

Copyright
by
Bahman Ghavimi-Alagha
2014

The Dissertation Committee for Bahman Ghavimi-Alagha Certifies that this is the approved version of the following dissertation:

**Synthesis and Receptor Affinity of 7 β -Substituted Analogs of Codeine;
Total Synthesis of 8,14-Dihydromorphinandienone Alkaloids**

Committee:

Philip D. Magnus, Supervisor

Eric V. Anslyn

Christopher W. Bielawski

Adrian T. Keatinge-Clay

Sean M. Kerwin

**Synthesis and Receptor Affinity of 7 β -Substituted Analogs of Codeine;
Total Synthesis of 8,14-Dihydromorphinandienone Alkaloids**

by

Bahman Ghavimi-Alagha, BA, MS

Dissertation

Presented to the Faculty of the Graduate School of

The University of Texas at Austin

in Partial Fulfillment

of the Requirements

for the Degree of

Doctor of Philosophy

The University of Texas at Austin

May 2014

Dedication

To my family.

Acknowledgements

I am indebted to Professor Magnus for his mentorship. He has been a tremendous source of intellectual guidance; and through his enormous experience, humility and integrity has created a truly nurturing environment for his students inside and outside the lab.

I am indebted to my wife Darlene for her perseverance and sacrifices which have allowed me to pursue my graduate studies. Without her daily encouragement, support, and assistance (including preparation of some compounds) this dissertation would not have materialized.

Dr. Phil Cox of Noramco, Inc. is thanked for providing us with codeine and thebaine. Dr. Xiao-Tao (Daniel) Chen and Dr. Jon Violin of Trevena, Inc. are thanked for the biological assays. Dr. Vince Lynch is thanked for obtaining the x-ray structures.

Synthesis and Receptor Affinity of 7 β -Substituted Analogs of Codeine; Total Synthesis of 8,14-Dihydromorphinandienone Alkaloids

Bahman Ghavimi-Alagha, PhD

The University of Texas at Austin, 2014

Supervisor: Philip D. Magnus

A series of morphinan-based compounds inspired by the semi-synthetic opioid metopon have been synthesized. An expedient route from (-)-codeine to the key intermediate, 6,7- α -epoxide has been developed giving access to enantio-enriched analogs. Classical diaxial opening of the α -epoxide has allowed for introduction of β -substituents at C7, emulating the 5 β -methyl group in metopon. Several analogs exhibited dual agonist activity at the μ - and δ -receptors while lacking significant affinity for κ -receptors, fulfilling a requirement for an opioid with a diminished side-effect profile. Additionally, a collective synthesis of 8,14-dihydronorsalutaridine, 8,14-dihydrosalutaridine, norisosinomenine and isosinomenine is reported. The strategy employed provides direct access to the correct oxidation level of the products by avoiding the biomimetic strategy of *o*, *p*-phenolic oxidative coupling. The combination of an organocatalyst guanidine superbases, a tertiary amine base and a dehydrating agent was found necessary for the successful Henry-Michael-dehydration cascade to form the phenanthrene motif. The requirement for an efficient and selective aliphatic nitro reduction could be achieved only under heterogeneous transfer-hydrogenation conditions. Conversion of 8,14-dihydrosalutaridine into salutaridine by oxidation of the C8-C14 into

a double bond would allow for subsequent biomimetic transformation of the resultant dienone structures consecutively into thebaine and codeine. The combination of these routes provide a highly practical racemic synthesis of certain 8,14-dihydromorphinandienone alkaloids, and by extension, of thebaine and codeine.

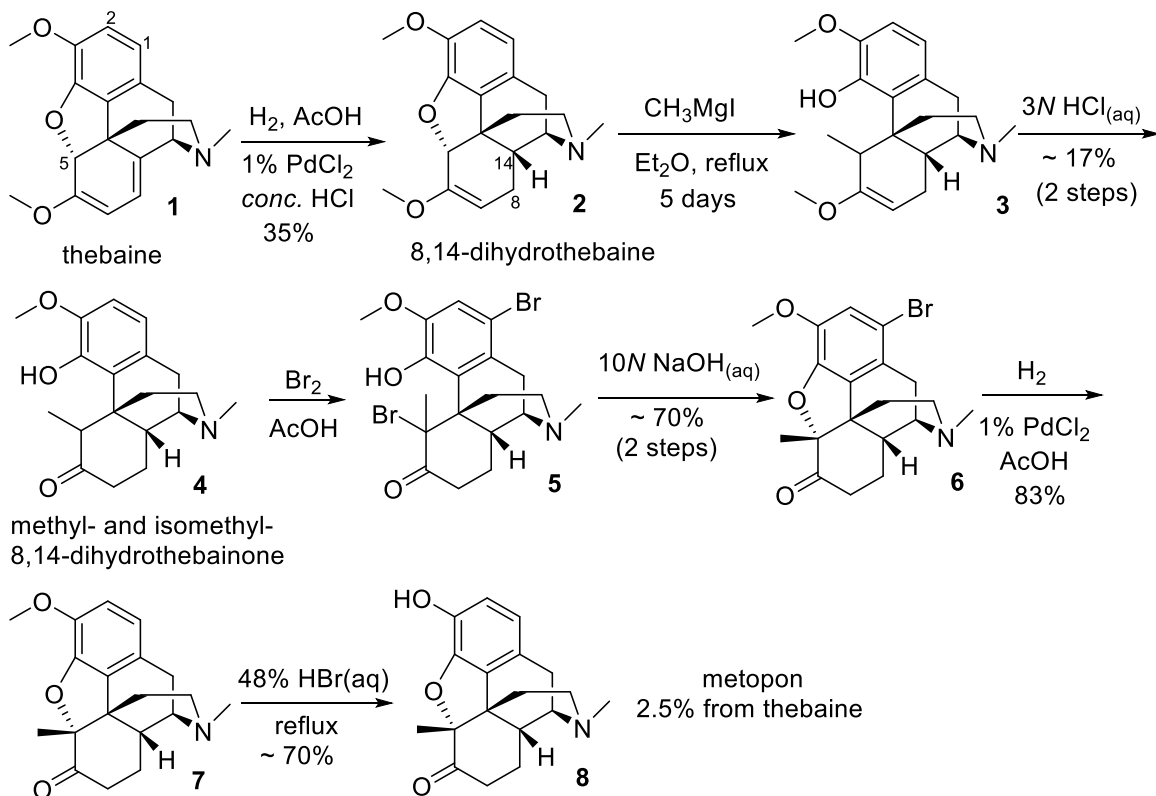
TABLE OF CONTENTS

	PAGE
CHAPTER 1: METOPON-INSPIRED ANALOGS	1
CHAPTER 2: 8,14-DIHYDROMORPHINANDIENONE ALKALOIDS	29
2.0 Background	29
2.1 Retrosynthesis	34
2.2 Biaryl	37
2.3 Dienone	40
2.4 Nitroalkene	43
2.5 Nitroalkane	53
2.6 Amine	56
2.7 Core	60
2.8 N-Methyl	61
CHAPTER 3: EXPERIMENTAL SECTION	64
3.0 General Information.....	64
3.1 Experimental Data for Chapter 1	65
3.2 Experimental Data for Chapter 2	94
Appendix A. X-Ray Data.....	112
Appendix B. Biological Data.....	212
REFERENCES.....	221

CHAPTER 1: METOPON-INSPIRED ANALOGS

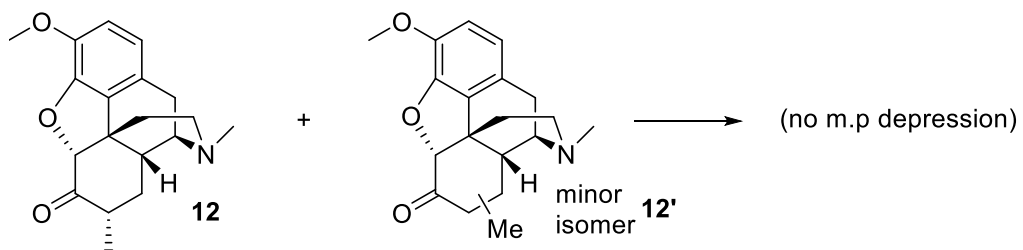
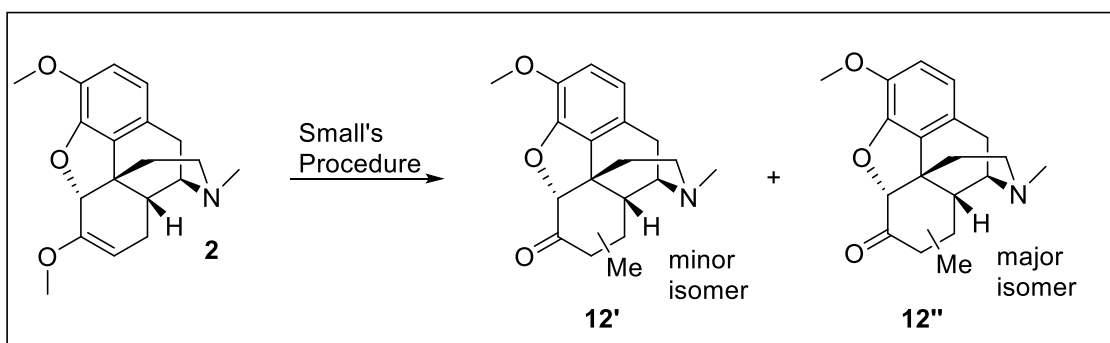
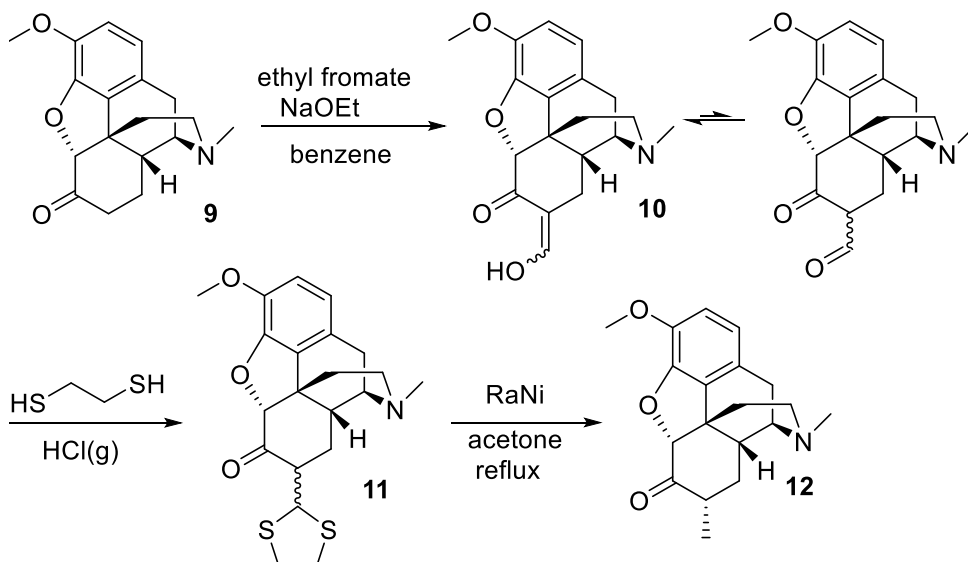
In 1936 Small¹ reported the synthesis of a new opioid, 5-methylhydrocodone **8** (metopon) derived from thebaine **1**, Scheme 1.1.

Scheme 1.1.



Confirmation of the structure was initially accomplished by Stork² using melting point comparison with a sample of 7 α -methyl **12** synthesized unambiguously, Scheme 1.2.

Scheme 1.2.



In 1982 Gates³ reported an efficient synthesis of metopon **8** in five highly efficient steps, Scheme 1.3; and, in 1989 provided an x-ray⁴ structure of the 5-methylheroin **8'** derivative, Figure 1.1.

Scheme 1.3.

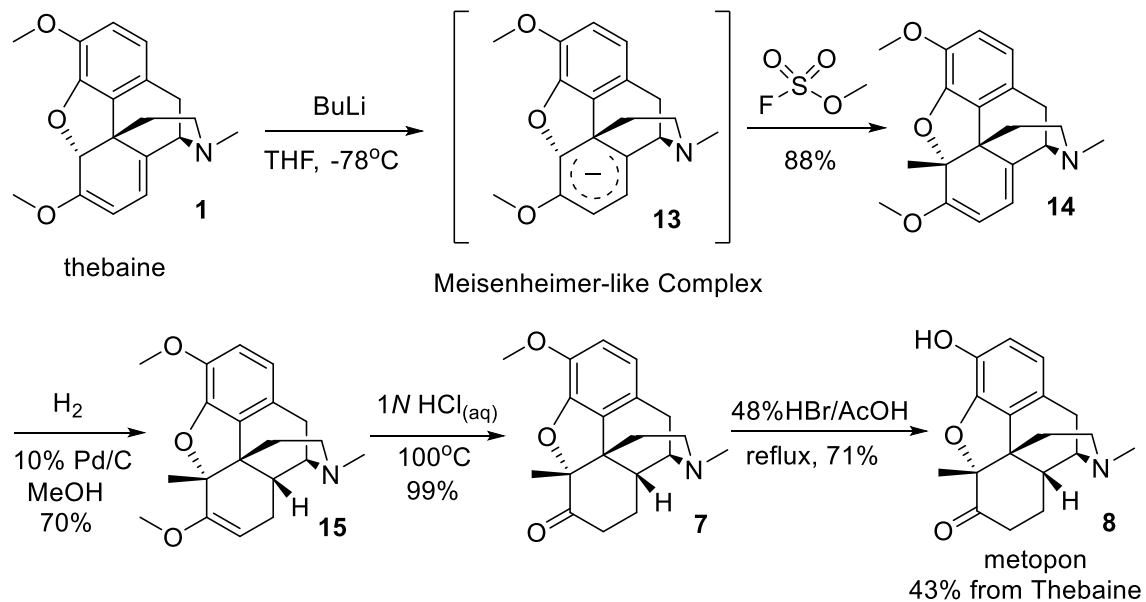
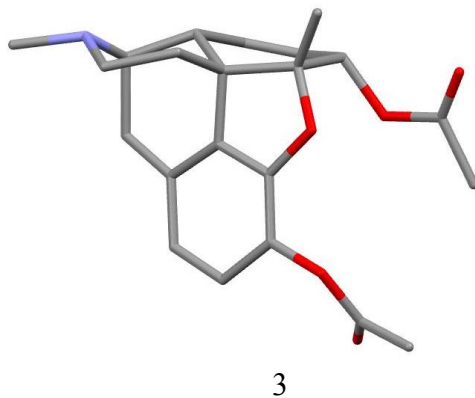


Figure 1.1. X-ray of **8'**.



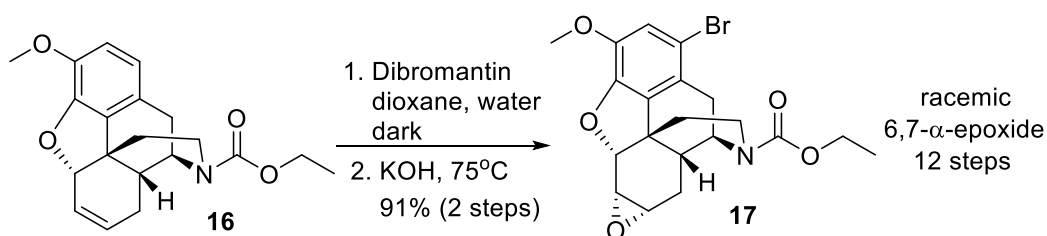
Prior to metopon, it was invariably observed that greater analgesic efficacy and potency caused more side effects.⁵ For example, morphine is about 10-fold more potent than codeine *in vivo*, but it also imparts significantly more side effects.⁶ Indeed, in many countries codeine is available as an over-the counter remedy for cough and other painful ailments, but morphine is a restricted substance. The side effects that are elicited by all opioid analgesics are constipation with the potential for paralytic ileus which can be lethal, respiratory depression which is the primary cause of death due to overdose, sedation or feeling “doped”, confusion, nausea and vomiting, development of tolerance to the analgesic effects, and addiction.⁷ Of these side effects respiratory depression, development of tolerance, and addiction are the most important.

The advent of metopon provided the first instance of an opioid with greater potency relative to morphine (3- to 10-fold), yet with less side effects, particularly with respect to development of tolerance and feeling “doped.” Although metopon did not demonstrate a dramatic improvement over morphine and semi-synthetic opioids as it too possessed all the typical aforementioned side effects to varying degrees, it did provide justification for continuation of the search for the “holy grail”⁸ of opioids. Ultimately, metopon fell out of favor due to the difficulty of its synthesis by the Small route.⁹ To this date the search for an opioid with morphine-like efficacy, but devoid of serious side effects continues with metopon as a *bona fide* lead.

The distinguishing structural feature of metopon is the 5 β -methyl group without which it is hydromorphone, the phenolic analog of hydrocodone that lacks the efficacy

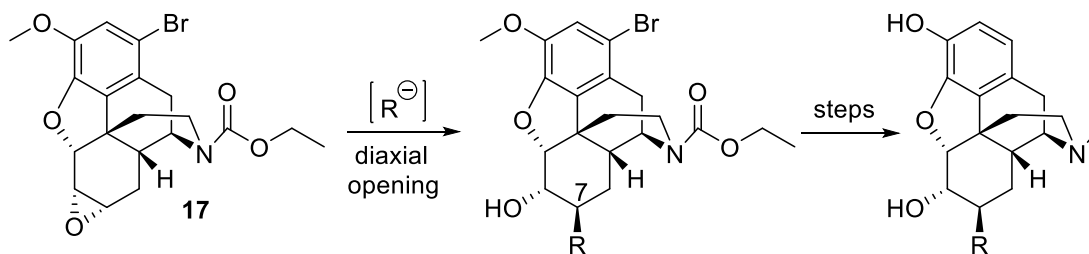
and side effect profile of metopon. Presumably, it is this structural feature that endows metopon with a greater therapeutic index relative to its congeners. Our approach to synthesis of analogs inspired by metopon capitalized on the existence of the 6,7- α -epoxide **17**, first reported by Magnus en route to the total synthesis of morphine, Scheme 1.4.¹⁰

Scheme 1.4.



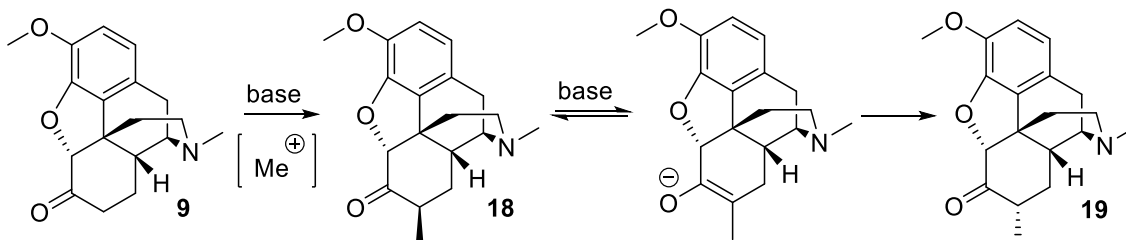
Given the relevance of the β -face of the morphinan skeleton *a la* metopon C5-methyl, we set out to investigate the effect of introducing a methyl group at C7. Diaxial opening of **17** would ensure the methyl group at C7 would be on the β -face, Scheme 1.5.

Scheme 1.5.



We anticipated that our epoxide **17** would be a versatile starting material for introduction of a variety of substituents at C7 allowing for an extensive structure-activity study. It should be noted that hydrocodone **9** is not a suitable starting material for introduction of 7 β -substituents even though the β -face is the preferred site of approach by an electrophile. The presence of the carbonyl group leads to epimerization at C7 with the resultant thermodynamic α -orientation. The 7 α -methylhydrocodone **19** analog has been reported to offer no advantage over hydrocodone **9**, Scheme 1.6.¹¹

Scheme 1.6.



In fact, reaction of hydrocodone-carbamate **20** with excess CH_3I in the presence of $^t\text{BuOK}$ in THF gave a mixture of four products: 8,14-dihydrothebaine **21**, 7-methyl-8,14-dihydrothebaine **22**, 7,7-dimethylhydrocodone **23**, and 5,7,7-trimethylhydrocodone **24** as their carbamates. The trimethylated compound **24** was subsequently subjected to LAH conditions to reduce the carbamate to N-methyl and inevitably, the ketone to an alcohol. Oxidation of the alcohol to ketone provided the trimethylated hydrocodone **25**, the structure of which was confirmed by x-ray analysis, Scheme 1.7. A notable feature of the structure is the pseudo-axial orientation of the β -methyl groups, Figure 1.2.

Scheme 1.7.

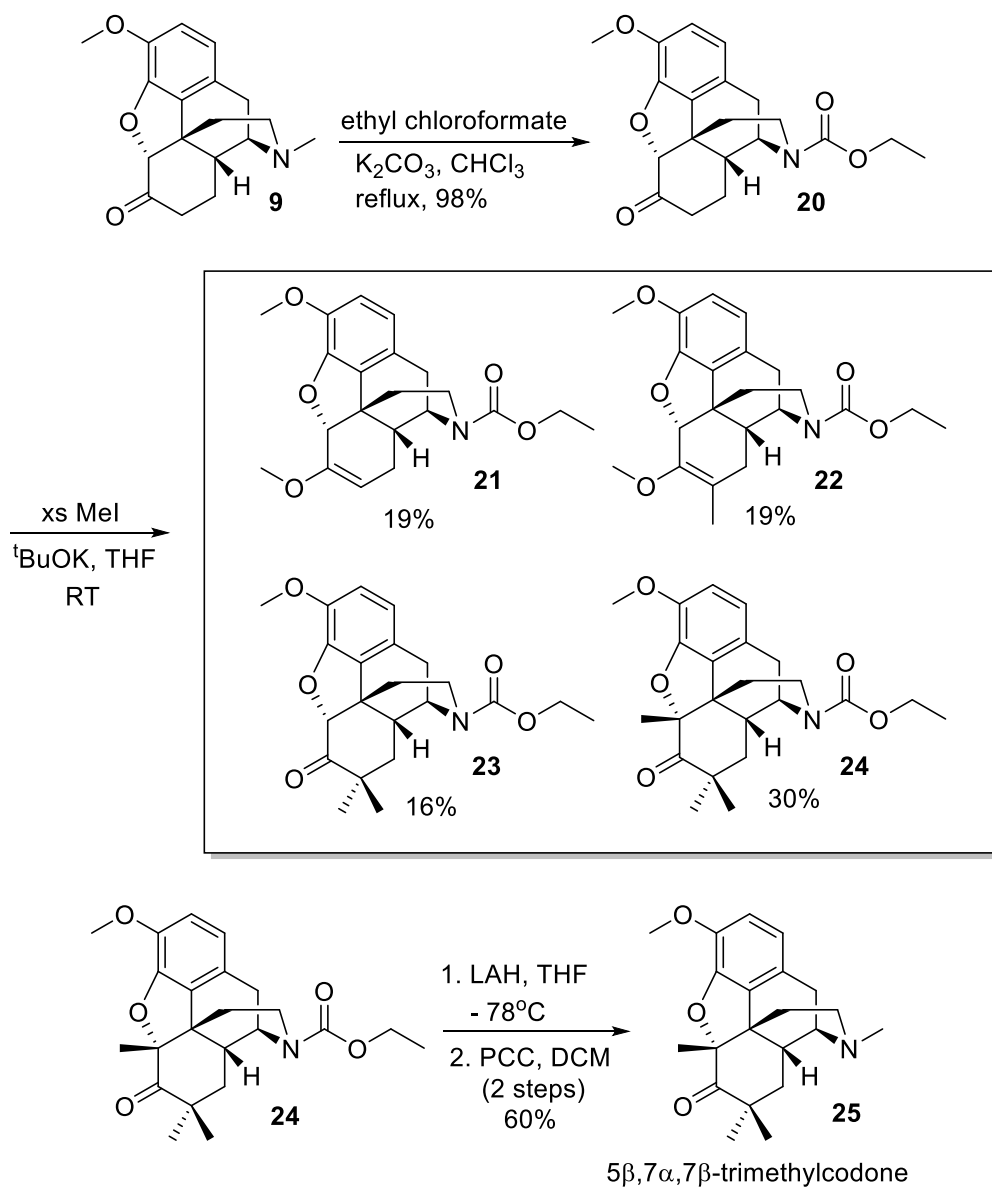
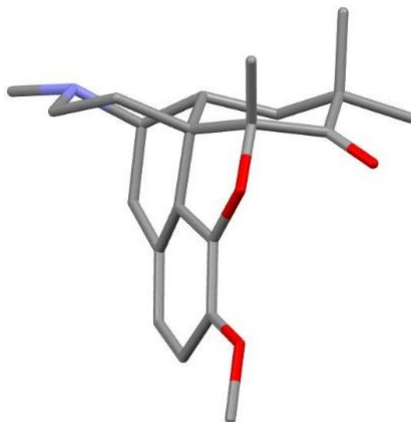
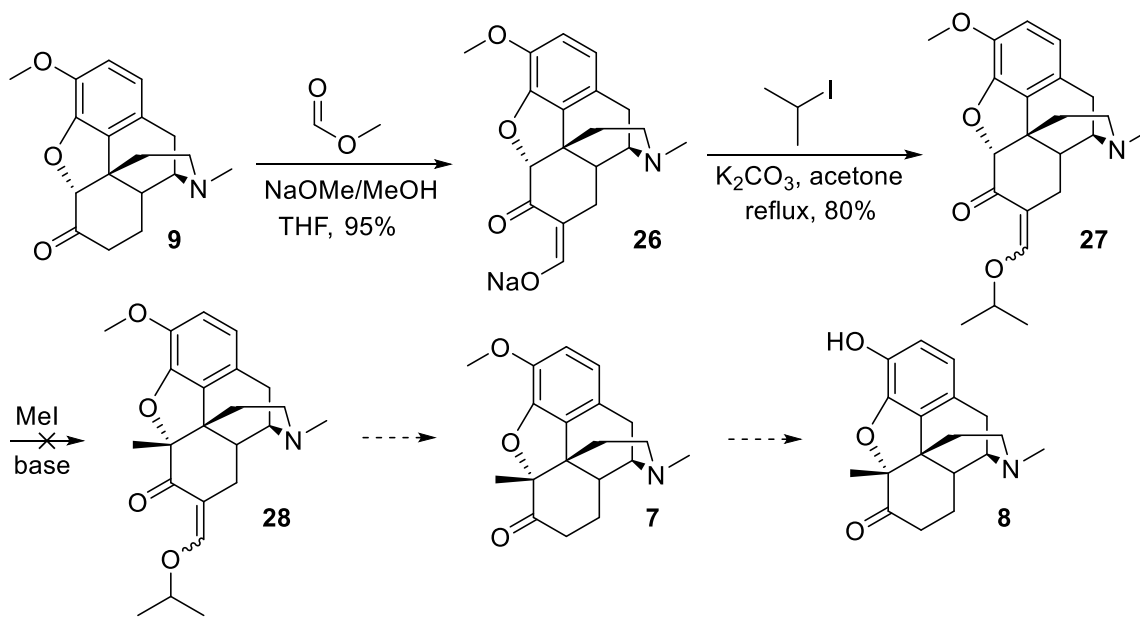


Figure 1.2. X-Ray of **25**.



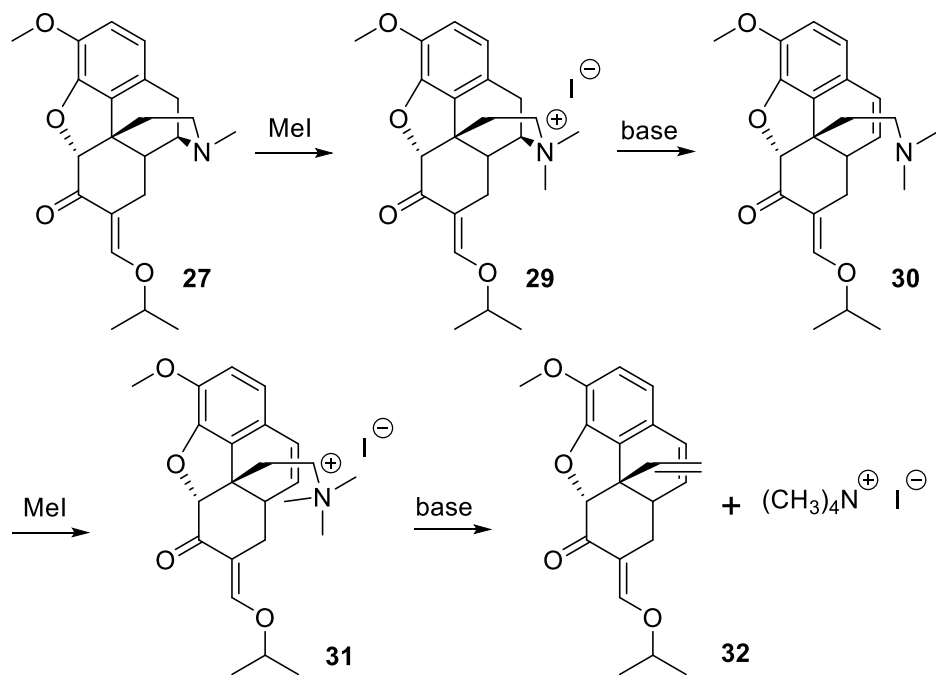
Hydrocodone **9** is an attractive alternative to thebaine **1** as starting material for a synthesis of metopon **8**, Scheme 1.8. Although hydrocodone itself is a semi-synthetic opioid, it is readily obtained in one step from (-)-codeine.¹² Thebaine, however, is a minor constituent of the opium poppy and is mainly used for the synthesis of oxycodone¹³ and Bentley compounds.¹⁴ The above experiment confirmed the problem of introducing the methyl group selectively at C5 and the necessity of “blocking” the C7 position before alkylation. Indeed, the strategy of “blocking” a methylene carbon possessing two active hydrogens over a methylene carbon with only one hydrogen was already inherent in Stork’s approach to the synthesis of the α -C7 methyl described earlier.

Scheme 1.8.



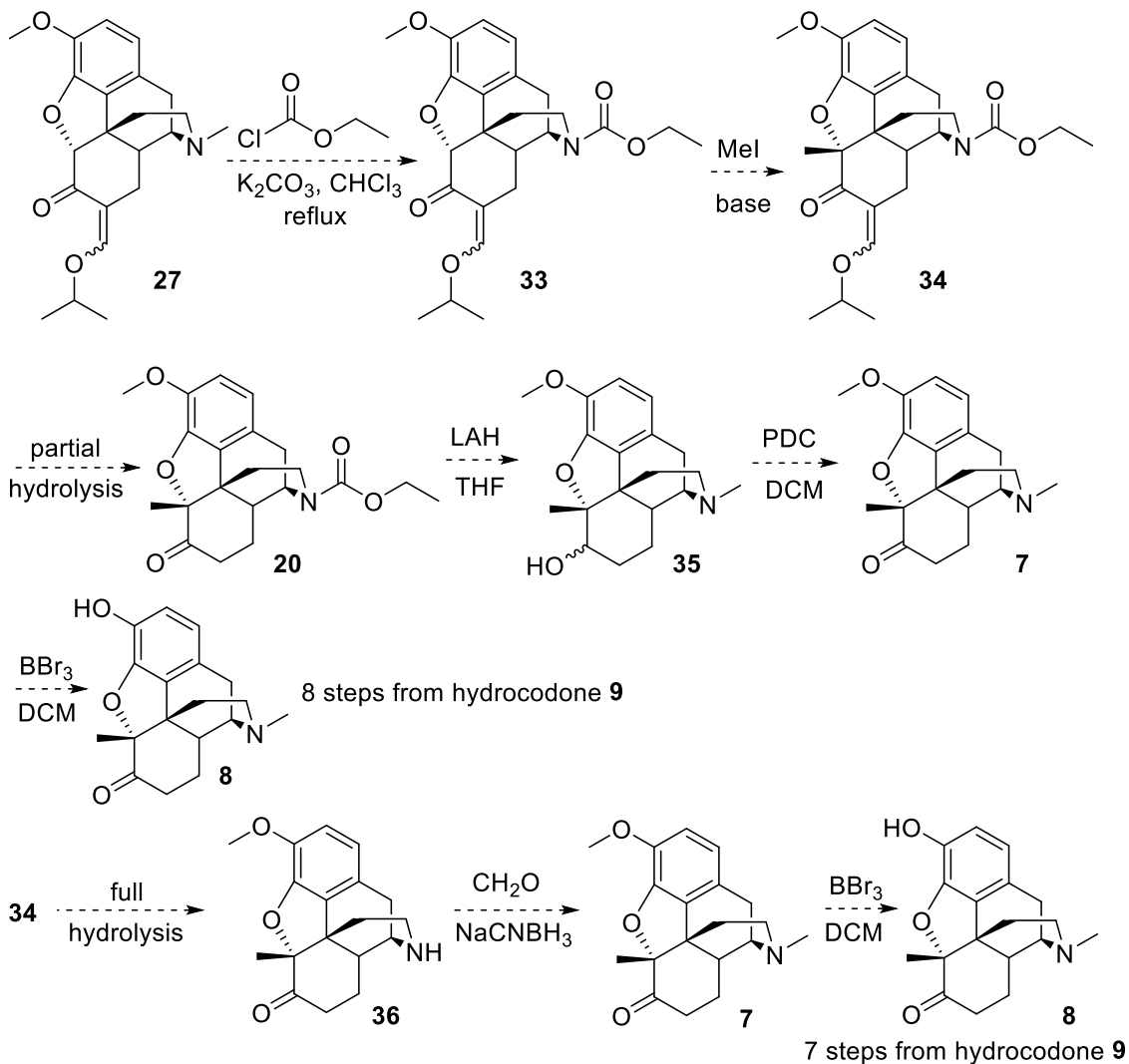
Although the C7 protection methodology worked smoothly, the subsequent methylation step did not. All attempts at methylation resulted in a mixture of products in which the N-methyl peak was absent in the NMR spectrum. We attributed the result to N-methylation with the subsequent Hoffman degradation, Scheme 1.9.

Scheme 1.9.



Using lower temperatures to avoid N-methylation as was done by Gates also prevented C-methylation, returning the starting material. This indicated the need to protect the nitrogen by forming its carbamate, compound **33**, Scheme 1.10. However, introducing another protecting group would render the synthesis inferior to Gates' and the project was halted.

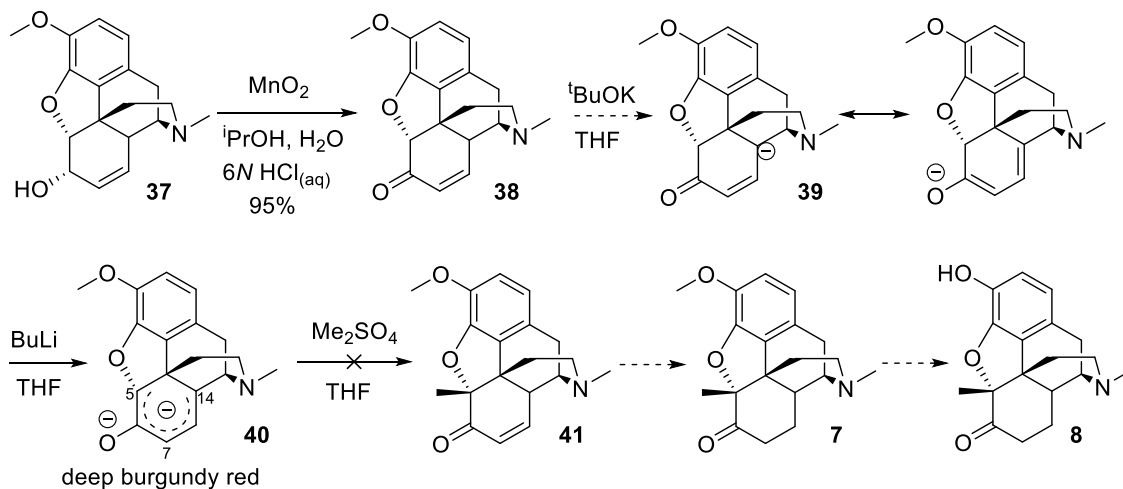
Scheme 1.10.



We also envisioned a more direct approach to metopon from codeine **37** employing dianion chemistry, Scheme 1.11.¹⁵ Treatment of codeinone **38** with a strong

base such as $t\text{BuOK}$ at $-78\text{ }^\circ\text{C}$ would deprotonate the compound at C14 to give **39**, while addition of a stronger base to this mixture such as BuLi would form the second anion, **39**, with the formation of the cyclopentadienyl anion intermediate acting as the driving force similar to that in Gates' procedure. The characteristic burgundy red color which is formed due to the conjugated anionic system would indicate the presence of the dianion. Quenching the solution with one equivalent of MeI would place the methyl group at C5 to give **41** (instead of C7 or C14) as in Gates' synthesis. Alkylation at C5 should be the preferred site due to the electron withdrawing effect of the oxo-bridge oxygen stabilizing the negative charge relative to C14. Alkylation at C7 would disrupt the conjugation.

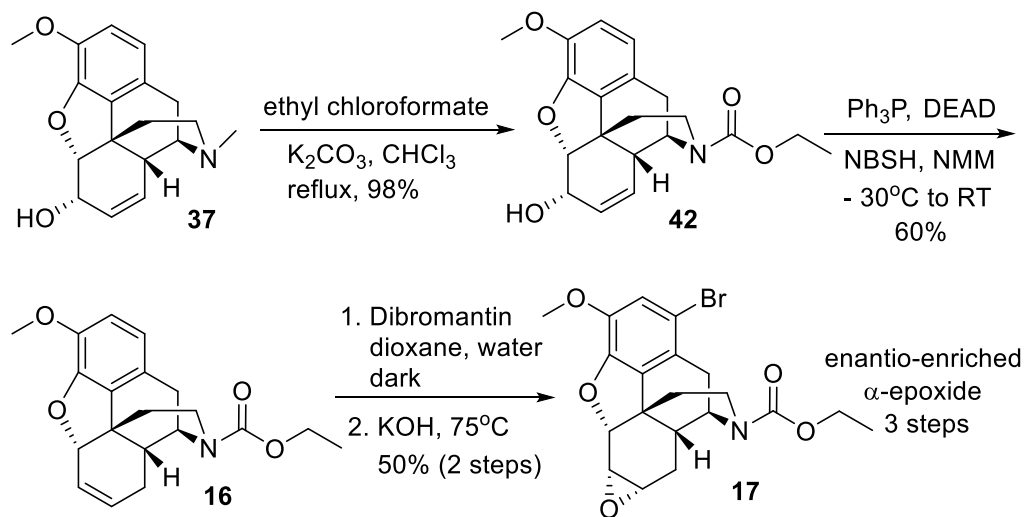
Scheme 1.11.



The 6,7- α -epoxide **17** available from the Magnus morphine route is racemic and requires 12 steps for its synthesis. From a practical and medicinal chemistry point of

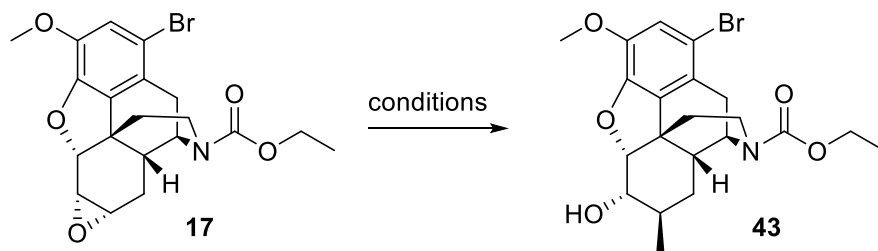
view, it is preferable to have a short and enantioselective synthesis of analogs. Our approach was to start from naturally occurring and enantio-enriched (-)-codeine **37** from the opium poppy which was supplied to us by Noramco, Inc. The allylic alcohol in (-)-codeine **37** was subjected to Myers' reductive transposition methodology¹⁶ to provide the precursor 6,7-olefin **16** from which the desired enantio-enriched 6,7- α -epoxide **17** could be obtained, Scheme 1.12.¹⁷

Scheme 1.12.



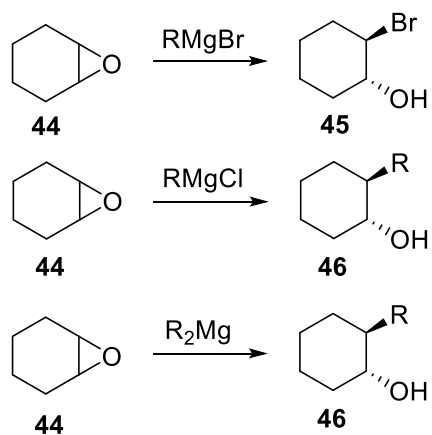
Following the successful application of Myers' protocol and availability of the 6,7- α -epoxide **17** in sufficient quantities, we set out to synthesize a few analogs. Our first attempt was to introduce the methyl group at C7, Scheme 1.13.

Scheme 1.13.



The standard protocol for epoxide opening with an alkyl nucleophile is to use an appropriate Grignard reagent. Although in the majority of cases this is a successful approach, Bedos¹⁸, and Bartlett¹⁹ reported that in the case of cyclohexene oxide **44** formation of halohydrin **45** is the exclusive product where the halide is bromine but not chlorine or dialkylmagnesium, Scheme 1.14.

Scheme 1.14.



Initially, we were not aware of these reports and our attempts at epoxide opening with CH_3MgBr resulted in 90% conversion to the bromohydrin 47, which was also confirmed by x-ray analysis, Scheme 1.15, Figure 1.3.

Scheme 1.15.

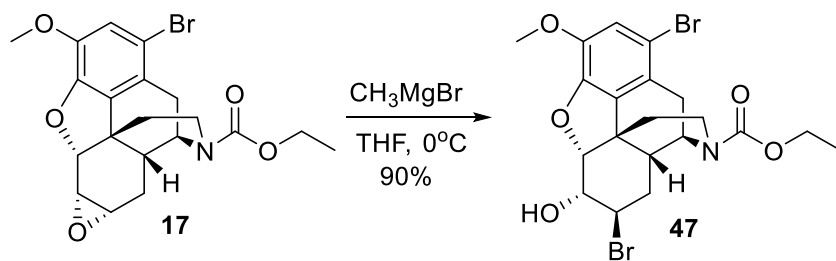
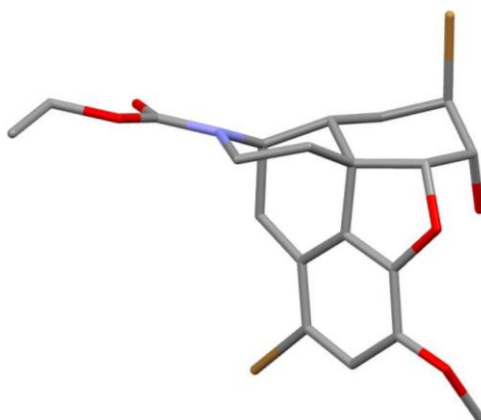
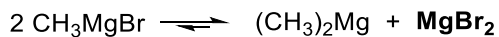


Figure 1.3. X-Ray of **47**.

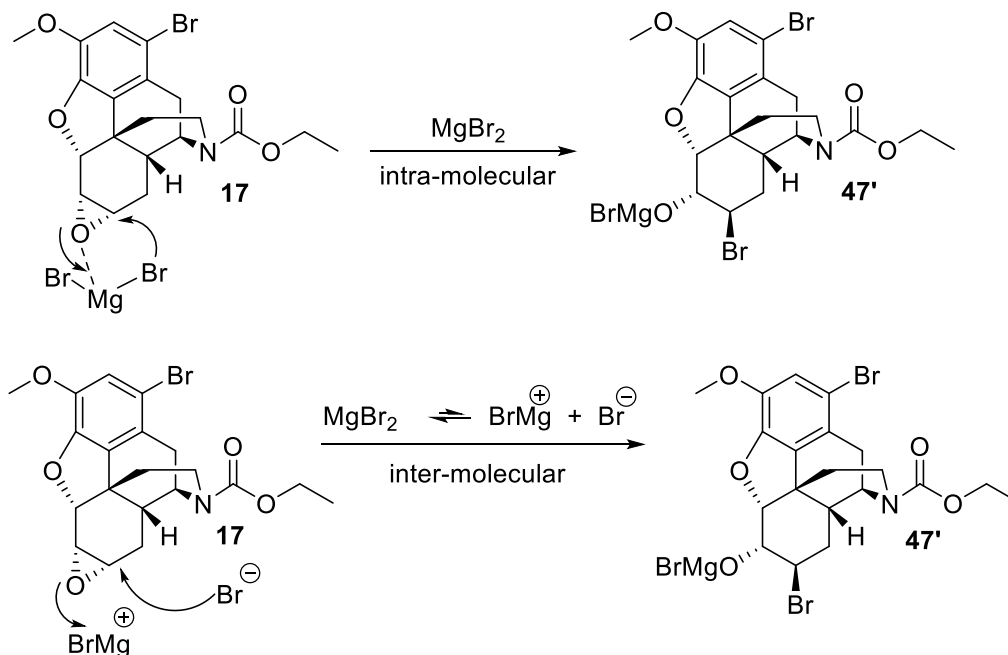


The x-ray structure revealed the diaxial relationship of the bromine and the hydroxyl group. We attribute the fact that the two groups retain their pseudo-axial conformations to the small A-values for bromine and hydroxyl groups, 0.48 and 0.60 kcal/mol respectively.²⁰ The relatively small values allow the dipoles of the two electronegative groups to orient themselves in an *anti*-periplanar conformation, effectively cancelling each other with the resultant chair-like conformation of the ring. Bartlett had demonstrated that the chloride form of the Grignard gave the expected alkylation product. In our case, we only observed the chlorohydrin product, albeit at a slower rate of formation. In the Schlenk equation²¹, MgX_2 is a Lewis acidic species that coordinates with the epoxide oxygen and catalyzes the ring opening to give **47**.



We postulated once coordination occurs the halide is readily transferred to C7 intra-molecularly. Alternatively, there may be a partial dissociation of MgX_2 into MgX^+ and X^- followed by an inter-molecular attack of X^- at C7, Scheme 1.16.

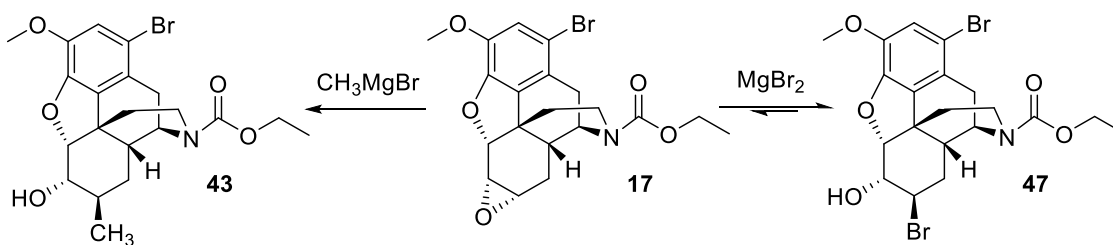
Scheme 1.16.



Regardless of the nature of the attack, we found it reasonable to use a source of methyl nucleophile that “carries” its own Lewis acid, analogous to MgBr_2 . Indeed, Bartlett demonstrated that R_2Mg was an efficient reagent for the epoxide opening, giving the desired product **46**. Before abandoning the use of CH_3MgBr , we considered running the reaction at higher temperatures and for longer duration. Our intention was to capitalize on

the reversibility of bromohydrin formation. We anticipated that once the bromohydrin is formed under the basic conditions of the Grignard reaction, it can re-form the α -epoxide **17**. Periodically the α -epoxide **17** can undergo diaxial opening with a nucleophilic methyl group giving **43** which is an irreversible reaction. This process would continue until all the α -epoxide **17** were consumed, Scheme 1.17. The C1 bromine would either survive the reaction conditions, or it would undergo Grignard exchange with the reagent which would lead to de-bromination during aqueous work up. Unfortunately, the reaction did not proceed as desired and a mixture of intractable products was observed.

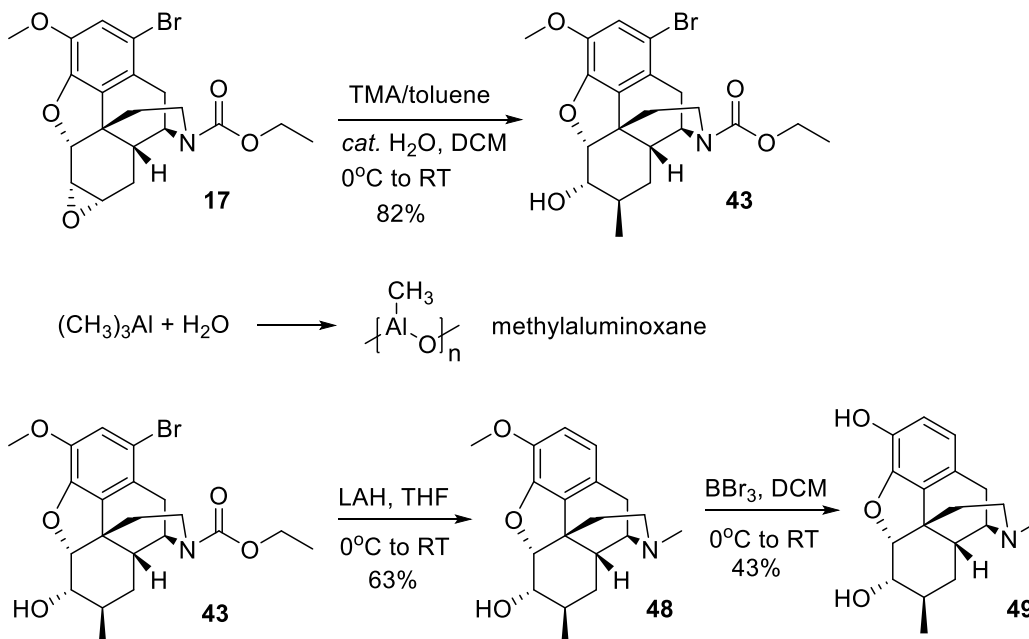
Scheme 1.17.



Before attempting to use the highly pyrophoric reagents $(\text{CH}_3)_2\text{Mg}$ or $(\text{CH}_3)_2\text{Zn}$, we investigated several reagents based on copper and aluminum. The copper reagents $(\text{CH}_3)_2\text{CuLi}$ as well as the more active CH_3CuCNLi resulted in no reaction. The use of the more reactive and stable $(\text{CH}_3)_2\text{CuCNLi}_2$ led to a moderate yield of 30%. The use of an aluminum-based alkylating reagent was initially the air-stable, powder $[(\text{CH}_3)_3\text{Al}]_2\cdot\text{dabco}$. No product **43** was observed even with the use of excess reagent and elevated temperatures. The use of $(\text{CH}_3)_3\text{Al}$ itself led to a 40% yield of the desired

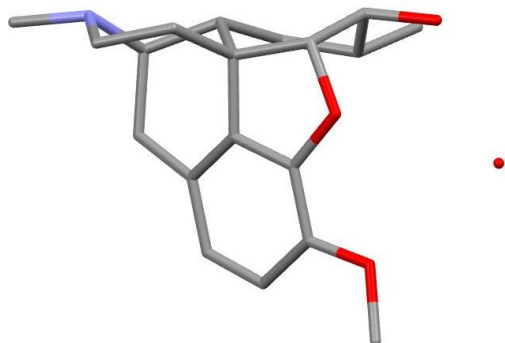
product **43**. This yield did not improve with higher temperatures or longer reaction time. At this point we considered various methods of “potentiating” the action of the reagent. First we considered an increase in nucleophilicity of the methyl group through the standard procedure of forming the “ate” complex. No improvement in yield was observed. The other approach was to use a strong Lewis acid based on the assumption that TMA was not adequately Lewis acidic. This, however, could readily be remedied with the addition of a catalytic amount of water to the solution of TMA and solvent. The controlled hydrolysis of TMA leads to generation of highly Lewis acidic oligomeric species, methylaluminumoxane (MAO) that act as co-catalysts in the Ziegler-Natta polymerization process. With this procedure the yield increased to 82%, Scheme 1.18.

Scheme 1.18.



Removal of the C1 bromine and reduction of the carbamate to the N-methyl were readily achieved through the action of LAH and the structure of the final compound **48** was confirmed by x-ray analysis, Figure 1.4.

Figure 1.4. X-Ray of **48**.

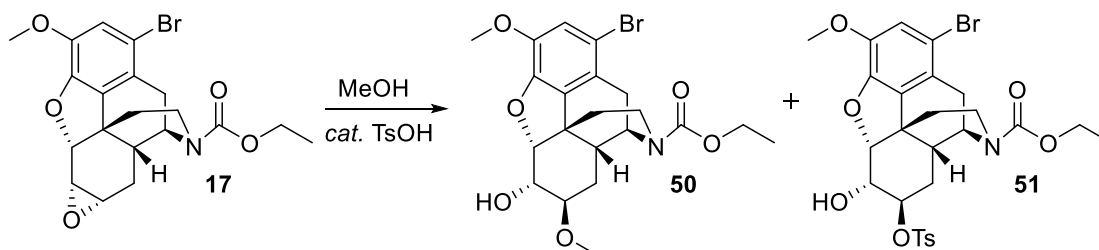


The x-ray shows that unlike the bromohydrin molecule **47**, the methyl and the hydroxyl group have relaxed into a pseudo-equatorial orientation following the initial diaxial opening with the resultant twist boat conformation of the ring. The A-value for a methyl group is 1.74 kcal/mol, significantly larger than bromine (0.48 kcal/mol).²² Additionally, the methyl group is not electronegative which precludes the need for an *anti*-periplanar orientation relative to the hydroxyl group. The final step was the conversion of the methyl ether into a phenol at C3 in the A-ring which was achieved by the action of BBr₃ to give **49**.

Preparation of other analogs was accomplished with the use of strong-acid catalysis. For example, hydrolysis of the epoxide **17** with KOH in water required refluxing temperatures with only partial conversion to the product **53** attesting to the stability of 6,7- α -epoxide **17** under basic conditions. However, MsOH catalysis allowed hydrolysis to occur readily at room temperature in a few minutes. The use of *p*-TsOH as a

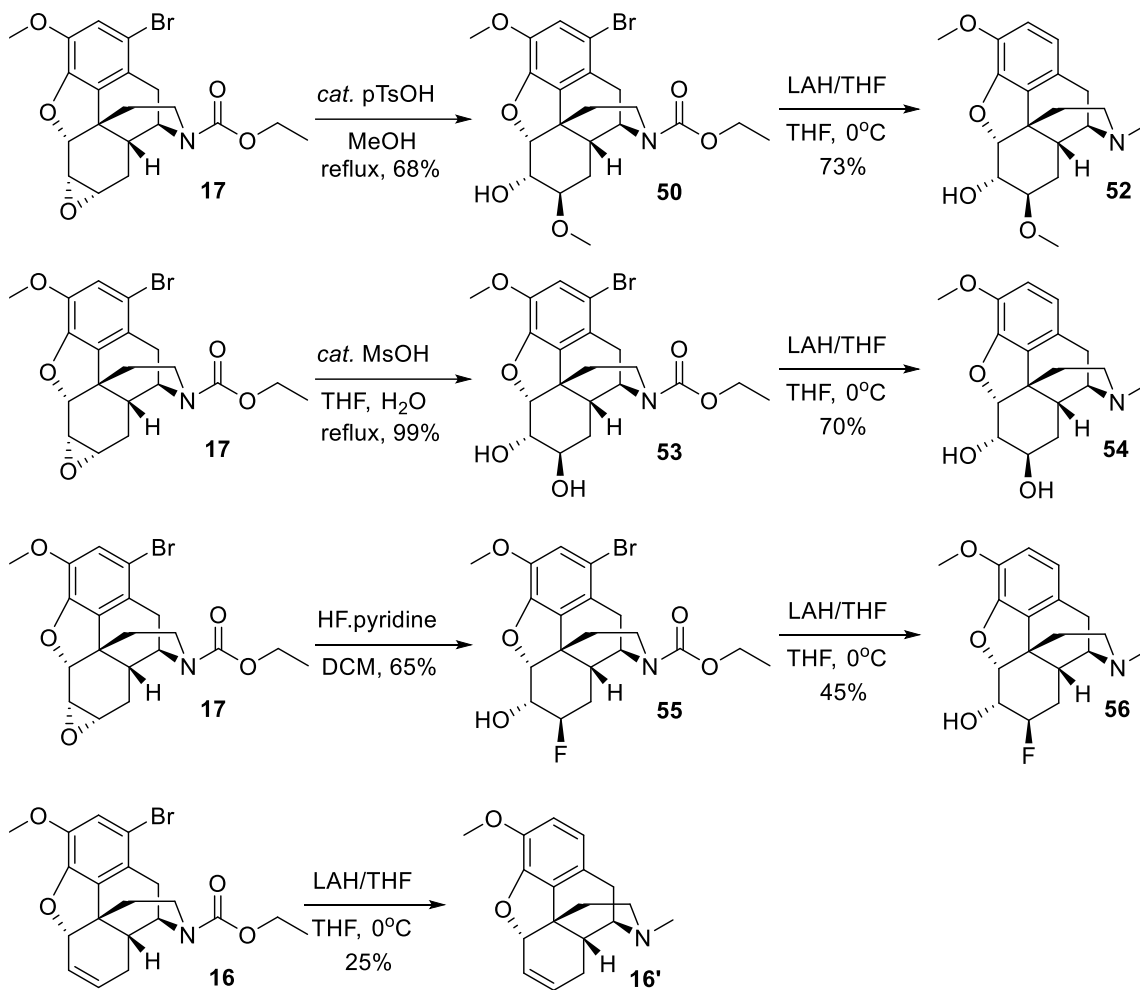
catalyst in methanolysis led to epoxide opening with *p*-TsO⁻ as the nucleophile to give **51** in 10% yield, Scheme 1.19. This did not occur with MsO⁻ anion, making MsOH the preferred catalyst.

Scheme 1.19.

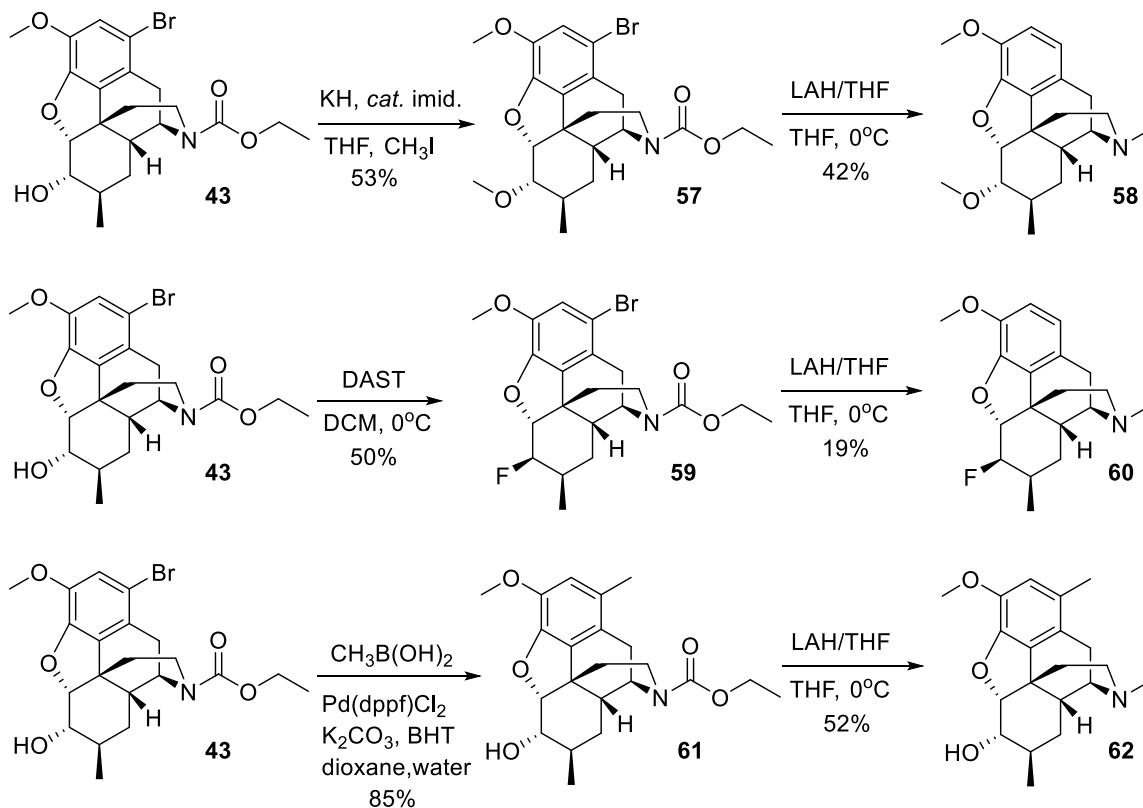


Representative compounds were prepared in order to demonstrate the versatility of the epoxide intermediate. In addition to the epoxide group, the C1 bromine allows for Suzuki coupling and the hydroxyl group at C6 can be converted into other groups such as ethers, halides as well as groups with the opposite stereochemistry, Scheme 1.20.

Scheme 1.20.

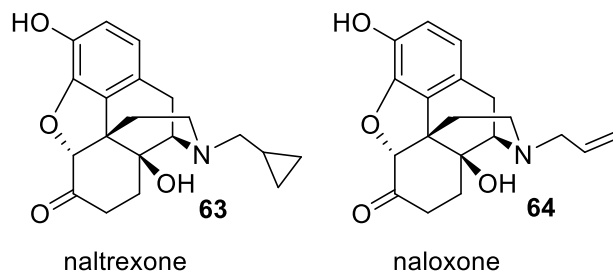


Scheme 1.20; continued,



We did not change the methyl group on the nitrogen. The substituent on the nitrogen determines whether the compound will function as an agonist or an antagonist (or even as a partial agonist depending on dose).²³ Opioid antagonists such as naltrexone **63** and naloxone **64**, are used to reverse the action of agonists by competitively displacement from the receptor site.

Figure 1.5.



In vitro activity of the analogs were determined by Trevena, Inc.²⁴ measuring binding affinity against the three opioid receptors of μ , δ , and κ . These are the three receptors associated with nociception as well as most of the side effects.²⁵ All the currently marketed opioid analgesics are μ -selective. It should be noted that there are several sub-receptors associated with each of the three receptors, significantly complicating attribution of biological effects.²⁶ Table 1.1 summarizes the binding affinity of the analogs.

Table 1.1.

Compound	hMOR, μ		hDOR, δ		hKOR, κ		$\mu : \delta : \kappa$	mMOR		mKOR	
	EC50 (μ M)	Span	EC50 (μ M)	Span	EC50 (μ M)	Span	selectivity ratios	EC50 (μ M)	Span	EC50 (μ M)	Span
48	2.0 \pm 0.2	98	3.2 \pm 0.5	97	25 \pm 2	29	13 : 8 : 1	0.6 \pm 0.1	97	32 \pm 13	30
49	0.020 \pm 0.004	98	0.08 \pm 0.02	107	1.6 \pm 0.3	46	80 : 20 : 1	0.010 \pm 0.002	99	1.6 \pm 0.3	62
52	16 \pm 2	68	13 \pm 2	84	50 \pm 23	38	3 : 4 : 1	4.0 \pm 0.6	86	N.Q.	--
54	16 \pm 1	84	100 \pm 28	117	126 \pm 87	41	8 : 1 : 1	6.3 \pm 0.6	96	159 \pm 128	60
56	40 \pm 6	68	79 \pm 15	90	N.Q.	--	2 : 1 : ---	8.0 \pm 0.9	79	N.Q.	--
58	3.2 \pm 0.4	78	2.5 \pm 0.6	94	32 \pm 4	52	10 : 13 : 1	0.8 \pm 0.2	92	50 \pm 9	51
62	5.0 \pm 0.5	69	16 \pm 2	73	N.Q.	--	3 : 1 : ---	2.0 \pm 0.2	77	50 \pm 37	18
60	3.2 \pm 0.4	59	3.2 \pm 0.6	86	5.0 \pm 0.6	55	1 : 1 : 1	0.8 \pm 0.1	78	10 \pm 2	40
Morphine	0.050 \pm 0.004	91	0.50 \pm 0.06	69	0.40 \pm 0.02	90	10 : 1 : 1	0.030 \pm 0.002	97	0.40 \pm 0.01	71
DAMGO	0.015 \pm 0.002	96	0.40 \pm 0.04	99	4.0 \pm 0.2	66	200 : 10 : 1	0.005 \pm 0.001	95	4.0 \pm 0.1	70
Oxycodone	0.50 \pm 0.02	93	4.0 \pm 0.2	93	16 \pm 2	47	32 : 4 : 1	0.160 \pm 0.007	97	16 \pm 1	59

Most analogs lack activity against κ -receptors. These receptors are associated with the side effect of intense dysphoria in addition to their desired analgesic effects.²⁷ Simultaneous agonist activity at μ - and δ -receptors has been found in animal studies to have a synergistic effect in that δ -receptor agonists significantly decrease the need for μ -activation to achieve same degree of pain relief. Furthermore, μ -agonists significantly

decrease the propensity of δ -agonists to cause convulsions which is their primary side effect. Thus, dual agonist compounds are regarded as a promising approach to discovery of opioids devoid of serious side effects. It is also highly desirable for practical as well as pharmacological reasons to achieve this dual activity by a single molecule. Several compounds tested exhibited this dual activity. As stated earlier, by changing the methyl group on the nitrogen into one of several established groups such as methylene cyclopropyl, or allyl, it is possible to convert an agonist into an antagonist. Although we did not pursue this route, it has been found that simultaneous agonist activity at μ -receptors and antagonist activity at δ -receptors prevents development of tolerance and addiction without loss of analgesia.²⁸ Although metopon itself is a μ -selective opioid²⁹, at least several different μ sub-receptors have been discovered in recent years.³⁰ The physiological function of each sub-receptor has yet to be fully elucidated adding another dimension to the complexity of opioid research and potentially providing another route for elimination of side effects.

In our collaboration with Pfizer Inc., we synthesized metopon according to Gates' procedure with some modifications, Scheme 1.21. The use of dimethyl sulfate instead of the highly toxic methyl fluorosulfonate or "magic methyl" as the methylating agent has already been reported.³¹ We also employed BBr_3 for the last step and obtained x-ray structures for **14**, Figure 1.6, and **8**, Figure 1.7. Further work on delineation of pharmacological properties of metopon according to modern assays is currently being pursued.

Scheme 1.21.

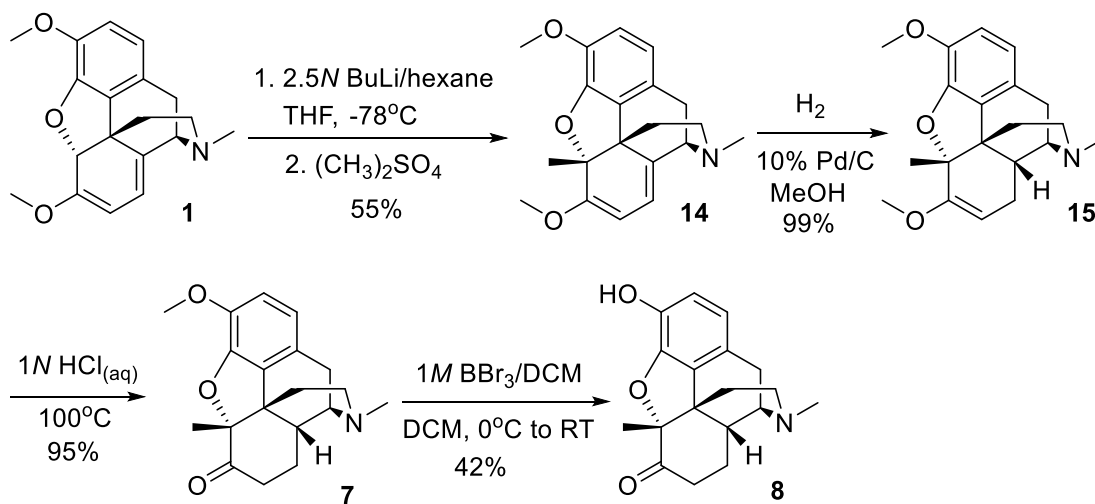


Figure 1.6. X-Ray of 14.

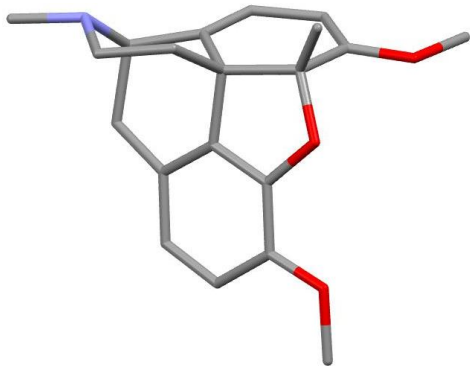
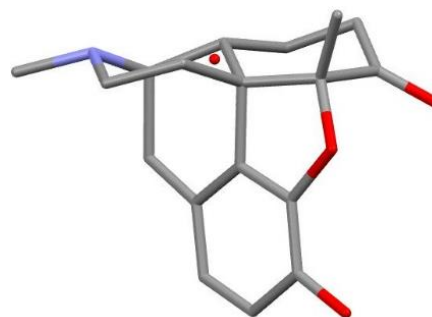


Figure 1.7. X-Ray of 8.

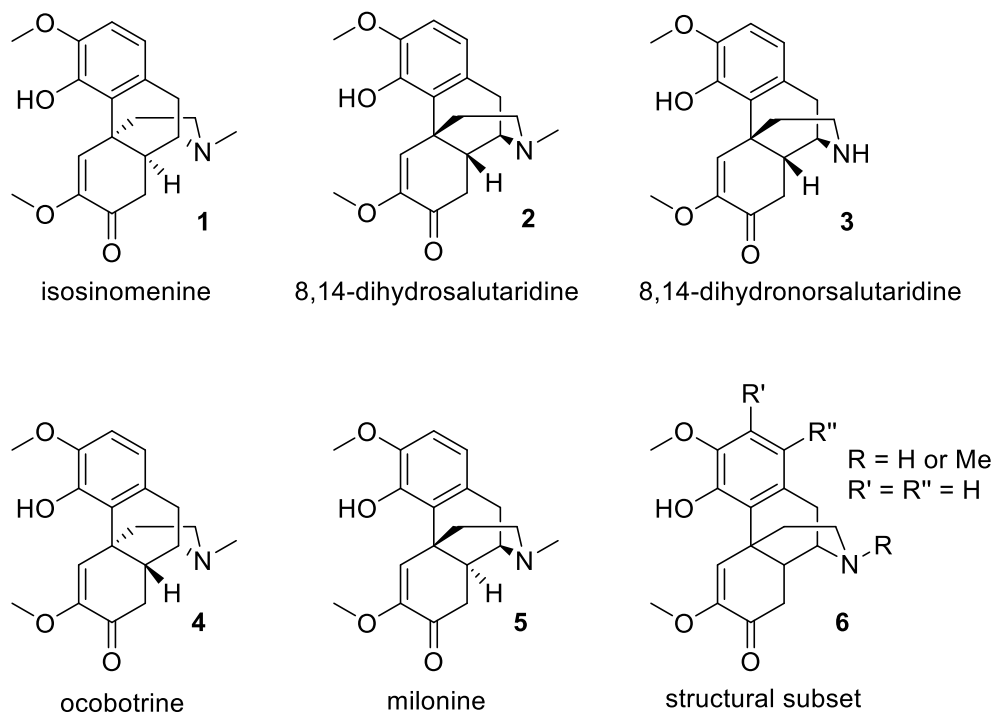


CHAPTER 2: 8,14-DIHYDROMORPHINANDIENONE ALKALOIDS

2.0 Background

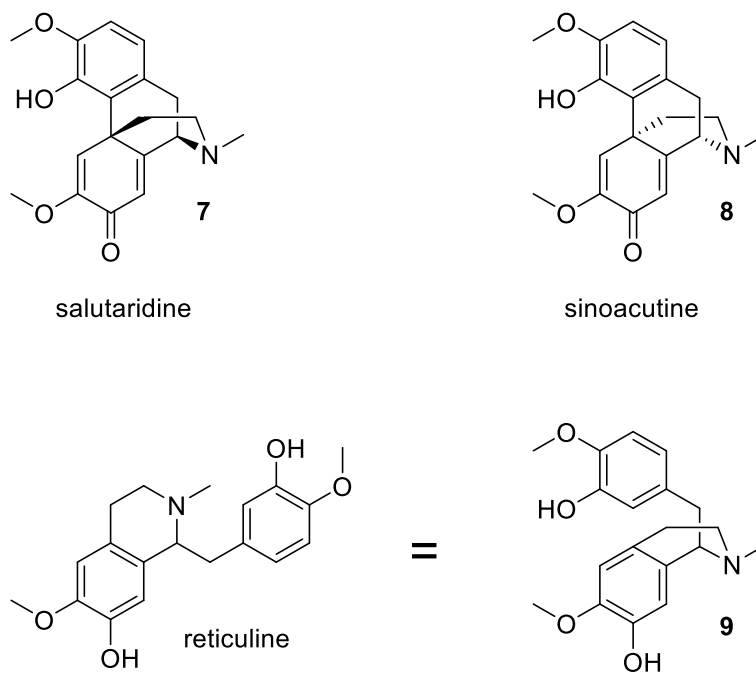
Isosinomenine **1**, 8,14-dihydrosalutaridine **2**, 8,14-dihydronorsalutaridine **3**, ocobotrine **4** and milonine **5** are to date the five known members of a subset of morphinandienone alkaloids (general structure **6**) in which the C8-C14 is a single bond, Figure 2.1. As such, they are a small and rare class of compounds whose formation and function has yet to be elucidated.³²

Figure 2.1.



This is in contrast to the well-known morphinandienone alkaloids salutaridine **7** and its enantiomer, sinoacutine **8** in which the C8-C14 is a double bond, biosynthetically originating from the intra-molecular oxidative *ortho-para* phenolic coupling of reticuline **9**, and in the case of salutaridine leading to formation of morphine, Figure 2.2.³³

Figure 2.2.



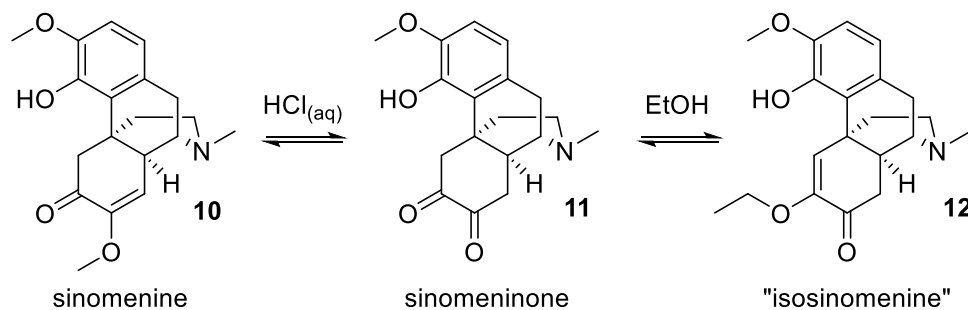
Little is also known about the pharmacological activity of these alkaloids. Milonine **5** has elicited hypotension and tachycardia upon injection into rats,³⁴ while by oral administration the compound exhibited potent anti-eosinophil and anti-leukotriene

activities³⁵. 8,14-Dihydrosalutaridine **2** has shown protective effects on the myocardial function in rats.³⁶

8,14-Dihydrosalutaridine **2** was first isolated as its O-acetyl derivative in 1963 by Haynes and Stuart from *Croton linearis* Jacq³⁷, and subsequently as its free base from *Croton discolor* Willd along with the establishment of its structure in 1967 by Stuart.³⁸ Later discoveries of this compound have been by Stuart from *Croton Plumieri* in 1969 together with salutaridine **7** and, possibly 8,14-dihydronorsalutaridine³⁹ **3**; and, from *Dehaasia longipedicellata* by Awang in 2004.⁴⁰ 8,14-Dihydronorsalutaridine **3** was first isolated in 1963 by Haynes and Stuart from *Croton linearis* Jacq,⁴¹ and subsequently, in 1968 by the same authors.⁴² Its structure was established in 1967 by Haynes, Husbands and Stuart⁴³; and was possibly isolated from *Croton Plumieri* in 1969 by Stuart.⁴⁴

Isosinomenine **1** isolation was first reported in 1958 by Sasaki from *Sinomenium Acutum* Rhed. Et Wils.⁴⁵ Initially, Sasaki correctly proposed the structure to be the methoxy enol ether. However, in 1963 Sasaki replaced the methoxy group by an ethoxy group **12** as the revised structure.⁴⁶ In 1968, Barton expressed doubt regarding the correctness of the revised structure due to the use of ethanolic hydrochloric acid during the isolation by Sasaki.⁴⁷ In 1968, Sawa expressed the same concern and prepared a compound from sinomeninone **11** that corresponded to Sasaki's sample and recommended the re-assignment of the name isosinomenine to the methoxy enol ether **1** as the correct structure, Scheme 2.1.⁴⁸

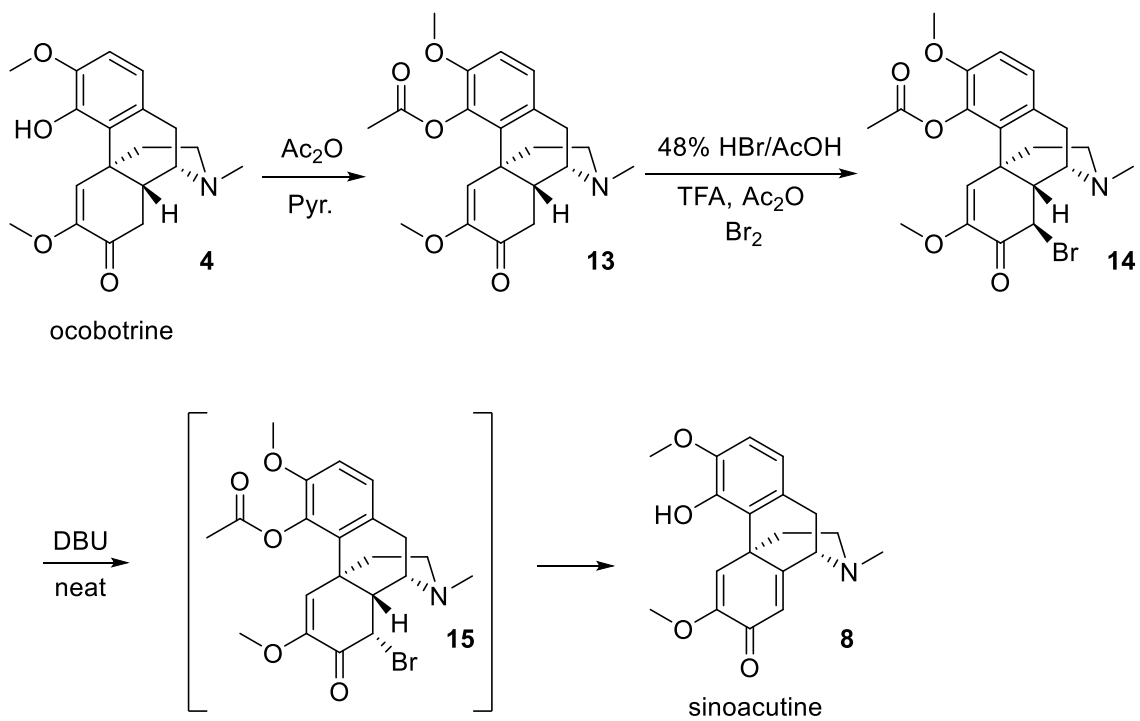
Scheme 2.1.



Isosinomenine **1** is the enantiomer of 8,14-dihydrosalutaridine **2**, and while 8,14-dihydronorsalutaridine **3** is a known natural product, its enantiomer, norisosinomenine has not yet been isolated.

Milonine **5** was first isolated in 1995 from leaves of *Cissampelos Sympodialis*⁴⁹, while ocobitrine **4** was first isolated in 1976 from *Ocotea Brachybotra*.⁵⁰ They possess a *trans* B/C ring-junction causing them to be epimeric at C14 relative to 8,14-dihydrosalutaridine **2** and isosinomenine **1** respectively. Ocobitrine **4** has been converted into sinoacutine **8** for the purpose of chemical correlation via a sequence of phenol protection/ α -bromination/dehydrobromination, but no yields were disclosed, Scheme 2.2.⁵¹

Scheme 2.2.



2.1 Retrosynthesis

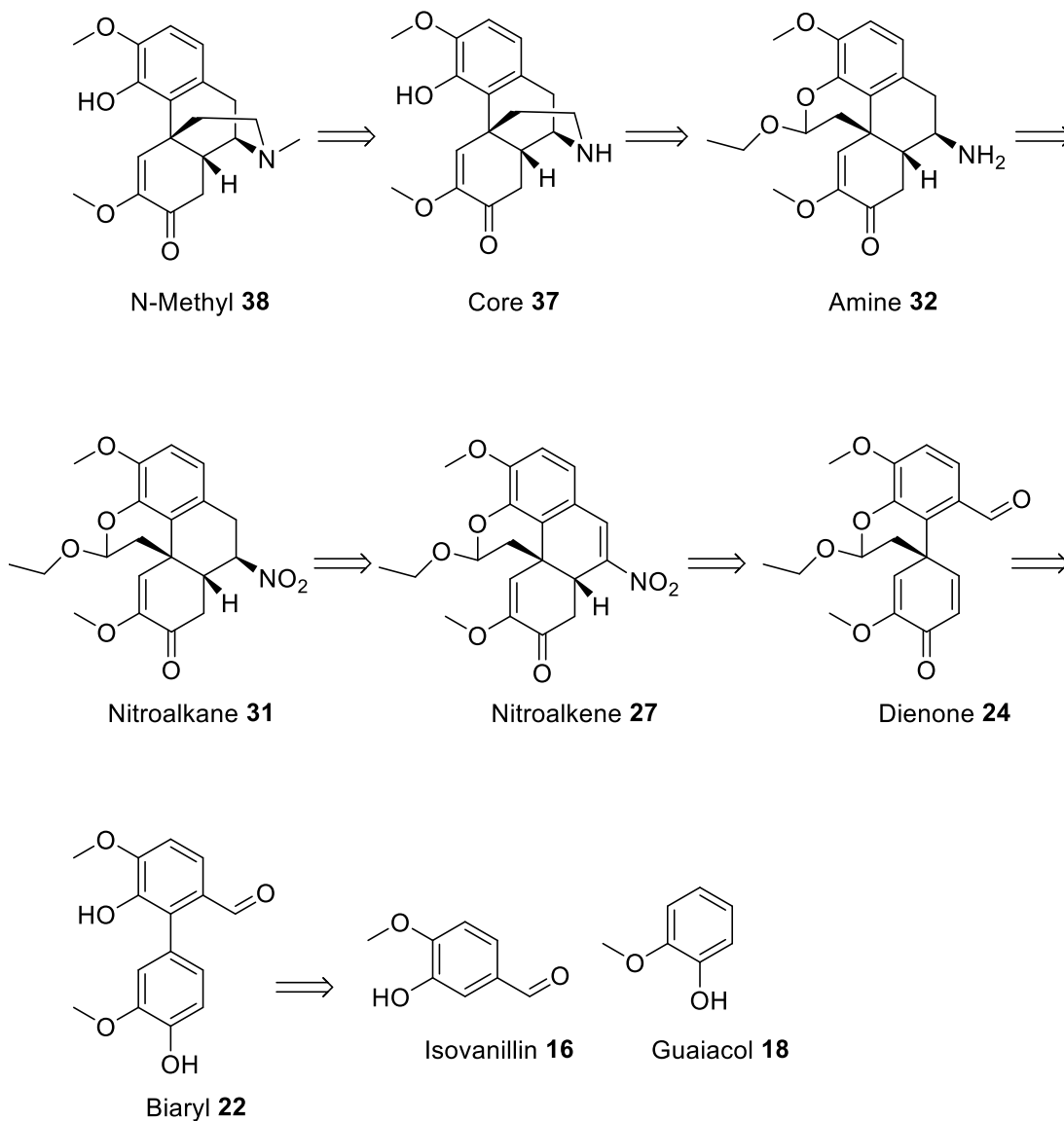
Our synthetic strategy is based on that used by Magnus in the total synthesis of morphine⁵² and allows for collective preparation of three of the five known 8,14-dihydromorphinandienone alkaloids discussed in the previous section, Scheme 2.3.⁵³ These are isosinomenine **1**, 8,14-dihydronorsalutaridine **3**, and 8,14-dihydrosalutaridine **2**. There are a total of four C-C and two C-N bond forming reactions along with the intermediacy of six key compounds leading to the formation of the aforementioned natural products. The synthesis is racemic, allowing for simultaneous formation of isosinomenine **1** and 8,14-dihydrosalutaridine **2** as well as their des-methyl precursors norisosinomenine (not a known natural product) and 8,14-dihydronorsalutaridine **3**.

The Suzuki coupling reaction is used to prepare the biaryl intermediate **22**. The reaction is the first C-C bond forming step and couples the A-ring with the C-ring. The coupling partners are prepared from the natural products guaiacol **18** and isovanillin **16**. Isovanillin **16** is converted to bromoisovanillin **17**, and guaiacol **18** to a silyl-protected boroxine trimer **21** via the intermediate **20**. Protection of the guaiacol **18** phenol serves to differentiate the C-ring hydroxyl group from that in the A-ring for the subsequent O-alkylation. It also serves as a handle for fluoride initiated intra-molecular *para*-alkylation using the established Magnus protocol. Following the O-alkylation of the hydroxyl group in the A-ring, the intra-molecular *para*-alkylation leads to formation of the dienone **24** unit in the C-ring and an acetal.

The dienone **24** synthesis is the second C-C bond forming step. From the dienone **24** the remaining two C-C bonds can be formed via a cascade Henry, Michael, and dehydration reactions. This yields the nitroalkene **27** intermediate along with the B-ring. The remaining D-ring requires modification of the nitroalkene **27** unit in preparation for the two C-N bond forming reactions. This is accomplished with a step wise reduction of the double bond of the nitroalkene **27** through conjugate reduction to **31**, and subsequently, the reduction of the nitro group into a primary amine **32**.

The first C-N bond formation is the reductive amination of the pendant aldehyde with the primary amine following hydrolysis of the acetal. This gives the racemic mixture of 8,14-dihydronorsalutaridine and norisosinomenine **37**. N-methylation is the last C-N bond forming reaction and completes the total synthesis of 8,14-dihydrosalutaridine and isosinomenine racemates **38**. The following section provides details for the synthesis of the key intermediates and their precursors.

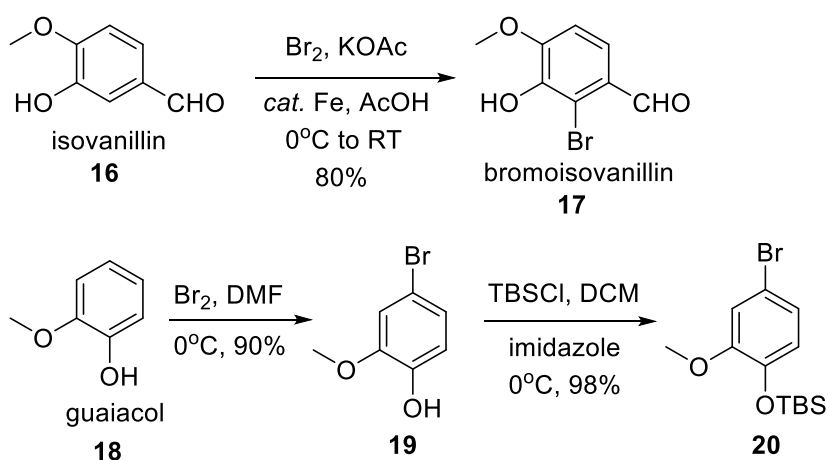
Scheme 2.3.



2.2 Biaryl

Preparation of the biaryl intermediate **22** (coupling of C12 and C13) began with the synthesis of the commercially available 4-bromoguaiacol **19** and bromoisovanillin **17**, Scheme 2.4. Conversion of 4-bromoguaiacol **19** was readily accomplished with the use of TBSCl in DCM using imidazole as both catalyst and base at 0 °C in 98% yield.

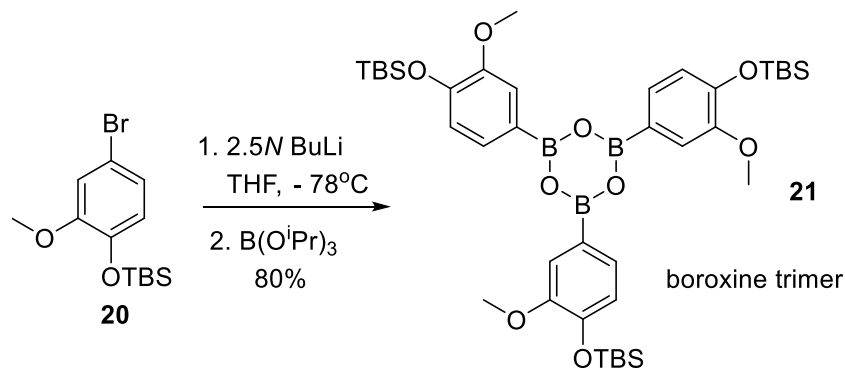
Scheme 2.4.



Synthesis of the boroxine intermediate **21** required freshly distilled triisopropyl borate as even new bottles often contained significant impurities presumably due to hydrolysis of the ester. Treatment of the bromide **20** with BuLi in dry THF at -78 °C followed by quenching with $(i\text{PrO})_3\text{B}$ provided an off-white solid which after azeotropic distillation and silica gel chromatography gave the boroxine trimer anhydride **21** in 80% yield. Recrystallization of the trimer from boiling hexane and a small quantity of ethyl

acetate was possible, but recovery was low and the quality of the recovered substance questionable. Chromatography provided the most convenient way for purification, Scheme 2.5.

Scheme 2.5.



The biaryl **22** synthesis was accomplished using Suzuki coupling and Pd(dppf)Cl₂ as the catalyst. Experiments were performed to determine the optimum catalyst loading. It was determined that as little as 0.1 mole% was sufficient for a yield of 57% which increased to 89% using 1 mole% loading. No improvement was observed by increasing the loading to 10 mole%, Scheme 2.6, Figure 2.3.

Scheme 2.6.

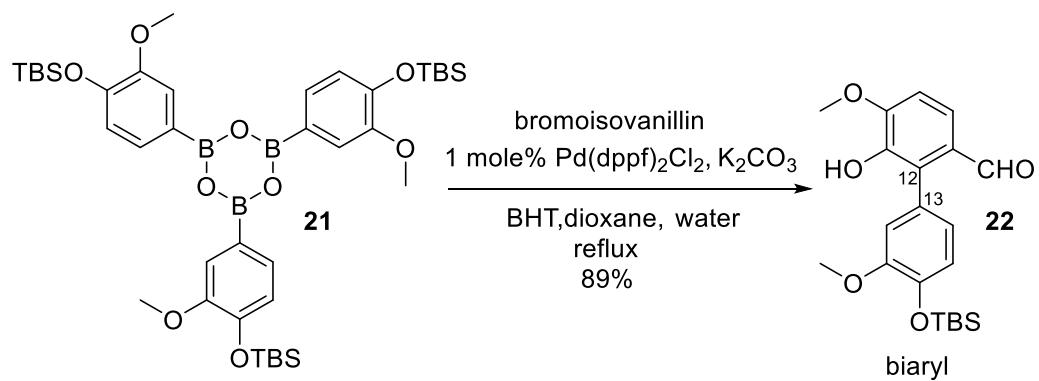
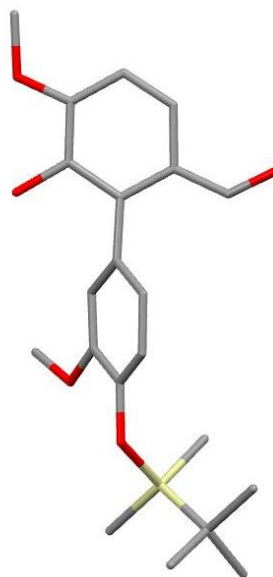


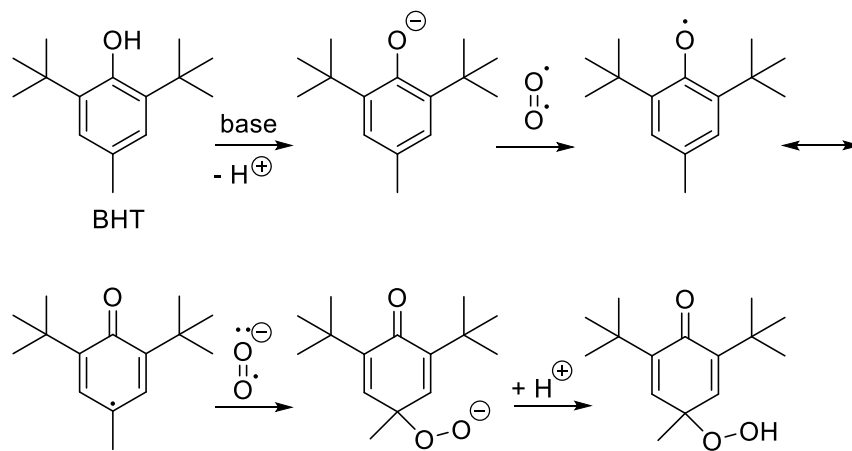
Figure 2.3. X-Ray of **22**.



De-oxygenation was accomplished by pre-heating the reaction mixture at approximately 60 °C for a few minutes while vigorously bubbling argon gas through the solution via a

needle. Additionally, butylated hydroxytoluene (BHT) was used as an oxygen scavenger as an additional measure, Scheme 2.7.

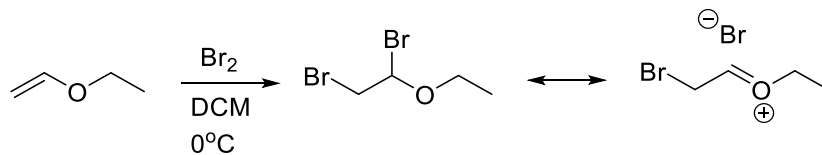
Scheme 2.7.



2.3 Dienone

Bromination of ethyl vinyl ether (EVE) in DCM at 0 °C generates the dibromide alkylating agent. The dibromide is preferentially reactive at the secondary carbon carrying the bromine due to activation by the ether oxygen, Scheme 2.8.

Scheme 2.8.



In the presence of Hunig's base (DIEA), the biaryl phenol **22** was alkylated resulting in the acetal-bromide intermediate **23**. This was then subjected to CsF conditions to form the quaternary center at C12, Scheme 2.9, Figures 2.4 and 2.5. The dienone intermediate **24** is a pair of diastereomers, each of which consists of a pair of enantiomers. The successful preparation of the dienone **24** required pre-treatment of a fresh bottle of DMF over 4Å molecular sieves for 72 hours. Furthermore, CsF is a highly hygroscopic salt and must be flame-dried under high vacuum for a few minutes and allowed to cool under high vacuum prior to use. If CsF is added to the solution of starting material in DMF and the mixture is heated to 135 °C, only de-silylated starting material is obtained. For this reason the reaction solution must be pre-heated to approximately 80 °C under Ar and rapidly and in one portion treated with CsF. Under the above conditions the reaction was completed in approximately 15 minutes with a yield of 84%. The use of KF was found to be inefficient since the mixture had to be heated for nearly 2 hours before all the starting material was consumed, and the yield was typically 10-20% lower. This is likely due to the poor solubility of KF in DMF.

Scheme 2.9.

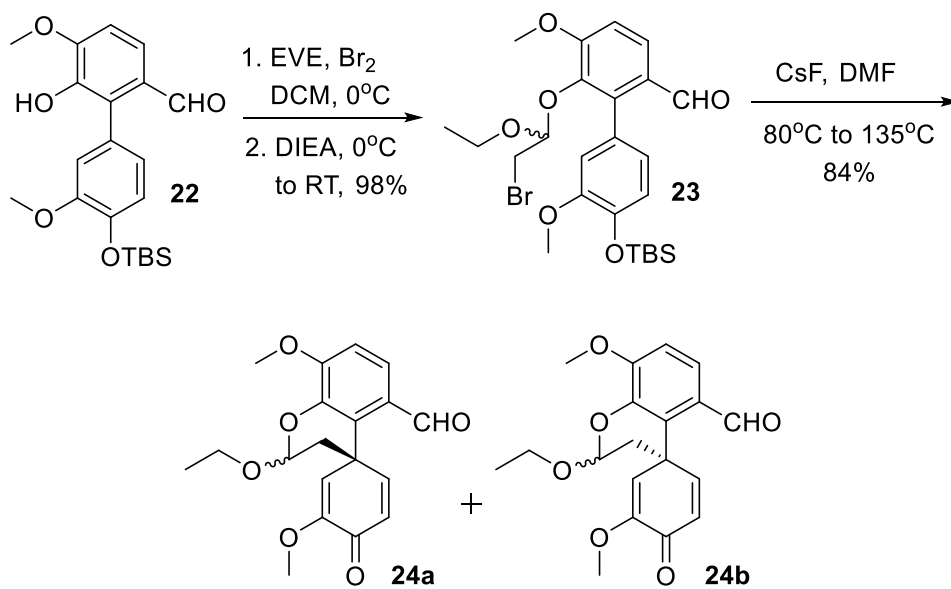


Figure 2.4. X-Ray of 24a.

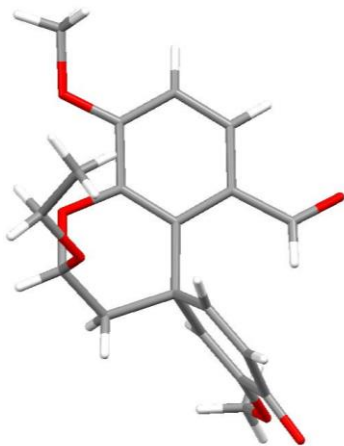
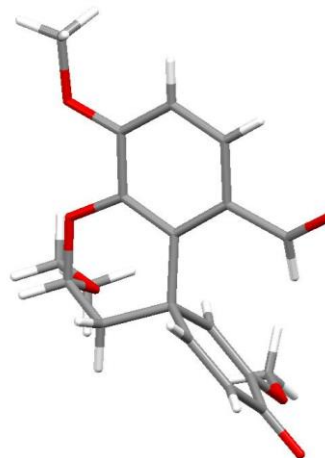


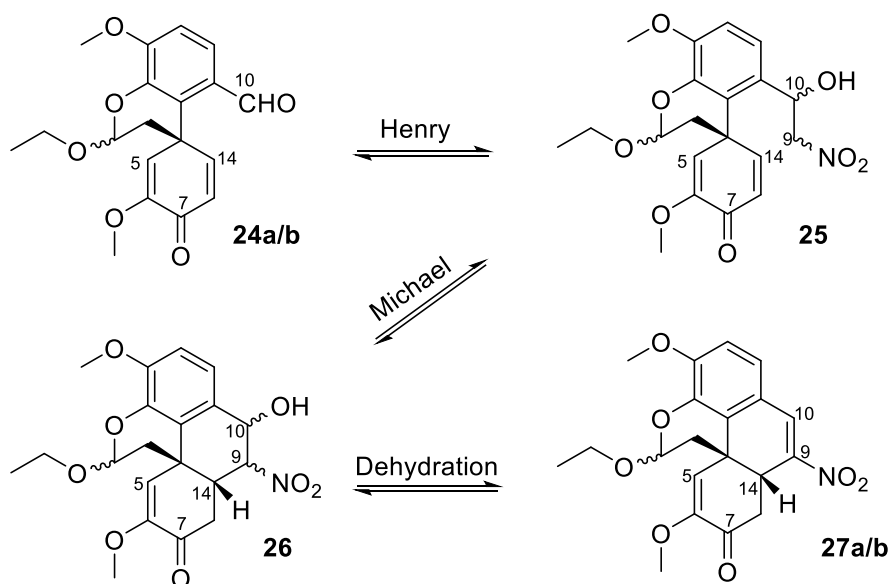
Figure 2.5. X-Ray of 24b.



2.4 Nitroalkene

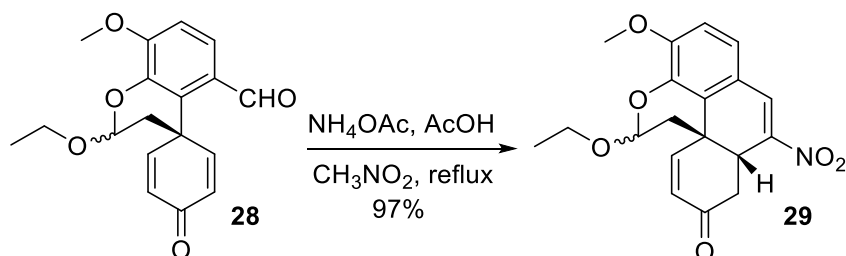
Preparation of the nitroalkene intermediate **27** posed the first and most significant challenge in the entire synthesis. The net transformation consists of three distinct steps: nitro-aldol (Henry)⁵⁴ reaction between nitromethane (providing C9) and the aldehyde C10 in the A-ring forming the first C-C bond; an intra-molecular conjugate addition (Michael) reaction between the newly introduced nitromethane C9, and the C-ring enone C14 forming the second C-C bond; and, a dehydration step to form the olefin moiety between C9 and C10, Scheme 2.10.

Scheme 2.10.



Initially, the combination of the $\text{NH}_4\text{OAc}/\text{AcOH}$ in CH_3NO_2 under refluxing conditions provided about 10% of the desired product. This was in stark contrast to the 97% yield reported by Magnus using the analogous substrate without the C-ring methoxy enol ether group, Scheme 2.11.⁵⁵

Scheme 2.11.



The presence of the methyl enol ether in the C-ring blocks the conjugate addition step (nucleophilic attack) at C5 by concentrating electron density at that carbon. Additionally, the carbonyl carbon (C7) is less electron deficient, and thereby less activating towards Michael addition. There is also the statistical advantage that the symmetrical dienone presents in that there are two equivalent β -carbon (two potential C5) Michael acceptors.

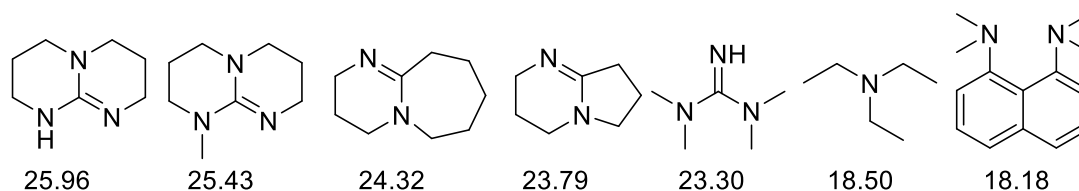
One of the most useful reagents for the Henry reaction is activated alumina, $\gamma\text{-Al}_2\text{O}_3$.⁵⁶ This reagent combines several features into one entity. It is a source of both Lewis acidic aluminum and nucleophilic, Lewis basic oxygen centers (ambiphilic).⁵⁷ Alumina is an effective dehydrating agent, and the combination of these properties could allow for reaction of nitromethane with the substrate across all three phases of the

transformation. Indeed, neutral and basic alumina provided a moderate yield of approximately 30% for the nitroalkene **27**. Further activation of alumina by flame drying under high vacuum (> 700 °C) for several minutes; use of a large excess of alumina; refluxing in nitromethane; and, sonication did not improve on the original yield. Other metal oxides, acidic alumina and the highly basic KF-Al₂O₃ gave little to no product.

The driving force for the reaction is probably the dehydration step. We pursued more effective dehydrating conditions by converting the hydroxyl group in the nitroalcohol intermediate into a “good” leaving group. Catalytic KOAc in Ac₂O is used in the synthesis of various nitrostyrenes. Ac₂O is a cheap and efficient water scavenger/desiccant used as solvent. A variety of conditions using these reagents did not improve on the 30% yield. Additionally, trimethyl- as well as triisopropyl orthoformate in AcOH were comparable to alumina. Orthoformates are also efficient dehydrating reagents used in condensation reactions under acid catalysis conditions.

At this point we focused our attention on organic superbases as applied to Henry and Knoevenagel condensation reactions.⁵⁸ A superbase is defined by Caubere as a base formed from the mixing of two or more bases resulting in a new basic species possessing inherently new properties.⁵⁹ Tetramethylguanidine (TMG) is the prototypical superbase which has found numerous applications in organic synthesis either in catalytic or stoichiometric quantities. The pK_a value in CH₃CN of some bases are listed below. They are in order from left to right TBD, MTBD, DBU, DBN, TMG, TEA and DMAN (proton sponge), Figure 2.6.⁶⁰

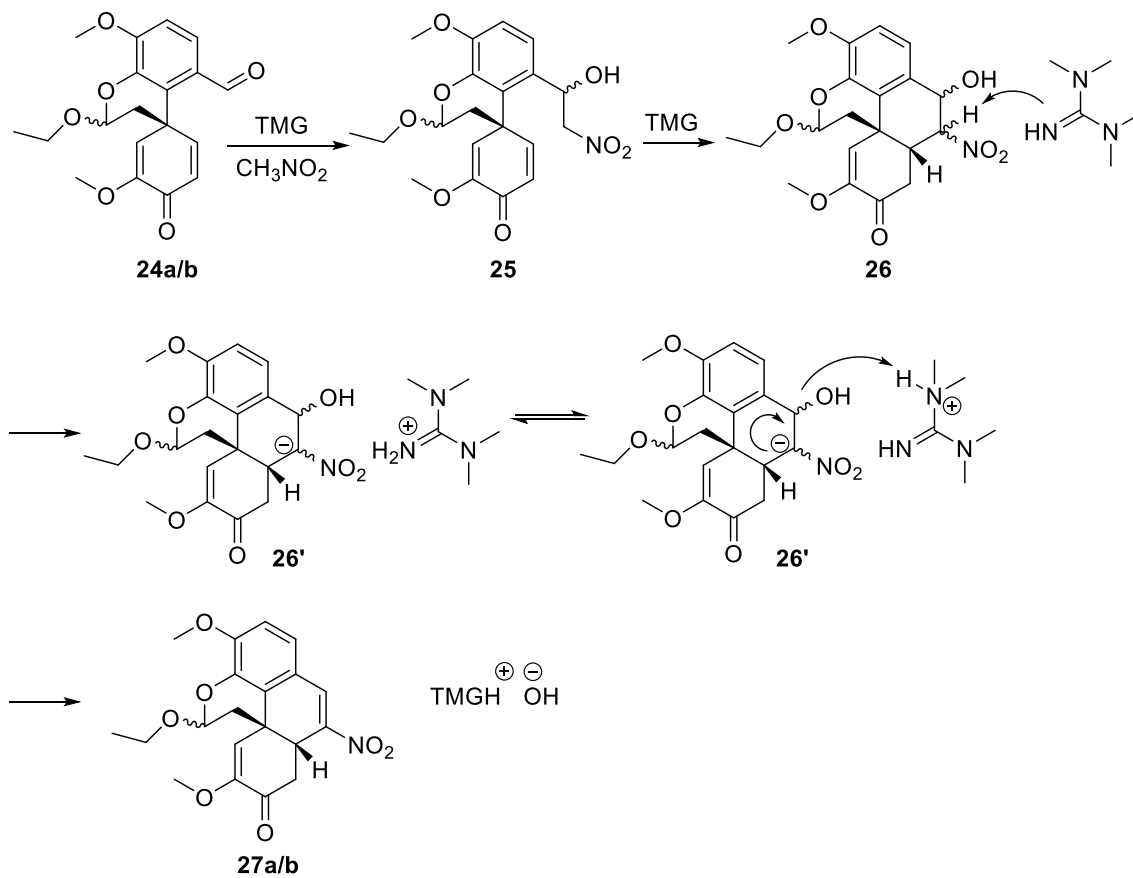
Figure 2.6.



Guanidine superbases owe their properties to the conjugated three-nitrogen guaidinyl system which allows for thermodynamic stability of both their acyclic structures and, upon protonation, the mono-protonated forms. This system exhibits resonance stabilization, γ -aromaticity, favorable Coulombic interactions due to effective distribution of positive charge in the protonated form, strong intra-molecular hydrogen bonding, and effective solvation of the protonated form.⁶¹

Using TMG in nitromethane led to an approximately 30% yield, Scheme 2.12. Although in principle, catalytic quantities of TMG should be adequate for the reaction to proceed, it was found that best results were obtained with 1.0-1.2 equivalents of the base. In fact, using either 2-4 equivalents or 0.5 equivalent resulted in lower yields (more baseline spots on TLC plate and a darker solution in the first case; and, an incomplete reaction in the second case). Heating at various temperatures, or longer reaction time also led to a drop in yield and darkening of the reaction solution. Strict purification of reagents and drying to prevent contamination with residual water did not improve the yield, although strictly anhydrous conditions were always necessary.

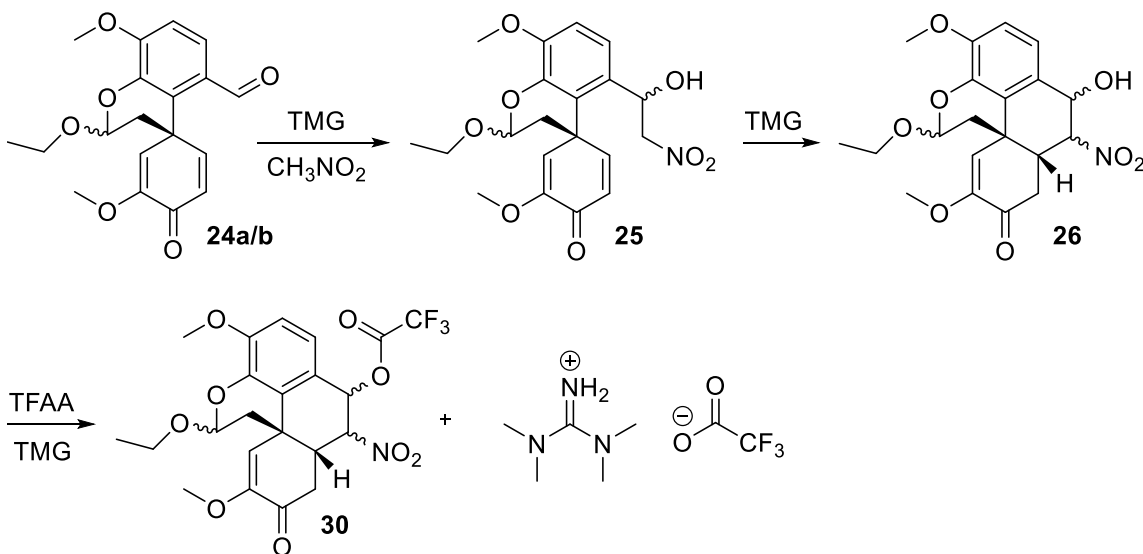
Scheme 2.12.



At this point we decided to use TFAA as a dehydrating agent which would convert the hydroxyl group in **26** into a trifluoroacetate, “good” leaving group **30**, Scheme 2.13. Addition of TFAA increased the yield to 40-50%. Once again, the yield did not improve with time or heating. The use of the Tf_2O led to a rapid darkening of the reaction medium at 0 °C and formation of polar/baseline spot on TLC, while Ac_2O

showed no advantage over TMG alone. A closer look at the reaction mechanism involving TFAA reveals that TMG is no longer catalytic in that it also acts as a stoichiometric base for esterification of the alcohol. Since a base is needed for the final elimination step, it appeared that formation of $(\text{TMG-H})^+ (\text{CF}_3\text{CO}_2)^-$ salt removed from the reaction any free TMG. Furthermore, $(\text{CF}_3\text{CO}_2)^-$ is not adequately basic to deprotonate the α -proton and induce elimination and regeneration of $(\text{CF}_3\text{CO}_2)^-$ in a new catalytic cycle.

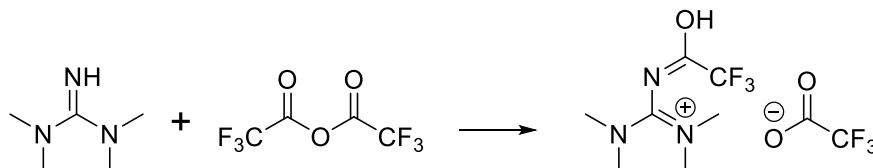
Scheme 2.13.



This necessitated using more base. Unfortunately, more TMG led to a decrease in yield due to greater formation of side products (baseline spots on TLC). There is the additional

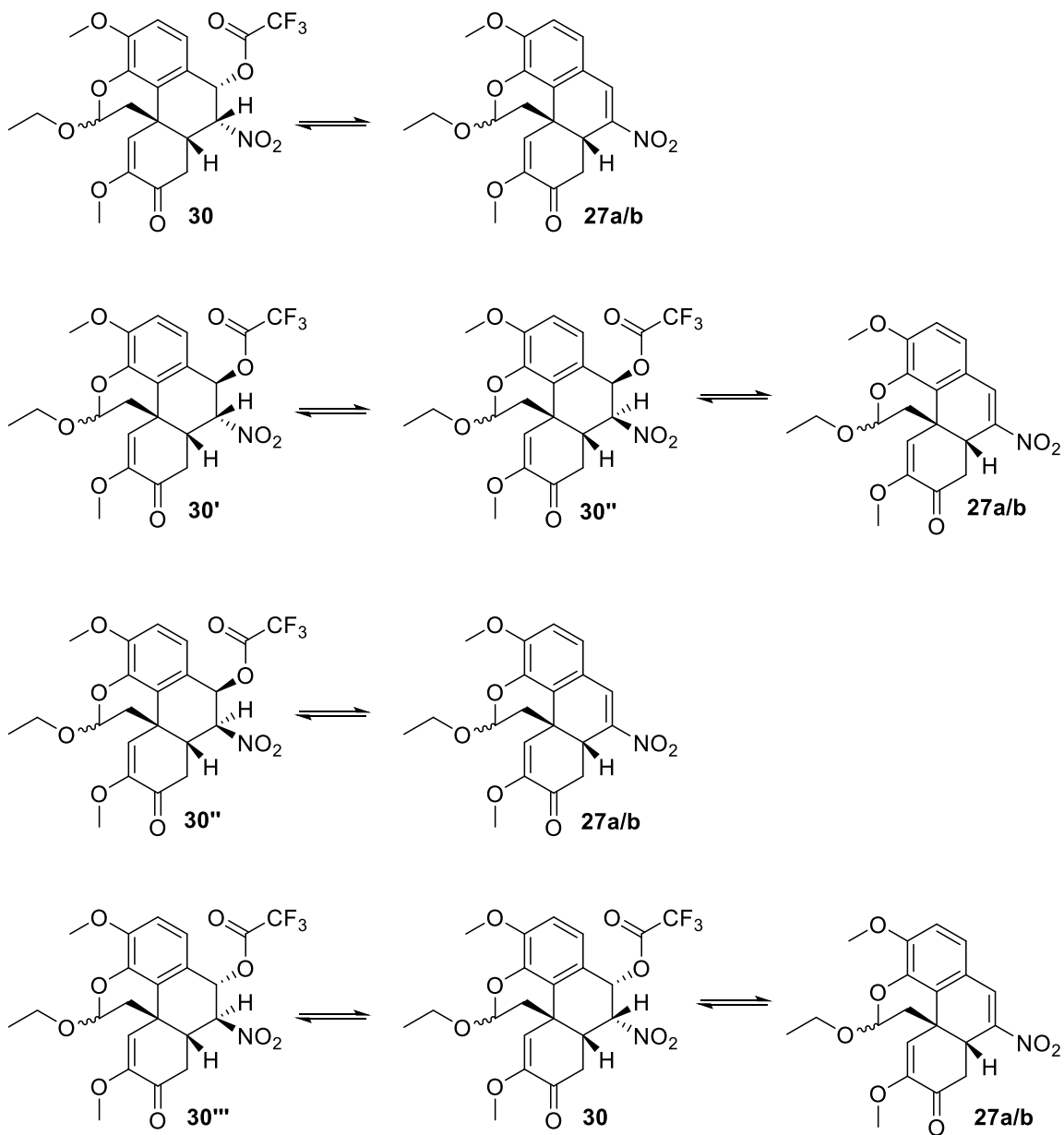
possibility of reaction between TMG and TFAA, albeit slowly, to form an “inactivated” TMG salt, Scheme 2.14.

Scheme 2.14.



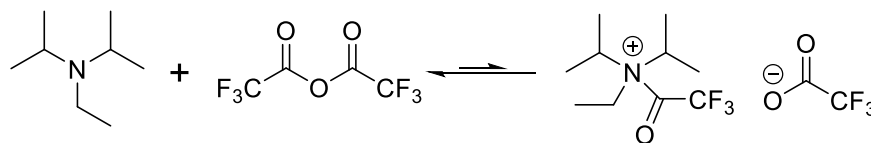
An important consideration in any elimination reaction is the requirement for *anti*-periplanar orientation of the leaving group and the α -proton. In our case, we suspected that all the intermediate isomers that have the correct *anti* relationship between the α -proton and the leaving group, be it the hydroxyl or the trifluoroacetate, eliminate readily, but those with the *syn* relationship require epimerization of the α -proton into the correct orientation which requires a base, Scheme 2.15.

Scheme 2.15.



Since both TMG and TFAA are necessary for the reaction to proceed and that excess TMG did not remedy the situation, we decided to incorporate DIEA as an “auxiliary” base. As a sterically hindered tertiary base, DIEA would not react with TFAA, or otherwise the equilibrium would be primarily in favor of the free base, Scheme 2.16.

Scheme 2.16.



DIEA is an effective base for epimerization (*syn/anti*) and elimination reactions. DIEA by itself did not lead to any appreciable amount of product, further emphasizing the vital role of the guanidine base. Presence of DIEA with TMG prior to addition of TFAA also failed to improve the yield over TMG alone. With the addition of DIEA as the auxiliary base after addition of TFAA the yield increased to 70%, Scheme 2.17, Figure 2.7. The reaction conditions tested are grouped according to their approximate yield, Table 2.1.

Scheme 2.17.

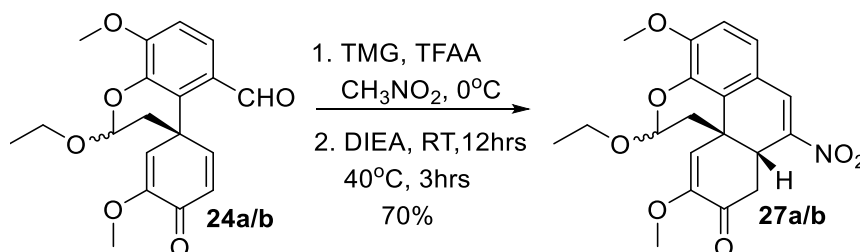
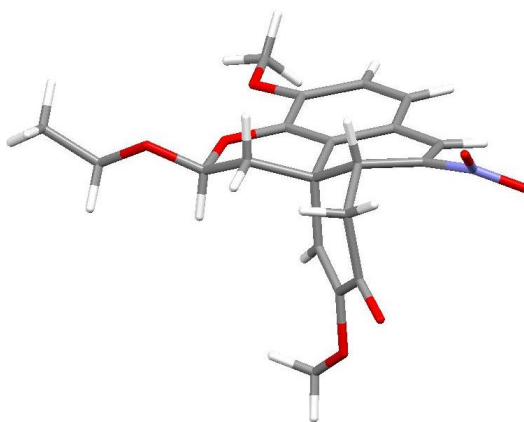


Table 2.1.

<u>0 - 5%</u>	<u>10 - 30%</u>	<u>40 - 50%</u>	<u>60 - 70%</u>
acidic Al ₂ O ₃	basic Al ₂ O ₃	TMG/TFAA	TMG/TFAA/DIEA
KF-Al ₂ O ₃	neutral Al ₂ O ₃	TBD/TFAA	
TiO ₂	NH ₄ OAc/AcOH		
V ₂ O ₅	KOAc/HC(OCH ₃) ₃ /MeOH/AcOH		
Nb ₂ O ₅	KOAc/HC(O ⁱ Pr) ₃ /AcOH		
CeO ₂	AcOH/KOAc/Sieves		
Ta ₂ O ₅	TMG		
BaO	Barton's base		
MgO			
sealed tube			
sonication			
Dean-Stark			
CsF			
Cs ₂ CO ₃			
Cs ₂ CO ₃ /TBAC/toluene			
NaOH/DCM/H ₂ O			
Cs ₂ CO ₃ /H ₂ O/EA			
DIEA			
TFAA			
DBU/Ac ₂ O/toluene			
TMG/DBU/Ac ₂ O			
TMG/AcOH			
TMG/Cs ₂ CO ₃ /Ac ₂ O			
KOAc/AcOH/PhthAnh			
TBAB			
ionic liquids			
Amberlyst-15			

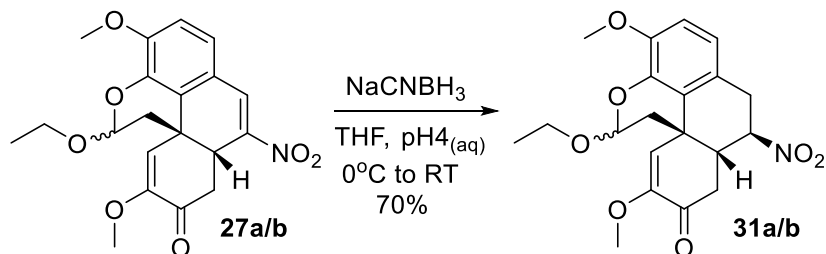
Figure 2.7. X-Ray of **27**.



2.5 Nitroalkane

The selective conjugate reduction of the nitroalkene **27** was accomplished with NaCNBH₃ in THF under buffered conditions at pH 4, Scheme 2.18.⁶²

Scheme 2.18.

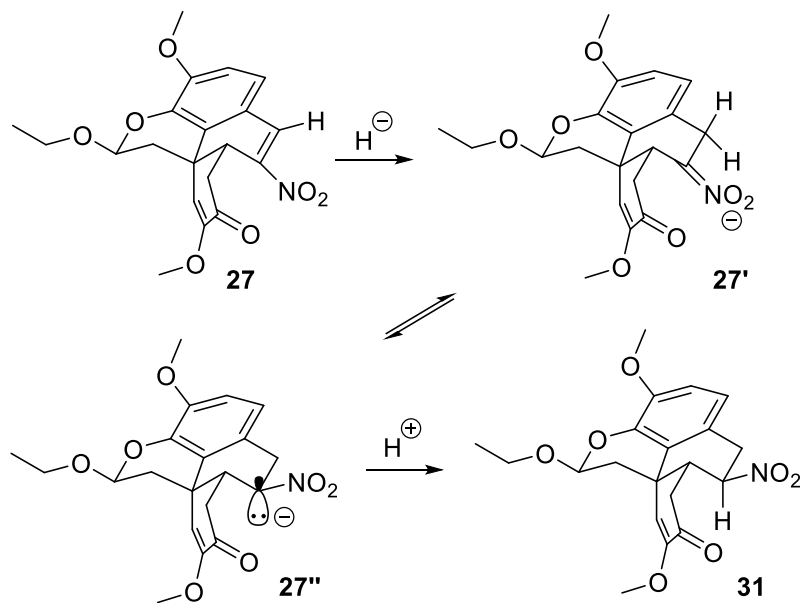


NaCNBH₃ is the ideal reagent for mild and selective conjugate reductions.⁶³ The milder and less toxic Na(OAc)₃BH failed to give any appreciable product even at elevated

temperatures. No reduction of the ketone group was observed under either conditions. Given the strong electron withdrawing ability of the nitro group relative to the carbonyl group, we did not anticipate any difficulty with selectivity. Furthermore, the enone system is electron-rich due to the electron-donating property of the methyl enol ether group and as in the case with nitroalkene **27** synthesis, the methyl enol ether concentrates electron density at the β -carbon, blocking approach by H^- from the reducing agent. Under these conditions a yield of 70% was obtained. The nitroalkene group is an excellent Michael acceptor and as such it is capable of hydrolysis to reform the nitroalcohol under aqueous conditions, and by TLC some nitroalcohol **26** was observed during the course of reaction. The extent of hydrolysis, however, was minimized by running the reaction at 0 °C. Using distilled AcOH as solvent in place of the pH 4 buffer led to significantly lower yields and greater nitroalcohol **26** formation.

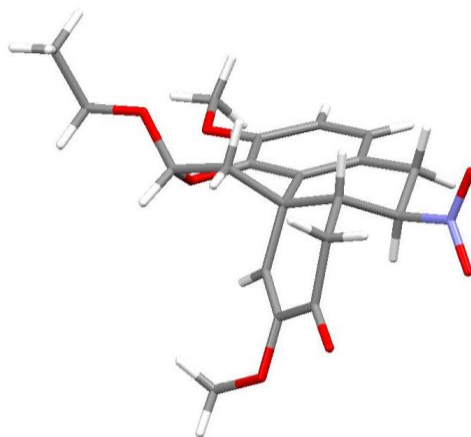
The conjugate reduction reaction is a thermodynamic process whereby the final product geometry places the nitro group in a pseudo-equatorial (more stable) conformation. Following hydride attack at the β -carbon, the nitronate intermediate **27'** is in equilibrium with the α -anion **27''** in which the lone pair occupies a pseudo-axial geometry. Protonation of the anion occurs from the axial position **31**.

Scheme 2.19.



Alternatively, any pseudo-axial nitro group can epimerize under the reaction conditions by α -deprotonation/re-protonation to achieve the thermodynamically favored orientation, Scheme 2.19, Figure 2.8. This result is crucial in that both the nitro group and the pendant aldehyde must be on the same face of the molecule for subsequent annulation.

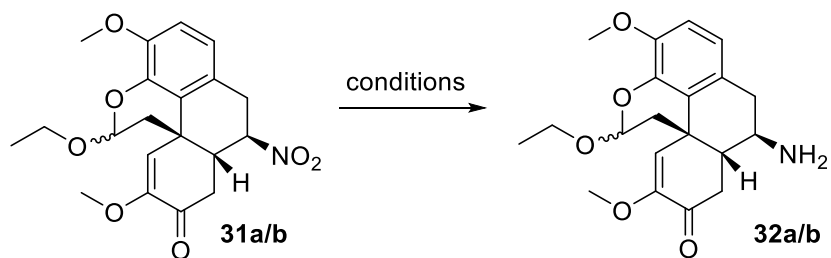
Figure 2.8. X-Ray of **31**.



2.6 Amine

Selective reduction of the nitro group of **31** in the presence of the α,β -unsaturated ketone presented the next major challenge in the synthesis, Scheme 2.20.

Scheme 2.20.

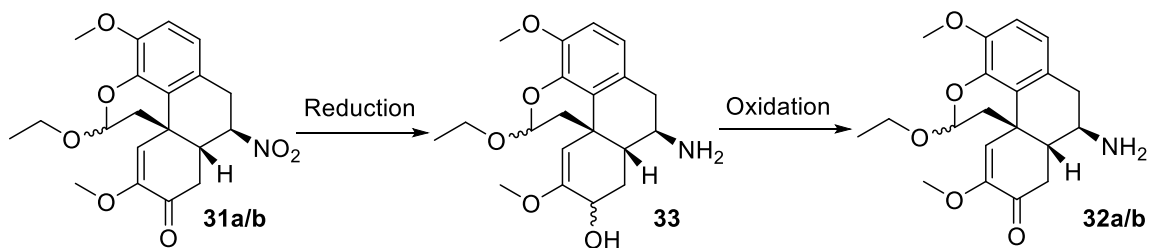


A large number of conditions were employed with no success. Aromatic nitro groups are more readily reduced than aliphatic ones and constitute the main bulk of the literature on

this topic. Typically, metals such as Fe⁶⁴, Zn⁶⁵, In⁶⁶, Mg, or SnCl₂ are used. Additives can be employed to further improve the reaction conditions with respect to selectivity and mildness. For example, FeCl₃⁶⁷ can be added in catalytic quantities to Fe suspension in AcOH. Other additives include formic acid, ammonium formate⁶⁸, and hydrazinium monoformate⁶⁹. All of the above conditions led to over-reduction or no reaction. In the case of In in AcOH some selectivity was discernable by TLC in that some amine could be spotted along with over-reduced products and starting material. Direct hydrogenation using a hydrogen balloon and 10% Pd/C, or PtO₂ (Adam's catalyst), or Pd/CaCO₃/PbCl₂ (Lindlar's catalyst) led to over-reduction.

At this point it was decided to employ a two-step approach by first reducing both the nitro and ketone groups in **31**, and then oxidizing the resultant allylic alcohol **33** to the α,β -unsaturated ketone **32**, Scheme 2.21.

Scheme 2.21.

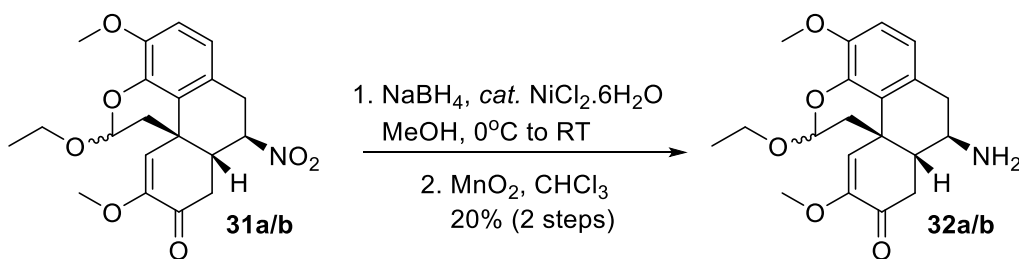


Metal hydride reduction with LAH gave an approximately 10% yield for the reduced nitro and ketone groups. This yield improved to about 20% with the use of Red-Al. Eventually, NaBH₄ with a catalytic amount of NiCl₂·6H₂O in MeOH (nickel boride)⁷⁰

gave the cleanest (TLC, LCMS) product mixture. The crude product was then subjected to oxidation conditions to recover the ketone moiety, Scheme 2.22.

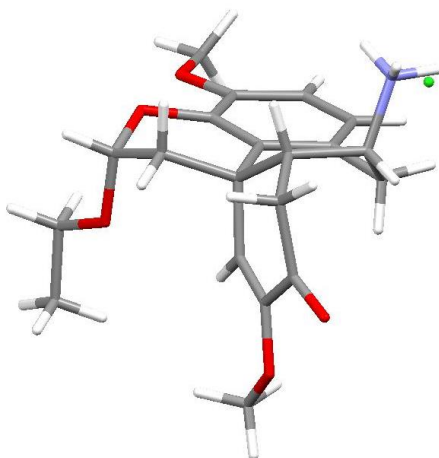
PCC, PDC, DMP and γ -MnO₂ were screened for oxidation efficiency, with active γ -MnO₂ powder in DCM providing the best results. The yields, however, were often inconsistent as is typical of γ -MnO₂ oxidation of allylic alcohols.

Scheme 2.22.



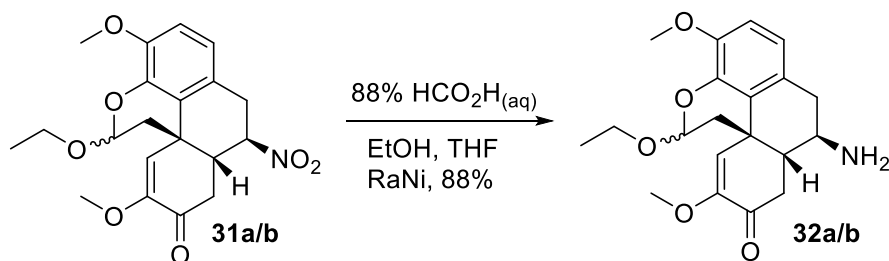
The x-ray of the amine confirmed the presence of the desired product **32**, and the β orientation of both the amine and the acetal groups, Figure 2.9. A striking feature of the structure is the near perfect boat conformation of the B-ring.

Figure 2.9. X-Ray of **32**.



Fortunately, conditions were found for selective, efficient and mild reduction of the aliphatic nitro group. Reaction of the starting material **31** under heterogeneous transfer-hydrogenation conditions with 10% Pd/C had afforded over-reduced products in earlier experiments. The same result was obtained using RaNi. Using HCO_2NH_4 with either of the catalysts returned the starting material. However, HCO_2H with RaNi^{71} in a solution of EtOH and THF provided a yield of 88% for amine **32**, Scheme 2.23.

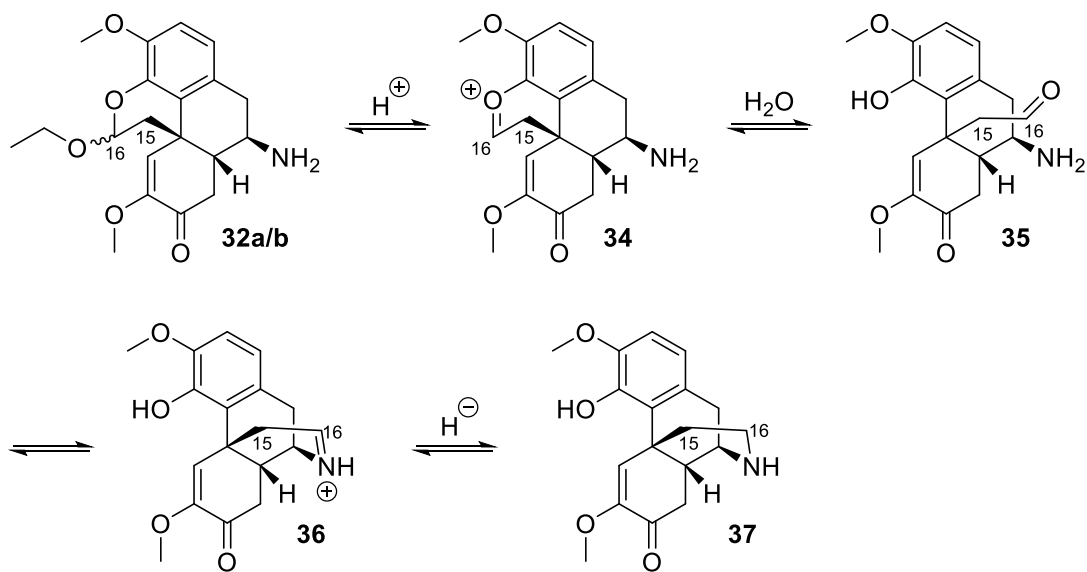
Scheme 2.23.



2.7 Core

Conversion of the amine **32** into the core structure **37** to form the D-ring was accomplished by an intra-molecular reductive amination between C16 and the nitrogen. The procedure involved the hydrolysis of the acetal to unmask the aldehyde, followed by formation of the iminium ion and its reduction with NaCNBH₃, Scheme 2.24.⁷²

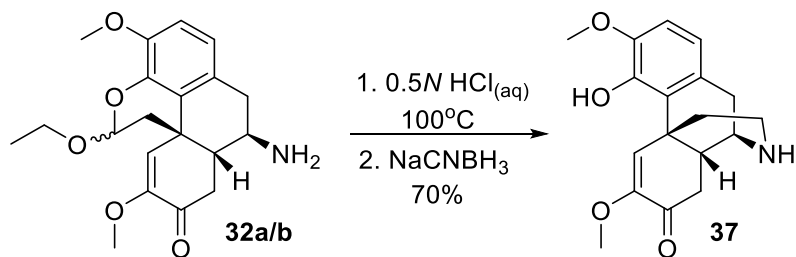
Scheme 2.24.



The hydrolysis step was accomplished with the use of 0.5 *N* aqueous HCl at 100 °C in approximately 10 minutes. Use of any co-solvent such as dioxane or ethanol significantly retarded the hydrolysis resulting in formation of unidentified side products. No hydrolysis of methyl enol ether occurred under these conditions, presumably due to the fact that it

would lead to formation of an unfavorable 1,2-diketone (carbonyls at C6 and C7). Following the reduction step a yield of 70% was obtained for core **37**, Scheme 2.25.

Scheme 2.25.



2.8 N-Methyl

Eschweiler-Clark is the method of choice for N-methylation.⁷³ We employed a modified version of that reaction in which aqueous formaldehyde, NaCNBH₃ and AcOH replaced formic acid as the hydride and proton source. The reaction was completed within a few minutes in 91% yield, Scheme 2.26. X-ray structure determination confirmed the correct relative stereochemistry of the chiral centers, and the presence of the racemic mixture of isosinomenine and 8,14-dihydrosalutaridine, Figure 2.10.

Scheme 2.26.

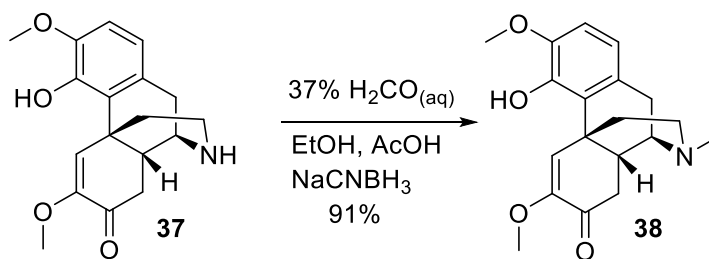
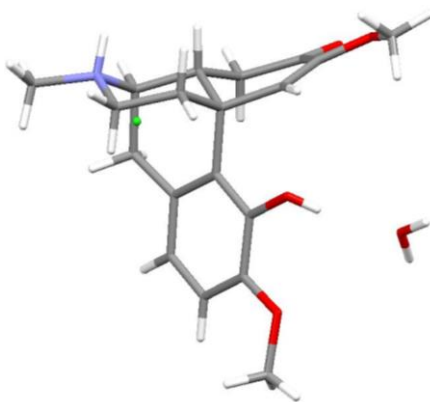


Figure 2.10. X-Ray of



In summary, our strategy represents the first efficient and collective synthesis of three 8,14-dihydromorphinandienone alkaloids, and the as yet undiscovered norisoinomenine. The total synthesis arrives directly at the correct oxidation level of the target compounds by avoiding the biomimetic strategy of *o,p*-phenolic oxidative coupling. A novel and unique route to a one-pot Henry-Michael-condensation cascade has been developed where a variety of other conditions failed. The fortuitously

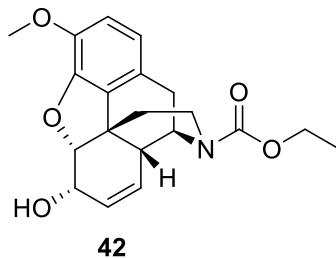
discovered aliphatic nitro reduction allowed for a direct and efficient route to the desired amine **32** avoiding a simultaneous nitro and enone reduction, and re-oxidation back to the enone. The current strategy is complementary to that reported by Magnus for the synthesis of codeine in that it begins with the C6 oxygen already in place (*vis-à-vis* guaiacol **18**) obviating the need for the introduction of the C6 oxygen later in the synthesis. Conversion of isosinomenine **1** and 8,14-dihydrosalutaridine **2** into sinoacutine **8** and salutaridine **7** respectively by oxidation of the C8-C14 into a double bond will allow for subsequent biomimetic transformation of the resultant dienone structures into thebaine and, therefore, codeine. This oxidation is exemplified by conversion of ocobotrine **4** into sinoacutine **8** via classical α -bromination-dehydrobromination mentioned earlier. The combination of these routes provide to date the most practical racemic synthesis of 8,14-dihydromorphinandienone alkaloids, and by extension, thebaine and codeine.

CHAPTER 3: EXPERIMENTAL SECTION

3.0 General Information

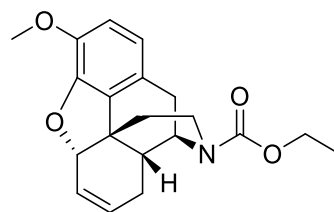
All reactions were setup under an atmosphere of argon and only degassed when specified. Melting points were taken on a Thomas-Hoover capillary tube apparatus and are uncorrected. Infrared spectra were recorded on a Nicolet FT-IR spectrophotometer neat unless otherwise indicated. ¹H NMR spectra were recorded on a Varian spectrometer at 300 MHz, or 500 MHz, or 600 MHz in the indicated solvent and are reported in ppm relative to tetramethylsilane (TMS) and referenced internally to the residually protonated solvent. ¹³C NMR spectra were recorded on a Varian spectrometer at 75 MHz or 125 MHz or 150 MHz in the solvent indicated and are reported in ppm relative to tetramethylsilane (TMS) and referenced internally to the residually protonated solvent. Mass spectra were obtained on a VG ZAB2E or a Finnigan TSQ70. Routine monitoring of reactions was performed using Merck 60 F₂₅₄ silica gel, aluminum-backed TLC plates. Flash column chromatography was performed using EMD silica gel (particle size 0.040-0.063 μm 22 x 250 mm). Solvents and commercial reagents were purified in accordance with Armarego, or used without further purification.

3.1 Experimental Data for Chapter 1



Ethyl chloroformate (5.8 mL, 60.4 mmol) was added to a mixture of codeine phosphate **37** (4 g, 10.07 mmol) and K_2CO_3 (8.4 g, 60.4 mmol) in $CHCl_3$ (300 mL), and the mixture was heated at reflux under Ar with stirring. The reaction was monitored by TLC. Upon completion (24 h), the mixture was cooled to 25 °C, diluted with $CHCl_3$ (100 mL), and washed with water (3 x 75 mL), followed by brine (50 mL), dried over Na_2SO_4 and concentrated *in vacuo*. The crude product was purified by chromatography (0-75% EtOAc/hexanes) to give **42** (3.5 g, 97%) as a white amorphous solid.

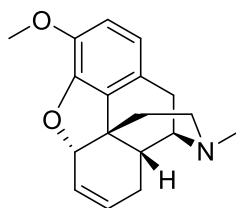
1H NMR (300 MHz, $CDCl_3$) δ 6.62 (1H, d, $J = 8.1$ Hz), 6.50 (1H, d, $J = 7.8$ Hz), 5.71 (1H, d, $J = 9.3$ Hz), 5.24 (1H, d, $J = 9.6$ Hz), 4.90 (0.6H, bs), 4.77 (0.4H, bs), 4.82 (1H, d, $J = 6$ Hz), 4.20 (4H, m), 3.74 (3H, s), 3.28 (1H, bs), 3.03-2.82 (1H, m), 2.78 (1H, d, $J = 6.3$ Hz), 2.67 (1H, d, $J = 18.6$ Hz), 2.48 (1H, m), 1.94-1.78 (2H, m), 1.22 (3H, m).
 ^{13}C NMR (75 MHz, $CDCl_3$) δ 155.6, 146.8, 142.6, 134.8, 130.2, 127.1, 126.1, 120.1, 113.5, 91.5, 66.4, 61.7, 56.4, 50.5, 43.6, 40.0, 37.4, 35.5, 29.6, 15.0.



16

Diethyl azodicarboxylate (0.61 mL, 3.9 mmol) was added to a solution of triphenylphosphine (1.1 g 4.2 mmol) in *N*-methylmorpholine (16 mL) under Ar at -30 °C. The mixture was stirred for 10 min, followed by addition of **42** (0.58 g, 1.62 mmol). The solution was stirred for 60 min at -30 °C and *o*-nitrobenzenesulfonyl hydrazine (0.85 g, 3.9 mmol) (NBSH) was added. The mixture was warmed to room temperature while stirring and monitored by TLC. Upon completion (2 h) the mixture was diluted with EtOAc (50 mL), washed with water (3 x 25 mL), brine (25 mL), dried over Na₂SO₄ and concentrated *in vacuo*. The crude product was purified by chromatography (0-10% EtOAc/hexanes) to give **16** (330 mg, 60%) as a clear oil.

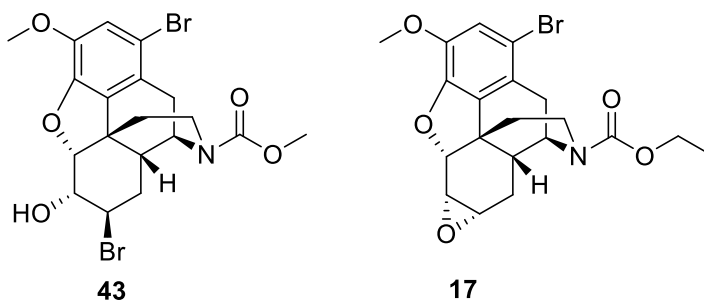
IR (thin film) 2978, 2931, 2838, 1695 cm⁻¹. ¹H NMR (300 MHz, CDCl₃) δ 6.69 (1H, d, *J* = 8.1 Hz), 6.58 (1H, d, *J* = 8.4 Hz), 5.81 (1H, m), 5.67 (1H, m), 4.91 (1H, bs), 4.67 (0.6H, bs), 4.54 (0.4H, bs), 4.18-3.88 (3H, m), 3.85 (3H, s), 3.04-2.80 (2H, m), 2.65 (1H, d, *J* = 18.9 Hz), 2.30-2.25 (1H, m), 2.02-1.91 (1H, m), 1.82-1.72 (2H, m), 1.53-1.37 (1H, m), 1.31-1.18 (3H, m). ¹³C NMR (75 MHz, CDCl₃) δ 155.4, 144.9, 143.5, 131.9, 128.6, 125.9, 124.7, 119.0, 113.3, 87.4, 61.4, 56.3, 50.2, 41.2, 37.9, 37.8, 35.1, 28.9, 24.1, 14.7.



16'

A solution of **16** (50 mg, 0.146 mmol) in THF (5 mL) was cooled to 0 °C under Ar. A solution of LAH (2M/THF, 0.4 mL) was added drop wise via a syringe to the above solution. Reaction progress was monitored by TLC. Upon completion the solution was quenched with ethyl acetate (0.5 mL). A solution of saturated aqueous Rochelle's salt (5 mL) was added and after stirring for 5 min, the solution was extracted with 5% MeOH/CHCl₃ (3 x 10 mL). Combined organic extracts were dried over Na₂SO₄, concentrated *in vacuo* and purified by prep-TLC to afford **16'** (12 mg, 25%).

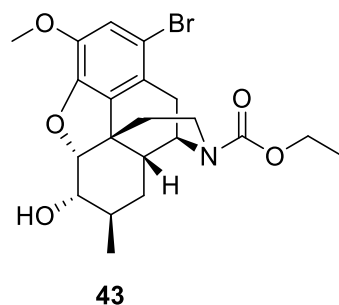
IR (thin film) 2916, 1505, 1440, 1276 cm⁻¹. ¹H NMR (300 MHz, CDCl₃) δ 6.72 (1H, d, *J* = 8.1 Hz), 6.64 (1H, d, *J* = 8.1 Hz), 5.87 (1H, m), 5.72 (1H, m), 4.99 (1H, bs), 3.87 (3H, s), 3.18 (1H, dd, *J*'s = 7.7, 2.7 Hz), 3.04 (1H, d, *J* = 18.6 Hz), 2.62 (1H, dd, *J*'s = 12.2, 3.6 Hz), 2.55-2.48 (2H, m), 2.47 (3H, s), 2.33 (1H, td, *J*'s = 24.3, 3.6 Hz), 2.04-1.91 (2H, m), 1.87-1.80 (1H, m), 1.61-1.49 (1H, m). ¹³C NMR (75 MHz, CDCl₃) δ 145.0, 143.6, 132.3, 129.7, 127.0, 124.9, 118.8, 113.3, 87.8, 59.6, 56.6, 47.2, 43.3, 40.9, 38.9, 35.5, 24.6, 20.3. HRMS C₁₈H₂₁NO₂ calculated for (M+H)⁺ 284.1651, found 284.1645.



To a stirred solution of **16** (330 mg, 0.97 mmol) in dioxane (20 mL) and water (20 mL) at -10 °C was added 1,3-dibromo-5,5-dimethylhydantoin (555 mg, 1.94 mmol) in the dark. The mixture was stirred and warmed to room temperature over 12 h to give compound **43**. The solution of **43** was directly treated with KOH (220 mg, 3.9 mmol) and heated at 75 °C. The reaction was monitored by TLC. Upon completion (24 h) the reaction was diluted with EtOAc (50 mL), washed with water (3 x 25 mL), brine (25 mL), dried over Na₂SO₄ and concentrated *in vacuo*. The crude product was purified by chromatography (0-30% EtOAc/hexanes) to give **17** (360 mg, 50%) as an off-white amorphous solid.

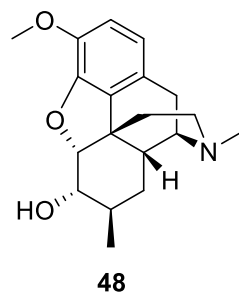
Compound **43**. IR (thin film) 3420, 2978, 2937, 2889, 1684 cm⁻¹. ¹H NMR (300 MHz, CDCl₃) δ 6.95 (1H, s), 4.90 (1H, d, *J* = 5.1 Hz), 4.74 (0.6H, bs), 4.59 (0.4H, bs), 4.28-4.10 (4H, m), 4.10-3.94 (1H, m), 3.87 (3H, s), 2.84-2.48 (5H, m), 1.92-1.62 (4H, m), 1.35-1.25 (3H, m). ¹³C NMR (75 MHz, CDCl₃) δ 155.6, 146.0, 143.1, 130.6, 125.3, 116.9, 113.2, 88.2, 70.4, 62.0, 56.7, 50.6, 50.3, 42.5, 38.0, 36.9, 36.1, 30.4, 26.7, 14.9. HRMS calculated for C₂₀H₂₃Br₂NO₅ (M+H)⁺ 516.0021, found 516.0018.

Compound **17**. IR (thin film) 2963, 2926, 2850, 1695, 1684 cm^{-1} . ^1H NMR (300 MHz, CDCl_3) δ 6.92 (1H, s), 4.89 (1H, dd, $J = 6.9$ Hz), 4.70 (0.7H, bs), 4.57 (0.3H, bs), 4.19-4.09 (3H, m), 3.87 (1H, bs), 3.86 (3H, s), 3.30-3.23 (2H, m), 2.83-2.70 (2H, m), 2.57 (1H, dd, J 's = 19.1, 12.2 Hz), 2.20-1.95 (2H, m), 1.85-1.62 (2H, m), 1.35-1.20 (3H, m), 1.15-1.06 (1H, m). ^{13}C NMR (75 MHz, CDCl_3) δ 155.2, 146.1, 143.0, 129.3, 124.3, 116.8, 112.1, 87.7, 61.6, 56.5, 53.6, 50.9, 50.2, 49.9, 41.2, 37.4, 37.2, 30.1, 23.0, 14.7. HRMS calculated for $\text{C}_{20}\text{H}_{22}\text{BrNO}_5$ ($\text{M}+\text{H}$) $^+$ 436.0760, found 436.0758.



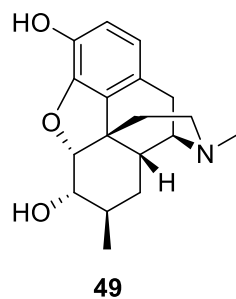
To a solution of **17** (160 mg, 0.37 mmol) in DCM (4 mL) and water (0.1 mL) was slowly added TMA (2M/hexane, 3.7 mL). Once the gas evolution subsided, the reaction was monitored by TLC. Upon completion the reaction was cooled to 0 °C and slowly quenched with water (5 mL), followed by a saturated aqueous solution of Rochelle's salt (5 mL). The reaction was extracted with EtOAc (3 x 10 mL), dried over Na₂SO₄ and concentrated *in vacuo*. The crude product was purified by chromatography (0-10% EtOAc/DCM) to give **43** (128 mg, 82%) as an off-white, amorphous solid.

IR (thin film) 3439, 2934, 1700, 1684, 1489, 1433 cm⁻¹. ¹H NMR (300 MHz, CDCl₃) δ 6.95 (1H, s), 4.71 (1H, d, *J* = 4.5 Hz), 4.66 (0.5H, bs), 4.56 (0.5H, bs), 4.21-4.10 (3H, m), 4.08-3.90 (2H, m), 3.86 (3H, s), 3.52-3.49 (1H, m), 2.90-2.70 (2H, m), 2.58 (1H, d, *J* = 18.6 Hz), 2.20-2.10 (2H, m), 1.88-1.68 (2H, m), 1.50-1.10 (4H, m), 0.91 (3H, d, *J* = 5.4 Hz). ¹³C NMR (75 MHz, CDCl₃) δ 155.5, 146.2, 143.1, 131.4, 126.0, 116.8, 112.9, 91.3, 72.4, 61.8, 56.7, 50.3, 43.7, 37.4, 37.3, 35.3, 30.6, 28.8, 26.6, 18.3, 14.6. HRMS calculated for C₂₁H₂₆BrNO₅ (M)⁺, 451.0994, found 451.0992.



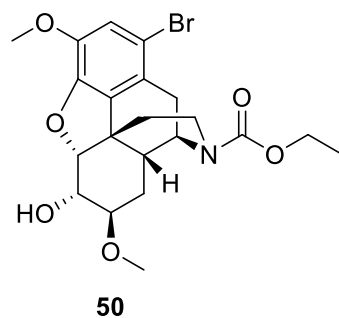
To a stirred solution of **43** (100 mg, 0.22 mmol) in THF (5 mL) under Ar at 0 °C was slowly added LAH (2M/THF, 1 mL). The reaction was monitored by TLC. Upon completion as judged by TLC the reaction was slowly quenched with MeOH (2 mL) and a saturated aqueous solution of Rochelle's salt (2 mL). The mixture was extracted with 5% MeOH/CHCl₃ (3 x 10 mL), dried over Na₂SO₄ and concentrated *in vacuo*. The crude product was purified by chromatography (0-5% MeOH/DCM) to give **48** (44 mg, 63%) as an off-white, amorphous solid.

M.p 136-138 °C. IR (thin film) 3600, 3442, 2932, 1653, 1601, 1499, 1452 cm⁻¹. ¹H NMR (300 MHz, CDCl₃) δ 6.69 (1H, d, *J* = 8.1 Hz), 6.58 (1H, d, *J* = 8.4 Hz), 4.66 (1H, d, *J* = 4.8 Hz), 3.82 (3H, s), 3.45 (1H, dd, *J*'s = 9.5, 4.7 Hz), 3.03 (1H, dd, *J*'s = 5.9, 2.8 Hz), 2.94 (1H, d, *J* = 18.6 Hz), 2.50-2.18 (5H, m), 2.35 (3H, s), 1.90 (1H, td, *J*'s = 24.9, 5.1 Hz), 1.68 (1H, dd, *J* = 12.6, 1.8 Hz), 1.26-1.11 (3H, m), 0.84 (3H, d, *J* = 6 Hz). ¹³C NMR (75 MHz, CDCl₃) δ 146.5, 141.9, 131.0, 127.7, 119.4, 113.7, 91.5, 72.9, 59.9, 56.7, 46.5, 43.3, 42.9, 37.6, 36.1, 29.8, 29.5, 20.1, 18.7. HRMS calculated for C₁₉H₂₅NO₃ (M+H)⁺ 316.1913, found 316.1912.



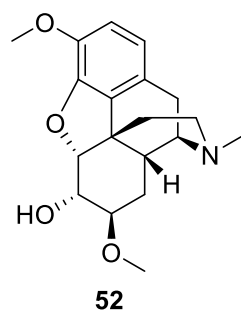
To a solution of **48** (27 mg as HCl salt, 0.077 mmol) in DCM (2 mL) at 0 °C under Ar was slowly added a solution of BBr₃ (1M/DCM, 0.4 mL) with stirring. The reaction was monitored by TLC allowing it to gradually warm to room temperature. The reaction was stirred at room temperature for 2 h and quenched with MeOH (0.5 mL), and a solution of saturated aqueous NaHCO₃ (2 mL). The mixture was extracted with DCM (4 x 20 mL), dried over Na₂SO₄ and concentrated *in vacuo*. The crude product was purified by prep-TLC to give **49** (10 mg, 43%).

IR (thin film) 3376, 2930, 1610, 1456 cm⁻¹. ¹H NMR (300 MHz, CD₃OD) δ 6.71 (1H, d, *J* = 8.1 Hz), 6.62 (1H, d, *J* = 8.1 Hz), 4.89 (2H, bs), 4.69 (1H, d, *J* = 4.5 Hz), 3.54-3.48 (2H, m), 3.11 (1H, d, *J* = 19.2 Hz), 2.93 (1H, dd, *J*'s = 12.9, 4.2 Hz), 2.79 (1H, dd, *J*'s = 19.4, 6.8 Hz), 2.72 (3H, s), 2.48 (1H, td, *J*'s = 18, 2.7 Hz), 2.11 (1H, td, *J*'s = 26.4, 5.1 Hz), 1.83 (1H, dd, *J*'s = 13.5, 2.4 Hz), 1.36-1.17 (4H, m), 0.90 (3H, d, *J* = 13.5 Hz). ¹³C NMR (75 MHz, CDCl₃) δ 147.2, 140.0, 130.6, 125.3, 120.6, 119.0, 92.0, 73.5, 62.1, 47.6, 43.4, 42.2, 36.5, 35.3, 30.8, 29.5, 22.0, 18.9. HRMS calculated for C₁₈H₂₃NO₃ (M+H)⁺ 302.1751, found 302.1753.



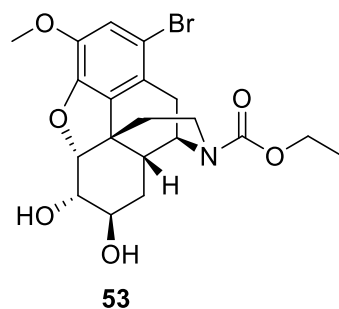
To a stirred solution of **17** (100 mg, 0.23 mmol) in MeOH (5 mL) was added *p*-toluenesulfonic acid (20 mg, 0.11 mmol) and the solution was heated at gentle reflux until all starting material was consumed as judged by TLC. Upon completion the reaction solution was concentrated *in vacuo* and purified by prep-TLC to yield **50** (88 mg, 68%).

IR (thin film) 3442, 2929, 1696, 1683, 1436 cm^{-1} . ^1H NMR (300 MHz, CDCl_3) δ 6.95 (1H, s), 4.75 (0.5H, bs), 4.56 (0.5H, bs), 4.70 (1H, d, $J = 5.7$ Hz), 4.24-4.03 (4H, m), 3.86 (3H, s), 4.51-3.37 (1H, m), 3.33 (3H, d, $J = 7.2$ Hz), 2.83-2.57 (3H, m), 2.40-2.25 (2H, m), 1.87-1.60 (3H, m), 1.35-1.17 (4H, m). ^{13}C NMR (75 MHz, CDCl_3) δ 155.7, 146.1, 143.0, 131.2, 125.4, 116.7, 112.9, 89.7, 68.2, 61.8, 60.6, 56.9, 56.7, 51.0, 42.3, 38.0, 36.2, 34.6, 30.3, 23.0, 15.0. HRMS calculated for $\text{C}_{21}\text{H}_{26}\text{BrNO}_6$ ($\text{M}+\text{Na}$) $^+$ 490.0841, found 490.0837.



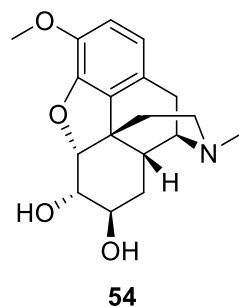
A solution of **50** (228 mg, 0.48 mmol) in THF (2 mL) at 0 °C was treated with a solution of LAH (2M/THF, 2 mL). The reaction was allowed to warm to room temperature and monitored by TLC. Upon completion the reaction was quenched with ethyl acetate (1 mL), saturated aqueous solution of Rochelle's salt (5 mL) and extracted with 5% MeOH/CHCl₃ (3 x 5 mL). The combined organic extracts were dried over Na₂SO₄ and concentrated *in vacuo*. The crude sample was purified by prep-TLC to afford **52** (80 mg, 73%).

IR (thin film) 3368, 2928, 1504, 1448, 1276 cm⁻¹. ¹H NMR (300 MHz, CDCl₃) δ 6.71 (1H, d, *J* = 8.4 Hz), 6.62 (1H, d, *J* = 8.4 Hz), 4.85 (1H, m), 4.71 (1H, d, *J* = 5.4 Hz), 3.98 (1H, t, *J* = 5.7 Hz), 3.85 (3H, s), 3.28 (3H, s), 3.27-2.22 (1H, m), 3.14 (1H, m), 3.02 (1H, d, *J* = 18.6 Hz), 2.64-2.51 (2H, m), 2.48-2.38 (1H, m), 2.47 (3H, s), 2.28 (1H, td, *J*'s = 24.6, 3.6 Hz), 1.97 (1H, td, *J*'s = 24.9, 4.8 Hz), 1.72-1.57 (2H, m), 1.38-1.29 (1H, m). ¹³C NMR (75 MHz, CDCl₃) δ 146.3, 142.1, 130.3, 126.4, 119.4, 113.7, 89.7, 69.2, 59.9, 56.7, 56.6, 47.1, 43.0, 41.7, 36.5, 35.4, 28.5, 24.3, 20.5. HRMS calculated for C₁₉H₂₅NO₄ (M+H)⁺ 332.1862, found 332.1829.



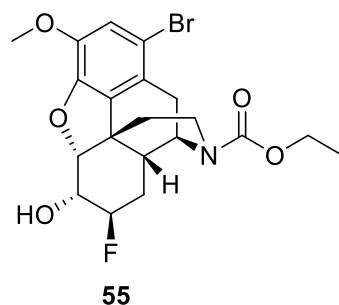
To a stirred solution of **17** (100 mg, 0.23 mmol) in water (2 mL) and THF (2 mL) was added methanesulfonic acid (3 drops) and the solution was heated at gentle reflux until all starting material was consumed as judged by TLC. Upon completion the solution was concentrated *in vacuo* and extracted with EtOAc (3 x 30 mL). The solution was dried over Na₂SO₄ and concentrated *in vacuo*. Purification of the crude product by prep-TLC gave **53** (100 mg, 99%).

IR (thin film) 3436, 2934, 1676, 1487, 1435 cm⁻¹. ¹H NMR (300 MHz, CDCl₃) δ 6.97 (1H, s), 4.80 (1H, d, *J* = 4.8 Hz), 4.78 (0.6H, bs), 4.63 (0.4H, bs), 4.24-4.10 (2H, m), 4.10-3.92 (1H, m), 3.88 (3H, s), 3.78-3.71 (1H, m), 3.46 (1H, dd, *J*'s = 14.7, 7.4 Hz), 2.94-2.70 (2H, m), 2.62 (1H, d, *J* = 19.2 Hz), 2.41 (1H, m), 2.24 (2H, bs), 1.90-1.70 (2H, m), 1.64 (1H, dd, *J*'s = 13.8, 6.9 Hz), 1.48-1.35 (1H, m), 1.23 (3H, m). ¹³C NMR (75 MHz, CDCl₃) δ 155.3, 145.4, 143.0, 130.7, 125.7, 116.8, 113.1, 90.3, 71.5, 66.9, 61.7, 56.5, 50.4, 43.4, 37.2, 36.4, 34.6, 30.1, 28.4, 14.6. HRMS calculated for C₂₀H₂₄BrNO₆ (M+H)⁺ 454.0860, found 454.0867.



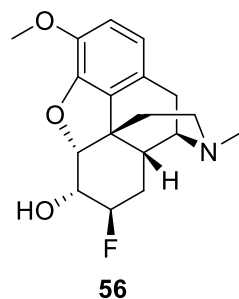
To a solution of **53** (100 mg, 0.22 mmol) in THF (10 mL) at room temperature under Ar was added a solution of LAH (2M/THF, 1.1 mL). The reaction was stirred and monitored by TLC. Upon completion it was slowly quenched with a saturated aqueous solution of Rochelle's salt (5 mL), and extracted with 5% MeOH/CHCl₃ (4 x 5 mL). Purification by prep-TLC gave **54** (50 mg, 70%).

IR: 3383, 2928, 1505, 1451, 1277, 1073 cm⁻¹. ¹H NMR (300 MHz, CDCl₃) δ 6.74 (1H, d, *J* = 8.1 Hz), 6.65 (1H, d, *J* = 8.4 Hz), 4.79 (1H, d, *J* = 5.1 Hz), 3.85 (3H, s), 3.77 (1H, dd, *J*'s = 8.6, 5.3 Hz), 3.54-3.32 (4H, m), 3.23-3.16 (1H, m), 3.01 (1H, d, *J* = 19.2 Hz), 2.71-2.48 (2H, m), 2.44 (3H, s), 2.30 (1H, td, *J*'s = 24, 3.7 Hz), 2.01 (1H, td, *J*'s = 25.1, 4.9 Hz), 1.72 (1H, d, *J* = 12.6 Hz), 1.55 (1H, *J*'s = 14, 7 Hz), 1.48-1.37 (1H, m). ¹³C NMR (75 MHz, CDCl₃) δ 146.1, 142.1, 130.3, 126.9, 119.7, 113.9, 90.5, 71.8, 67.1, 59.9, 56.7, 46.7, 43.0, 42.5, 36.7, 35.6, 29.2, 20.3. HRMS calculated for C₁₈H₂₃NO₄ (M+H)⁺ 318.1705, found 318.1702.



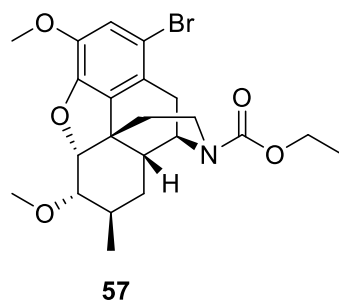
To a solution of **17** (100 mg, 0.22 mmol) in DCM (5 mL), was added HF.pyridine (2 mL) and the mixture stirred at room temperature under Ar. More reagent was added if reaction was found to progress too slowly. Upon completion as judged by TLC the reaction was diluted with water (10 mL) and extracted with DCM (3 x 10 mL). The mixture was dried over Na₂SO₄ and concentrated *in vacuo*. The crude product was purified by prep-TLC to give **55** (70 mg, 65%).

IR (thin film) 3447, 2952, 1684, 1488 cm⁻¹. ¹H NMR (300 MHz, CDCl₃) δ 6.96 (1H, s), 4.75 (2H, d, *J* = 5.1 Hz), 4.59 (1H, bs), 4.24-4.10 (3H, m), 4.09-3.90 (1H, m), 3.87 (3H, s), 2.85-2.60 (3H, m), 2.51-2.38 (2H, m), 1.91-1.65 (3H, m), 1.50-1.35 (1H, m), 1.34-1.20 (3H, m). ¹³C NMR (75 MHz, CDCl₃) δ 155.6, 145.9, 143.1, 130.6, 125.3, 116.9, 113.2, 90.9, 89.2, 88.6, 67.7, 67.3, 61.9, 56.7, 50.5, 42.6, 37.9, 34.3, 30.1, 15.3. HRMS calculated for C₂₀H₂₃BrFNO₅ (M+H)⁺ 458.0978, found 458.0799.



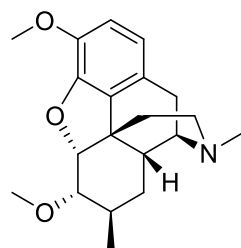
To a solution of **55** (60 mg, 0.13 mmol) in THF (2 mL) at room temperature under Ar was added a solution of LAH (2M/THF, 0.3 mL). The reaction was stirred and monitored by TLC. Upon completion, it was slowly quenched with a saturated aqueous solution of Rochelle's salt (2 mL), and extracted with DCM (4 x 5 mL). Purification by prep-TLC gave **56** (19 mg, 45%).

IR (thin film) 3367, 2917, 1505, 1450, 1277, 1046 cm^{-1} . ^1H NMR (300 MHz, CDCl_3) δ 6.77 (1H, d, $J = 8.4$ Hz), 6.68 (1H, d, $J = 8.1$ Hz), 4.80 (1H, dd, J 's = 5.4, 3 Hz), 4.55 (0.5H, m), 4.39 (0.5H, m), 3.88 (3H, s), 3.35-3.15 (1H, bs), 3.27 (1H, m), 3.08 (1H, d, $J = 18.9$ Hz), 2.80-2.70 (2H, m), 2.62 (1H, dd, J 's = 31.7, 5 Hz), 2.52 (3H, s), 2.37 (1H, td, J 's = 24.6, 3.6 Hz), 2.13-1.99 (1H, m), 1.89-1.67 (3H, m), 1.58-1.39 (1H, m). ^{13}C NMR (75 MHz, CDCl_3) δ 146.0, 142.4, 129.5, 125.9, 120.0, 114.1, 90.8, 89.2, 88.6, 68.8, 68.4, 59.7, 56.6, 47.0, 42.8, 41.8, 36.0, 20.5. HRMS calculated for $\text{C}_{18}\text{H}_{22}\text{FNO}_3$ ($\text{M}+\text{H}$) $^+$ 320.1662, found 320.1659.



To a stirred solution of **43** (60 mg, 0.14 mmol) in THF (5 mL) was added imidazole (10 mg, 0.14 mmol), and KH (56 mg, 1.4 mmol). After 5 min of stirring, CH₃I (70 μL, 1.4 mmol) was added and the reaction stirred at room temperature to completion as judged by TLC. The reaction was quenched with MeOH (1 mL) and water (10 mL). The mixture was extracted with EtOAc (3 x 10 mL), dried over Na₂SO₄ and concentrated *in vacuo*. Purification by prep-TLC afforded **57** (37 mg, 53%).

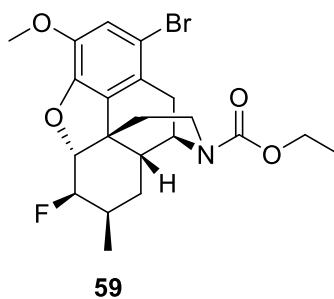
IR (thin film) 2934, 1694, 1487, 1435 cm⁻¹. ¹H NMR (300 MHz, CDCl₃) δ 6.94 (1H, s), 4.82 (1H, d, *J* = 4.5 Hz), 4.70 (0.6H, bs), 4.55 (0.4H, bs), 4.25-4.10 (2H, m), 4.10-3.88 (1H, m), 3.86 (3H, s), 3.41 (3H, s), 3.20-3.10 (1H, m), 2.90-2.75 (2H, m), 2.59 (1H, d, *J* = 18.9 Hz), 2.20-2.10 (1H, m), 1.82-1.70 (2H, m), 1.71-1.60 (1H, m), 1.35-1.10 (5H, m), 0.90 (3H, d, *J* = 6 Hz). ¹³C NMR (75 MHz, CDCl₃) δ 155.6, 146.9, 143.2, 131.0, 116.8, 112.1, 108.0, 88.5, 81.5, 61.8, 61.7, 58.5, 56.7, 51.0, 43.5, 37.7, 35.3, 30.7, 29.0, 28.2, 17.8, 14.9. HRMS calculated for C₂₂H₂₈BrNO₅ (M+H)⁺ 466.1229, found 466.1224.



58

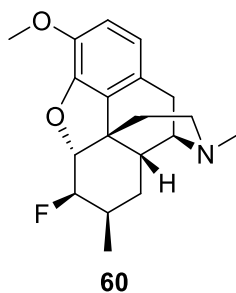
A solution of **57** (37 mg, 0.08 mmol) in THF (2 mL) was treated with LAH (2M/THF, 0.25 mL) at room temperature under Ar. Upon completion as judged by TLC the solution was quenched with a saturated aqueous solution of Rochelle's salt (5 mL) and extracted with DCM (4 x 10 mL). The combined extracts were dried over Na₂SO₄ and concentrated *in vacuo*. The crude sample was purified by prep-TLC to give **58** (11 mg, 42%).

IR (thin film) 3420, 2928, 1506, 1456 cm⁻¹. ¹H NMR (300 MHz, CDCl₃) δ 6.78 (1H, d, *J* = 9.5 Hz), 6.65 (1H, d, *J* = 9.5 Hz), 4.87 (1H, d, *J* = 4.8 Hz), 3.87 (3H, s), 3.45 (3H, s), 3.34 (1H, m), 3.18 (1H, dd, *J* = 9.3, 4.6 Hz), 3.03 (1H, d, *J* = 18.6 Hz), 2.87-2.82 (1H, m), 2.77-2.62 (2H, m), 2.61 (3H, s), 2.57-2.47 (1H, m), 2.23 (1H, td, *J*'s = 25.5, 4.2 Hz), 1.82 (1H, dd, *J*'s = 12.9, 2.4 Hz), 1.58 (1H, m), 1.34-1.17 (2H, m), 0.91 (3H, d, *J* = 6.9 Hz). ¹³C NMR (75 MHz, CDCl₃) δ 146.0, 142.6, 134.0, 132.0, 119.0, 115.8, 87.7, 81.5, 60.8, 58.3, 56.6, 47.1, 42.6, 42.1, 36.0, 34.0, 28.7, 28.4, 21.0, 18.1. HRMS calculated for C₂₀H₂₇NO₃ (M+H)⁺ 330.2069, found 330.2065.



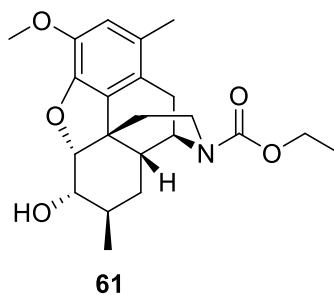
To a solution of **43** (310 mg, 0.69 mmol) in DCM (10 mL) at 0 °C and under Ar was added diethylaminosulfur trifluoride (0.2 mL, 1.4 mmol) via a syringe. Upon completion as judged by TLC the reaction was quenched with a saturated aqueous solution of NaHCO₃ (10 mL) and extracted with DCM (3 x 5 mL). The combined organic extracts were dried over Na₂SO₄ and concentrated *in vacuo*. The crude product was purified by prep-TLC to afford **59** (160 mg, 50%).

IR (thin film) 2930, 1694, 1487, 1430 cm⁻¹. ¹H NMR (300 MHz, CDCl₃) δ 6.95 (1H, s), 4.70 (1H, d, *J* = 15.3 Hz), 4.55 (1H, *J* = 20.1 Hz), 4.36 (1H, d, *J* = 8.1 Hz), 4.22-4.09 (3H, m), 4.05-3.87 (1H, m), 3.86 (3H, s), 2.69 (4H, m), 2.42 (1H, m), 2.02-1.97 (1H, m), 1.79-1.71 (3H, m), 1.26 (5H, m). ¹³C NMR (75 MHz, CDCl₃) δ 155.7, 145.1, 144.2, 140.4, 131.0, 125.2, 117.2, 112.7, 94.7, 93.7, 91.3, 61.7, 56.9, 50.9, 50.6, 43.1, 38.3, 38.1, 34.9, 29.8, 16.0. HRMS calculated for C₂₁H₂₅BrFNO₄ (M+Na)⁺ 476.0849, found 476.0843.



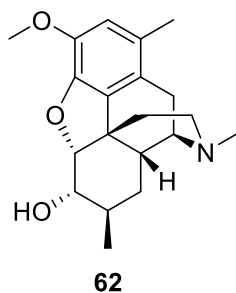
To a solution of **59** (150 mg, 0.33 mmol) in THF (5 mL) at 0 °C under Ar was added a solution of LAH (2M/THF, 1.32 mL). The reaction was stirred and monitored by TLC. Upon completion it was quenched with a saturated aqueous solution of Rochelle's salt (5 mL), and extracted with 5% MeOH/CHCl₃ (3 x 5 mL). The combined extracts were dried over Na₂SO₄ and concentrated *in vacuo*. Purification by prep-TLC gave **60** (20 mg, 19%).

IR (thin film) 2930, 1503, 1440, 1280 cm⁻¹. ¹H NMR (300 MHz, CDCl₃) δ 6.73 (1H, d, *J* = 8.1 Hz), 6.64 (1H, d, *J* = 8.4 Hz), 4.60 (1H, dt, *J*'s = 48, 2.3 Hz), 4.38 (1H, d, *J* = 8.1 Hz), 3.89 (3H, s), 3.09 (1H, m), 2.68-2.65 (1H, m), 2.63-2.57 (1H, m), 2.55 (1H, dd, *J*'s = 6, 3 Hz), 2.44 (3H, s), 2.37 (1H, dd, *J*'s = 18.8, 5.6 Hz), 2.20 (1H, td, *J*'s = 24.3, 3.8 Hz), 2.00-1.83 (2H, m), 1.69 (1H, d, *J*'s = 7.8 Hz), 1.39-1.24 (2H, m), 1.27 (3H, d, *J* = 6.6 Hz). ¹³C NMR (75 MHz, CDCl₃) δ 144.4, 144.0, 130.5, 127.1, 119.1, 114.0, 94.6, 91.8, 59.5, 56.9, 47.7, 43.2, 42.3, 38.6, 38.3, 36.0, 35.0, 20.2, 16.1. HRMS calculated for C₁₉H₂₄FNO₂ (M+H)⁺ 318.1869, found 318.1864, calculated for (M+Na)⁺ 340.1689, found 340.1683.



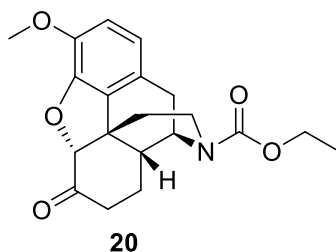
To a solution of **43** (100 mg, 0.22 mmol) in dioxane (10 mL) and water (5 mL) was added K_2CO_3 (185 mg, 1.32 mmol), BHT (25 mg, 0.11 mmol), $CH_3B(OH)_2$ (66 mg, 1.1 mmol) and $Pd(dppf)Cl_2$ (20 mg, 0.1 mmol). The mixture was heated at reflux for 10 min and cooled to room temperature. The mixture was extracted with EtOAc (3 x 10 mL), dried over Na_2SO_4 and concentrated *in vacuo*. The crude product was purified by prep-TLC to afford **61** (75 mg, 85%).

IR (thin film) 3447, 2932, 1684, 1436 cm^{-1} . 1H NMR (300 MHz, $CDCl_3$) δ 6.66 (1H, s), 4.70 (0.5 H, bs), 4.55 (0.5H, bs), 4.67 (1H, d, $J = 4.5$ Hz), 4.15 (2H, m), 4.10-3.88 (1H, m), 3.88 (3H, s), 3.51 (1H, m), 2.83 (2H, m), 2.54 (1H, d, $J = 18.6$ Hz), 2.17 (3H, s), 2.12-2.04 (1H, m), 1.85-1.74 (2H, m), 1.4 (1H, m), 1.36-1.23 (2H, m), 1.27 (3H, m), 0.91 (3H, d, $J = 6.6$ Hz). ^{13}C NMR (75 MHz, $CDCl_3$) δ 144.6, 141.8, 129.8, 128.5, 124.5, 114.9, 90.9, 72.7, 61.7, 56.6, 50.9, 43.4, 37.6, 37.3, 35.1, 30.0, 29.1, 28.0, 21.3, 18.3, 18.0, 15.0. HRMS $C_{22}H_{29}NO_5$ calculated for $(M+H)^+$ 388.2124, found 388.2119; calculated for $(M+Na)^+$ 410.1943, found 410.1938.



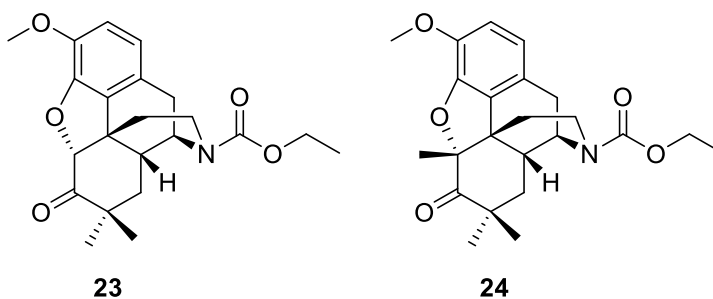
To a solution of **61** (75 mg, 0.19 mmol) in THF (5 mL) at room temperature under Ar was added drop wise a solution of LAH (2M/THF, 0.4 mL). The reaction was stirred and monitored by TLC. Upon completion it was quenched with a saturated aqueous solution of Rochelle's salt (5 mL), and extracted with CHCl₃ (3 x 5 mL). The combined extracts were dried over Na₂SO₄ and concentrated *in vacuo*. Purification by prep-TLC gave **62** (34 mg, 52%).

IR (thin film) 3378, 2929, 1502, 1447 cm⁻¹. ¹H NMR (300 MHz, CDCl₃) δ 6.59 (1H, s), 4.70 (1H, d, *J* = 4.5 Hz), 3.87 (3H, s), 3.51 (1H, dd, *J*'s = 8.3, 4.7 Hz), 3.17 (1H, dd, *J*'s = 3, 2.7 Hz), 2.83 (1H, d, *J* = 18.6 Hz), 2.58 (1H, dd, *J*'s = 12.2, 4.7 Hz), 2.46 (3H, s), 2.45-2.25 (3H, m), 2.21 (3H, s), 1.99 (1H, td, *J*'s = 19.6, 5.1 Hz), 1.74 (1H, dd, *J*'s = 12.8, 2 Hz), 1.35-1.15 (4H, m), 0.91 (3H, d, *J* = 6.3 Hz). ¹³C NMR (75 MHz, CDCl₃) δ 144.5, 141.6, 130.7, 128.0, 125.4, 114.7, 91.1, 72.9, 60.0, 56.7, 46.6, 43.3, 42.9, 37.4, 35.7, 29.7, 29.6, 19.1, 18.6, 18.1. HRMS C₂₀H₂₇NO₃ calculated for (M+Na)⁺ 352.1889, found 352.1883.



Ethyl chloroformate (0.9 mL, 60.4 mmol) was added to a mixture of hydrocodone **9** (0.3 g, 10 mmol) and K_2CO_3 (1.4 g, 10 mmol) in $CHCl_3$ (50 mL), and the mixture was heated at reflux under Ar with stirring. The reaction was monitored by TLC. Upon completion the mixture was cooled to room temperature and washed with water (3 x 75 mL), brine (50 mL), dried over Na_2SO_4 and concentrated *in vacuo*. The crude product was purified by prep-TLC to give **20** (325 mg, 90%).

IR (thin film) 2931, 1729, 1690, 1505, 1427 cm^{-1} . 1H NMR (300 MHz, $CDCl_3$) δ 6.70 (1H, d, $J = 8.1$ Hz), 6.61 (1H, d, $J = 8.1$ Hz), 4.74 (0.7H, bs), 4.60 (0.3, bs), 4.65 (1H, s), 4.16-4.06 (2H, m), 4.05-3.90 (1H, m), 3.87 (3H, s), 2.81-2.67 (3H, m), 2.43-2.30 (2H, m), 2.00-1.75 (3H, m), 1.30-1.17 (5H, s). ^{13}C NMR (75 MHz, $CDCl_3$) δ 207.4, 155.7, 145.8, 143.3, 126.4, 125.2, 120.5, 115.1, 91.4, 61.8, 56.9, 50.7, 47.4, 41.6, 40.0, 38.2, 35.2, 28.7, 25.6, 14.9. HRMS $C_{20}H_{23}NO_5$ calculated for $(M+H)^+$ 358.1654, found 358.1649; calculated for $(M+Na)^+$ 380.1474, found 380.1468.

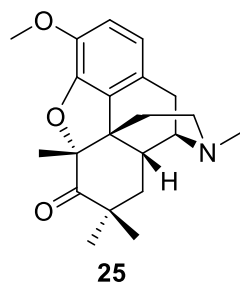


To a solution of **20** (200 mg, 0.56 mmol) in THF (5 mL) at room temperature and under Ar was added ^tBuOK (315 mg, 2.8 mmol) followed by CH₃I (0.35 mL, 5.6 mmol) in one portion. The reaction was monitored by TLC. Upon completion the reaction was quenched with water (10 mL) and extracted with ethyl acetate (3 x 10 mL). The combined extracts were dried over Na₂SO₄ and concentrated *in vacuo*. Purification by prep-TLC afforded four products, **23** (35 mg, 16%) and **24** (65 mg, 30%) which were fully characterized. The remaining two products were identified as **21**, and **22** in approximately 19% yield each.

Data for **24**: IR (thin film) 2979, 2924, 1694, 1506, 1437 cm⁻¹. ¹H NMR (300 MHz, CDCl₃) δ 6.69 (1H, d, *J* = 8.4 Hz), 6.60 (1H, d, *J* = 8.4 Hz), 4.69 (0.65 H, bs), 4.53 (0.35H, bs), 4.22-4.10 (2H, m), 3.99 (1H, dd, *J*'s = 12, 3.9 Hz), 3.86 (3H, s), 2.88 (1H, dd, *J*'s = 18.6, 5.7 Hz), 2.76 (1H, m), 2.66 (2H, d, *J* = 18.3 Hz), 2.48 (1H, dt, *J* = 12.9, 3.5 Hz), 1.84 (1H, td, *J* = 25.1, 5.2 Hz), 1.63 (3H, s), 1.62-1.59 (1H, m), 1.53 (1H, dd, *J* = 13.7, 4.1 Hz), 1.34-1.15 (6H, m), 0.93 (3H, s). ¹³C NMR (75 MHz, CDCl₃) δ 214.8, 155.5, 145.2, 142.7, 128.0, 125.2, 120.0, 114.2, 95.4, 61.8, 56.6, 50.8, 47.5, 44.7, 38.3,

37.5, 36.3, 31.2, 28.8, 26.2, 24.8, 19.3, 15.0. HRMS $C_{23}H_{29}NO_5$ calculated for $(M+H)^+$ 400.2124, found 400.2119; calculated for $(M+Na)^+$ 422.1943, found 422.1938.

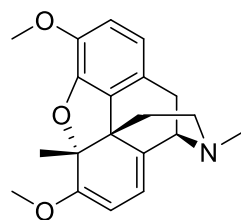
Data for **23**: IR (thin film) 2967, 2927, 1694, 1505, 1436 cm^{-1} . 1H NMR (300 MHz, $CDCl_3$) δ 6.74 (1H, d, $J = 8.1$ Hz), 6.64 (1H, d, $J = 8.1$ Hz), 4.90 (1H, s), 4.72 (0.64 H, bs), 4.56 (0.36 H, bs), 4.21-4.13 (2H, m), 4.06- 3.95 (1H, m), 3.93 (3H, s), 2.90-2.63 (4H, m), 2.58 (1H, dt, $J's = 12.9, 3.8$ Hz), 1.94 (1H, td, $J's = 24.5, 4.9$ Hz), 1.85 (1H, m), 1.60 (1H, dd, $J's = 13.7, 4.7$ Hz), 1.35-1.15 (6H, m), 0.98 (3H, s). ^{13}C NMR (75 MHz, $CDCl_3$) δ 210.4, 202.7, 145.6, 143.4, 126.6, 123.9, 115.4, 94.5, 61.8, 57.2, 51.2, 47.3, 45.0, 38.8, 38.3, 37.2, 34.9, 31.3, 28.9, 26.4, 24.8, 14.9. HRMS $C_{22}H_{27}NO_5$ calculated for $(M+H)^+$ 386.1967, found 386.1962; calculated for $(M+Na)^+$ 408.1787, found 408.1781.



To a solution of **24** (60 mg, 0.15 mmol) in THF (10 mL) at room temperature and under Ar was added a solution of LAH (2M/THF, 0.4 mL) with stirring. The reaction was monitored by TLC and upon completion it was quenched with a MeOH (1 mL) and saturated aqueous solution of Rochelle's salt (5 mL). The solution was then extracted with 5% MeOH/CHCl₃ (3 x 5 mL), dried over Na₂SO₄ and concentrated *in vacuo* to afford crude product. The crude product was then dissolved in DCM (10 mL), to which was added 4-angstrom molecular sieves (100 mg) followed by PCC (65 mg, 0.29 mmol). The reaction was stirred and monitored by TLC. Upon completion the solution was filtered through Celite and the filtrate was concentrated *in vacuo*. The crude product was purified by prep-TLC to afford **25** (29 mg, 60%).

IR (thin film) 3409, 2927, 1717, 1506 cm⁻¹. ¹H NMR (300 MHz, CDCl₃) δ 6.72 (1H, d, *J* = 8.1 Hz), 6.66 (1H, d, *J* = 8.4 Hz), 3.88 (3H, s), 3.53 (1H, d, *J* = 3.6 Hz), 3.22 (1H, d, *J* = 11.7 Hz), 3.06 (1H, d, *J* = 18.9 Hz), 3.05-2.97 (1H, bs), 2.72 (3H, s), 2.67-2.35 (3H, m), 1.74-1.69 (1H, bs), 1.68 (3H, s), 1.54 (1H, dd, *J*'s = 13.4, 3.2 Hz), 1.28 (3H, s), 1.23 (1H, d, *J* = 14.1 Hz), 0.94 (3H, s). ¹³C NMR (75 MHz, CDCl₃) δ 214.4, 145.2, 143.2, 127.9, 123.5, 119.9, 114.6, 95.4, 60.7, 56.7, 47.1, 46.1, 44.7, 42.2, 37.9,

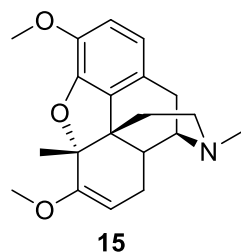
35.2, 30.3, 26.1, 24.7, 20.9, 19.4. HRMS calculated for $C_{21}H_{27}NO_3$ (M+H)⁺ 342.2069, found 3342.2064, calculated for (M+Na)⁺ 364.1889, found 364.1883.



14

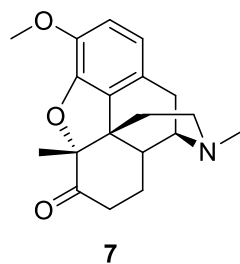
To a solution of thebaine **1** (1 g, 3.2 mmol) in THF (50 mL) at -78 °C and under Ar was added a solution of BuLi (2.5M, 1.9 mL) via a syringe. After stirring for 5 min, (CH₃)₂SO₄ (0.3 mL, 3.2 mmol) was added. The reaction was monitored by TLC. Upon completion it was diluted with water (20 mL) and extracted with CHCl₃ (3 x 10 mL). The combined extracts were dried over Na₂SO₄ and concentrated *in vacuo*. Crystallization from CHCl₃ afforded **14** (0.55 g, 55%).

IR (thin film) 2952, 2915, 2832, 1437, 1045 cm⁻¹. ¹H NMR (300 MHz, CDCl₃) δ 6.63 (1H, d, *J* = 8.1 Hz), 6.57 (1H, d, *J* = 8.1 Hz), 5.53 (1H, d, *J* = 6.3 Hz), 4.91 (1H, d, *J* = 6.3 Hz), 3.82 (3H, s), 3.63 (1H, d, *J* = 6.6 Hz), 3.55 (3H, s), 3.28 (1H, d, *J* = 17.7 Hz), 2.72-2.57 (3H, m), 2.45 (3H, s), 2.20-2.08 (1H, m), 1.74 (3H, s), 1.73-1.67 (1H, m). ¹³C NMR (75 MHz, CDCl₃) δ 156.6, 144.2, 142.6, 134.4, 131.8, 127.5, 119.4, 112.5, 112.4, 94.6, 93.7, 61.7, 56.4, 55.2, 47.7, 46.0, 42.6, 31.0, 29.9, 20.4. HRMS calculated for C₂₀H₂₃NO₃ (M+H)⁺ 326.1756, found 326.1756; calculated for (M+Na)⁺ 348.1576, found 348.1571.



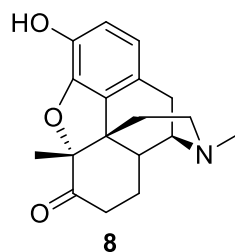
To a solution of **14** (350 mg, 1.1 mmol) in MeOH (30 mL) was added 10% Pd/C (100 mg) under Ar. The reaction vessel was then charged with H_{2(g)} using a balloon and the suspension stirred and monitored by TLC. Upon completion the reaction was filtered through Celite and concentrated *in vacuo* to afford **15** (0.33 mg, 99%). No purification was necessary.

IR (thin film) 2914, 1664, 1505, 1441 cm⁻¹. ¹H NMR (300 MHz, CDCl₃) δ 6.67 (1H, d, *J* = 8.1 Hz), 6.59 (1H, d, *J* = 8.4 Hz), 4.58 (1H, d, *J* = 4.8 Hz), 3.81 (3H, s), 3.40 (3H, s), 3.13-3.10 (1H, m), 2.98 (1H, d, *J* = 18.6 Hz), 2.57-2.43 (1H, m), 2.41 (3H, s), 2.31-2.15 (2H, m), 2.00 (1H, dt, *J*'s = 16.8, 6.3 Hz), 1.88 (1H, td, *J*'s = 24.6, 5.1 Hz), 1.66 (3H, s), 1.64-1.56 (3H, m). ¹³C NMR (75 MHz, CDCl₃) δ 154.2, 144.5, 143.0, 131.2, 127.0, 118.6, 112.9, 96.5, 92.6, 60.0, 56.4, 54.7, 46.6, 43.8, 43.3, 38.4, 32.3, 23.9, 20.2, 18.0. HRMS calculated for C₂₀H₂₅NO₃ (M+H)⁺ 328.1913, found 328.1910, calculated for (M+Na)⁺ 350.1732, found 350.1727.



A solution of **15** (130 mg, 0.4 mmol) in aqueous HCl (1N, 6 mL) was heated at 100 °C for 10 min. The solution was then basified using a saturated aqueous solution of NaHCO₃ to pH 8 and extracted with CHCl₃ (3 x 10 mL), dried over Na₂SO₄ and concentrated *in vacuo* to afford crystalline **7** (118 mg, 95%). No purification was necessary.

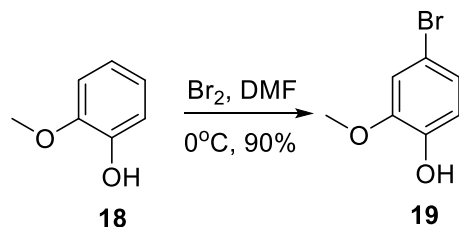
IR (thin film) 2932, 1726, 1505, 1439 cm⁻¹. ¹H NMR (300 MHz, CDCl₃) δ 6.67 (1H, d, *J* = 8.1 Hz), 6.60 (1H, d, *J* = 8.1 Hz), 3.87 (3H, s), 3.15 (1H, dd, *J*'s = 5.3, 2.9 Hz), 2.99 (1H, d, *J* = 18.6 Hz), 2.56 (1H, dd, *J*'s = 11.9, 3.2 Hz), 2.47 (1H, dd, *J*'s = 4.1, 2.9 Hz), 2.42 (3H, s), 2.41-2.37 (1H, m), 2.35-2.31 (1H, m), 2.30-2.25 (1H, m), 2.17 (1H, td, *J*'s = 24.2, 5.0 Hz), 1.95 (1H, td, *J*'s = 24.2, 5.0 Hz), 1.81 (1H, m), 1.59 (3H, s), 1.55 (1H, m), 1.27 (1H, m). ¹³C NMR (75 MHz, CDCl₃) δ 211.4, 145.3, 142.7, 128.8, 126.5, 119.7, 113.9, 96.3, 59.6, 56.6, 47.8, 46.5, 43.1, 42.3, 39.0, 31.7, 26.0, 20.1, 16.2. HRMS calculated for C₁₉H₂₃NO₃ (M+H)⁺ 314.1756, found 314.1752, calculated for (M+Na)⁺ 336.1576, found 336.1573.



To a solution of **7** (100 mg, 0.32 mmol) in DCM (3 mL) at $-20\text{ }^{\circ}\text{C}$ and under Ar was added a solution of BBr_3 (1M/DCM, 1.6 mL) via a syringe. The reaction was stirred and monitored by TLC. Upon completion MeOH (1 mL) and a saturated aqueous solution of Rochelle's salt (5 mL) were added with stirring. The product was extracted using CHCl_3 (4 x 5 mL), dried over Na_2SO_4 and concentrated *in vacuo*. The crude product was crystallized from MeOH to afford **8** (40 mg, 42%).

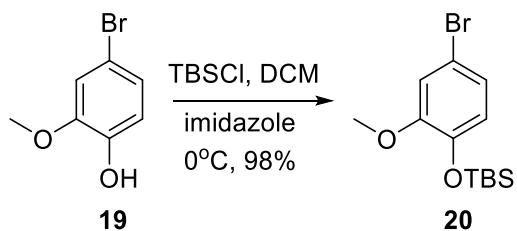
^1H NMR (500 MHz, CD_3OD) δ 6.60 (1H, d, $J = 8.0$ Hz), 6.56 (1H, d, $J = 8.5$ Hz), 5.81 (1H, s), 3.19 (1H, dd, J 's = 6.0, 3.0 Hz), 3.01 (1H, d, $J = 18.5$ Hz), 2.64-2.56 (2H, m), 2.51 (1H, m), 2.43 (3H, s), 2.38 (1H, dd, J 's = 19, 5.5 Hz), 2.26-2.19 (2H, m), 1.99 (1H, td, J 's = 24.8, 4.8 Hz), 1.88-1.82 (1H, m), 1.58 (3H, s), 1.51 (1H, m), 1.25-1.16 (1H, m). ^{13}C NMR (75 MHz, CDCl_3) δ 214.8, 145.1, 140.4, 129.4, 126.2, 120.9, 118.7, 97.2, 60.7, 49.9, 47.4, 42.8, 42.2, 39.5, 32.1, 26.8, 21.0, 16.4. HRMS calculated for $\text{C}_{18}\text{H}_{21}\text{NO}_3$ ($\text{M}+\text{H}$) $^+$ 300.1600, found 300.1597, calculated for ($\text{M}+\text{Na}$) $^+$ 322.1419, found 322.1414.

3.2 Experimental Data for Chapter 2



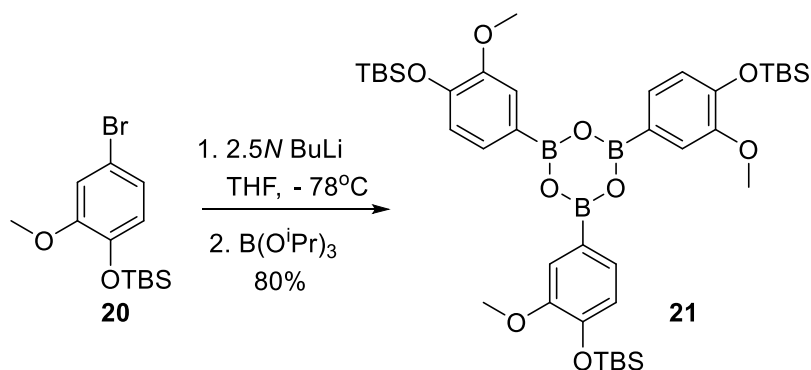
To a solution of guaiacol **18** (28.4 g, 228.8 mmol) in DMF (150 mL) at 0 °C was slowly added a solution of NBS (40.7 g, 228.8 mmol) in DMF (150 mL). The reaction mixture was stirred for 0.5 h and quenched by addition of ice (150 g). The mixture was then allowed to warm to room temperature and extracted with ethyl acetate (3 x 50 mL). The combined organic extracts were washed with water (100 mL) and brine (100 mL). The ethyl acetate solution was dried over Na₂SO₄ and concentrated *in vacuo*. The crude mixture was purified using column chromatography (0-5% ethyl acetate/hexanes) to afford **19** (42 g, 90%).

IR (thin film) 3508, 2917, 2849, 1498 cm⁻¹. ¹H NMR (300 MHz, CDCl₃) δ 6.99 (2H, s), 6.84 (1H, s), 5.32 (1H, s), 3.90 (3H, s). ¹³C NMR (75 MHz, CDCl₃) δ 147.5, 145.1, 124.4, 116.0, 114.4, 111.8, 56.4. HRMS calculated for C₇H₇BrO₂ (M-H)⁻ 200.9551, found (M-H)⁻ 200.9557.



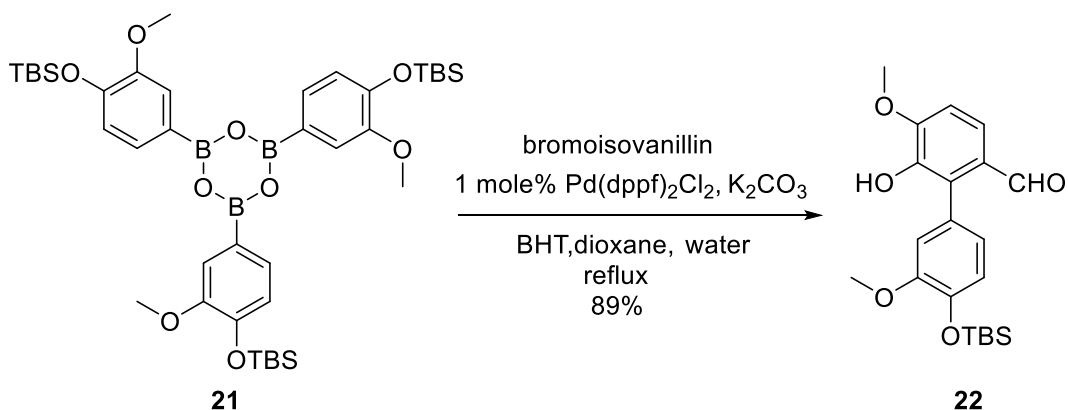
To a stirring solution of **19** (153 g, 754 mmol) in DCM (1500 mL) at 0 °C was added imidazole (80 g, 1167 mmol). After 15 min TBSCl (129 g, 856 mmol) was added in portions. The reaction was monitored by TLC and upon completion poured into a saturated aqueous solution of NH₄Cl (1000 mL). The organic phase was separated, and the aqueous layer extracted with DCM (2 x 250 mL). The combined organic extracts were dried over Na₂SO₄ and concentrated *in vacuo*. The crude mixture was purified using column chromatography (0-5% ethyl acetate/hexanes) to afford **20** (227 g, 95%).

IR (thin film) 2956, 2930, 2857, 1497 cm⁻¹. ¹H NMR (300 MHz, CDCl₃) δ 7.01 (1H, s), 6.99 (1H, d, *J* = 9 Hz), 6.77 (1H, d, *J* = 8.1 Hz), 3.81 (3H, s), 1.06 (9H, s), 0.21 (6H, s). ¹³C NMR (75 MHz, CDCl₃) δ 152.1, 144.6, 125.3, 122.4, 115.7, 113.8, 55.8, 26.0, 18.7, - 4.4. HRMS calculated for C₁₃H₂₁BrO₂Si (M+H)⁺ 317.0572, found (M+H)⁺ 317.0571.



To a solution of **20** (51.5 g, 162.3 mmol) in THF (500 mL) at -78 °C under Ar was slowly added a solution of BuLi (2.5 M, 76 mL) via a syringe. The solution was stirred for 10 min followed by slow addition of B(ⁱPrO)₃ via a syringe. The reaction was stirred for 12 h, slowly warming to room temperature. The reaction was quenched with a solution of 10% aqueous NaHSO₄ (200 mL) and extracted with ethyl acetate (3 x 150 mL). The combined extracts were washed with brine (200 mL), dried over Na₂SO₄ and concentrated *in vacuo*. The crude product was azeotroped with toluene (2 x 50 mL) and purified by column chromatography (0-40% ethyl acetate/hexanes) to afford **21** (34.3 g, 80%).

IR (thin film) 2951, 2931, 2857, 1597, 1516 cm⁻¹. ¹H NMR (300 MHz, CDCl₃) δ 7.82 (1H, d, *J* = 8.1 Hz), 7.74 (1H, s), 7.06 (1H, d, *J* = 8.1 Hz), 4.00 (3H, s), 1.13 (9H, s), 0.29 (6H, s). ¹³C NMR (75 MHz, CDCl₃) δ 150.9, 149.7, 129.9, 124.0, 121.1, 118.9, 55.7, 26.0, 18.9, - 4.2. HRMS calculated for C₃₉H₆₃B₃O₉Si₃ (M+H)⁺ 793.4137, found (M+H)⁺ 793.4151.

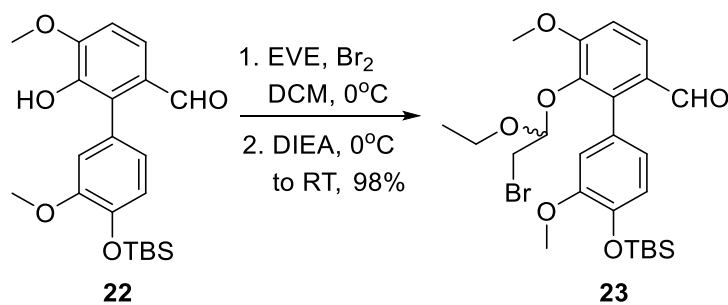


A solution of dioxane (45 mL) and water (15 mL) was heated at 60 °C and degassed with Ar via a needle inside the solution for 20 min. K₂CO₃ (5.5 g) and BHT (1.3 g) were added. Bubbling of Ar through the solution was continued for 0.5 h at 40 °C. Bromoisovanillin (2.8 g, 11.9 mmol), **21** (2.9 g, 11 mmol) and Pd(dppf)Cl₂ (95 mg, 0.11 mmol) were added successively and the reaction mixture was heated at 110 °C. Reaction progress was monitored by TLC. Upon completion (15 min), the mixture was cooled to room temperature and diluted with water (50 mL). The reaction mixture was extracted with ethyl acetate (3 x 50 mL) and the combined organic extracts were washed with brine (100 ml), dried over Na₂SO₄ and concentrated *in vacuo*. Purification by column chromatography (0-30% ethyl acetate/hexanes) afforded **22** (3.8 g, 89%).

MP: 145-146 °C. IR (thin film) 3220, 2952, 2929, 1667, 1587 cm⁻¹. ¹H NMR (300 MHz, CDCl₃) δ 9.69 (1H, s), 7.65 (1H, d, *J* = 8.7 Hz), 6.99 (1H, d, *J* = 7.8 Hz), 6.95 (1H, s), 6.89 (1H, d, *J* = 1.8 Hz), 6.84 (1H, d, *J* = 7.8 Hz), 5.79 (1H, s), 4.01 (3H, s), 3.81 (3H, s), 1.04 (9H, s), 0.02 (6H, s). ¹³C NMR (75 MHz, CDCl₃) δ 191.9, 151.3, 151.0,

145.5, 142.9, 132.0, 128.8, 125.6, 121.0, 120.7, 115.0, 109.8, 56.5, 55.8, 30.6, 26.0, 18.7,

-4.3. HRMS calculated for $C_{21}H_{28}O_5Si$ (M+H)⁺ 389.1784, found (M+H)⁺ 389.1780.

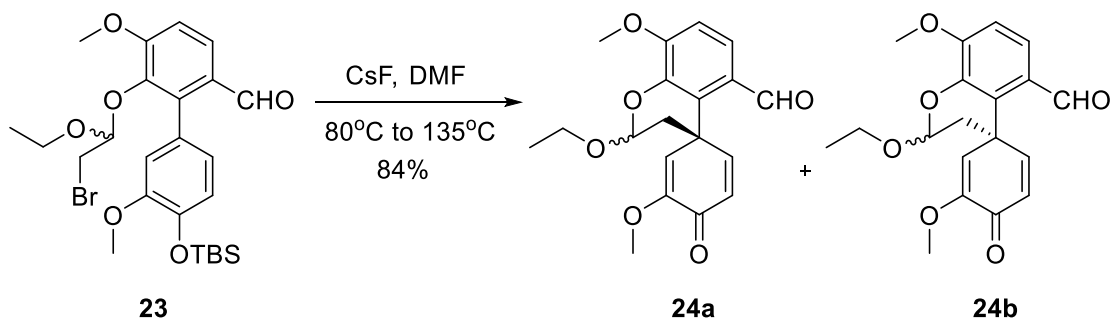


To a solution of Br_2 (6.5 g, 40.5 mmol) in DCM (100 mL) at 0 °C under Ar was slowly added ethyl vinyl ether (3.5 g, 48.3 mmol). The solution was stirred for 5 min, followed by addition of DIEA (10 g, 77.2 mmol). A solution of **22** (7.5 g, 19.3 mmol) in DCM (100 mL) was slowly added to the above solution. The reaction was stirred for 12 h, slowly warming to room temperature. The reaction was diluted with a solution of saturated aqueous NaHCO_3 (100 mL) and the layers separated. The aqueous layer was extracted with DCM (2 x 50 mL), the combined extracts were dried over Na_2SO_4 and concentrated *in vacuo*. Purification by column chromatography (0-20% ethyl acetate/hexanes) afforded **23** (10.2 g, 98%).

IR (thin film) 3245, 2929, 2857, 1668, 1588, 1516, 1273 cm^{-1} . ^1H NMR (300 MHz, CDCl_3) δ 9.66 (1H, s), 7.87 (1H, d, $J = 8.7$ Hz), 7.06 (1H, d, $J = 8.7$ Hz), 6.95 (1H, d, $J = 6.9$ Hz), 6.87 (1H, bs), 6.77 (1H, bs), 5.06 (1H, t, $J = 5.4$ Hz), 4.00 (3H, s), 3.82 (3H, s), 3.68-3.27 (2H, m), 3.26-3.08 (2H, m), 1.05-0.98 (3H, m), 1.04 (9H, s), 0.20 (6H, s). ^{13}C NMR (75 MHz, CDCl_3) δ 196.0, 161.7, 155.2, 150.0, 145.3, 133.6, 133.3,

132.9, 130.6, 129.9, 125.1, 119.8, 115.7, 108.3, 60.6, 60.2, 36.5, 30.3, 23.1, 19.6, -0.01.

HRMS calculated for $C_{25}H_{35}BrO_6Si$ ($M+Na$)⁺ 561.1284, found ($M+Na$)⁺ 561.1277.

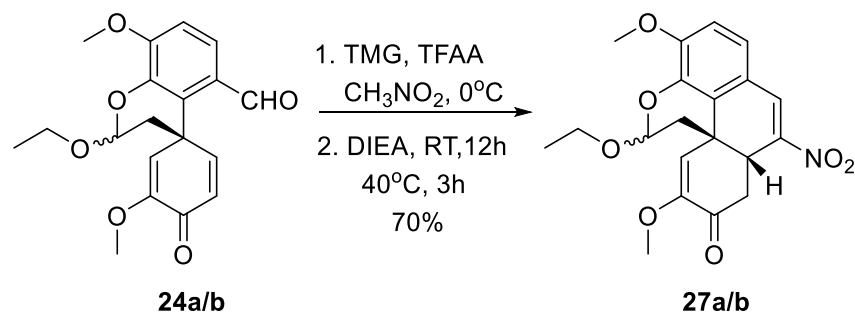


A solution of **23** (4.4 g, 8.16 mmol) in DMF which had been dried over 4-angstrom molecular sieves for 2 days (100 mL) was heated to 80 °C under Ar. CsF (3.7 g, 24.5 mmol) was flame-dried under high vacuum for 10 min and after cooling to room temperature (under high vacuum) was added rapidly and in one portion to the above solution. The reaction temperature was rapidly raised to 135 °C. The reaction progress was monitored by TLC and after completion (20 min), it was cooled to room temperature and diluted with water (200 mL). The product was extracted with ethyl acetate (3 x 50 mL) and the combined extracts were washed with brine, dried over Na₂SO₄, and concentrated *in vacuo*. The remaining DMF was removed under high vacuum. The crude product was purified by column chromatography (0-20% ethyl acetate/hexanes) to afford **24a/b** (2.35 g, 84%). The diastereomers were separated by prep-TLC and characterized individually.

Data for **24a**. IR (thin film) 2975, 2935, 1668, 1634 cm⁻¹. ¹H NMR (500 MHz, CDCl₃) δ 9.96 (1H, s), 7.79 (1H, d, *J* = 16.8 Hz), 7.62 (1H, d, *J* = 14.3 Hz), 6.97 (1H, d, *J* = 14 Hz), 6.35 (1H, d, *J* = 16.5 Hz), 6.00 (1H, d, *J* = 4 Hz), 5.50 (1H, t, *J* = 4 Hz), 3.97

(3H, s), 3.96-3.90 (1H, m), 3.75-3.65 (1H, m), 3.68 (3H, s), 2.47 (1H, d, $J = 25.3$ Hz), 2.06 (1H, d, $J = 23.8$ Hz), 1.24 (3H, t, $J = 11.8$ Hz). ^{13}C NMR (125 MHz, CD_3Cl) δ 189.8, 179.9, 155.9, 154.4, 150.8, 140.2, 128.8, 125.8, 123.9, 123.6, 123.2, 110.5, 95.2, 64.7, 56.3, 55.1, 41.4, 40.7, 15.0. HRMS calculated for $\text{C}_{19}\text{H}_{20}\text{O}_6$ ($\text{M}+\text{H}$) $^+$ 345.1338, found ($\text{M}+\text{H}$) $^+$ 345.1337.

Data for **24b**. IR (thin film) 2974, 2934, 1669, 1586 cm^{-1} . ^1H NMR (500 MHz, CDCl_3) δ 9.96 (1H, s), 7.63 (1H, d, $J = 16.3$ Hz), 7.08 (1H, d, $J = 14$ Hz), 6.97 (1H, d, $J = 13.5$ Hz), 6.82 (1H, d, $J = 2$ Hz), 6.42 (1H, d, $J = 16.3$ Hz), 5.55 (1H, d, $J = 2$ Hz), 3.97 (3H, s), 3.96-3.93 (1H, m), 3.73-3.68 (1H, m), 3.69 (3H, s), 2.46 (1H, d, $J = 23$ Hz), 1.99 (1H, d, $J = 23$ Hz), 1.24 (3H, t, $J = 11.5$ Hz). ^{13}C NMR (125 MHz, CDCl_3) δ 189.7, 179.6, 155.7, 154.5, 149.3, 140.0, 128.6, 127.6, 124.3, 123.5, 123.2, 110.5, 95.2, 64.7, 56.3, 54.8, 40.7, 40.6, 15.0. HRMS calculated for $\text{C}_{19}\text{H}_{20}\text{O}_6$ ($\text{M}+\text{H}$) $^+$ 345.1338, found ($\text{M}+\text{H}$) $^+$ 345.1338.

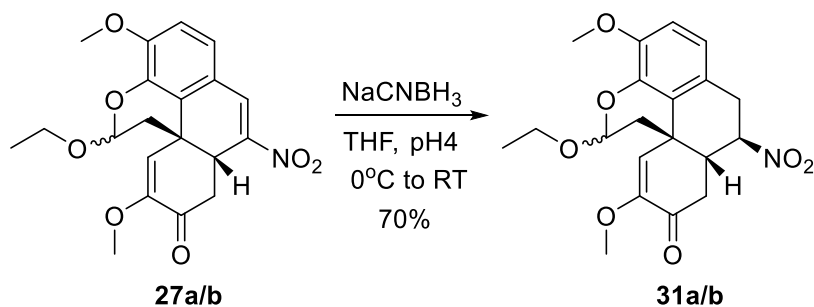


To a solution of **24a/b** (1 g, 2.9 mmol), in CH_3NO_2 (20 mL) at 0°C under Ar, was added TMG (0.4 g, 3.5 mmol) drop wise via a syringe. After stirring the reaction for 20 min TFAA (1.8 g, 8.7 mmol) was added drop wise. The reaction was stirred for 5 min and DIEA (0.45 g, 3.5 mmol) was added drop wise. The ice bath was removed and the reaction stirred for 12 h at room temperature. After heating the reaction at 40°C for 3 h, it was cooled to room temperature, diluted with water (100 mL) and extracted with ethyl acetate (3 x 50 mL). The combined organic extracts were washed with brine (100 mL), dried over Na_2SO_4 and concentrated *in vacuo*. Purification using column chromatography (0-30% ethyl acetate/hexanes) afforded **27a/b** (0.8 g, 70%). The diastereomers were separated by prep-TLC and characterized individually.

Data for **27a**. IR (thin film) 2974, 2934, 1694, 1623, 1494, 1266 cm^{-1} . ^1H NMR (500 MHz, CDCl_3) δ 7.57 (1H, d, $J = 2\text{ Hz}$), 6.99 (1H, d, $J = 7\text{ Hz}$), 6.88 (1H, d, $J = 7\text{ Hz}$), 5.71 (1H, s), 5.59 (1H, dd, J 's = 3, 1.5 Hz), 4.01 (1H, m), 3.94 (3H, s), 3.65 (1H, m), 3.43 (3H, s), 3.41-3.38 (1H, m), 3.35 (1H, s), 2.94 (1H, dd, J 's = 14.3, 3.8 Hz), 2.68 (1H, dd, J 's = 11.3, 1.5 Hz), 2.29 (1H, dd, J 's = 11, 2.5 Hz), 1.19 (3H, t, $J = 5.5\text{ Hz}$). ^{13}C

NMR (125 MHz, CDCl₃) δ 189.7, 152.2, 148.9, 147.1, 140.0, 132.4, 124.0, 122.4, 121.9, 120.2, 110.8, 96.8, 64.7, 56.2, 54.6, 42.8, 37.7, 35.9, 34.9, 15.2. HRMS calculated for C₂₀H₂₂NO₇ (M+H)⁺ 388.1396, found (M+H)⁺ 388.1386.

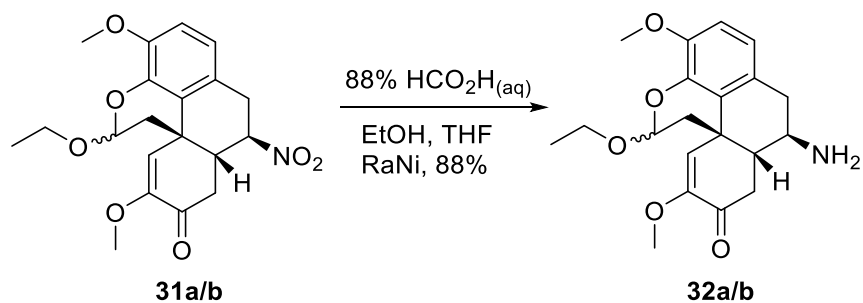
Data for **27b**. IR (thin film) 2975, 1699, 1496, 1265 cm⁻¹. ¹H NMR (500 MHz, CDCl₃) δ 7.60 (1H, d, *J* = 2 Hz), 6.99 (1H, d, *J* = 8.5 Hz), 6.89 (1H, d, *J* = 8.5 Hz), 5.43 (1H, dd, *J*'s = 10, 3 Hz), 5.30 (1H, s), 4.21 (1H, m), 3.95 (3H, s), 3.77 (1H, m), 3.47 (3H, s), 3.46-3.43 (2H, m), 3.00 (1H, dd, *J*'s = 18.5, 5.5 Hz), 2.67 (1H, dd, *J*'s = 13, 3 Hz), 2.26 (1H, dd, *J*'s = 13, 10 Hz), 1.33 (3H, t, *J* = 7 Hz). ¹³C NMR (125 MHz, CDCl₃) δ 189.6, 152.2, 150.3, 146.5, 141.2, 132.3, 124.1, 122.1, 121.1, 115.8, 111.2, 98.2, 65.3, 56.2, 55.1, 41.7, 39.9, 38.6, 34.8, 15.1. HRMS calculated for C₂₀H₂₂NO₇ (M+H)⁺ 388.1396, found (M+H)⁺ 388.1387.



A solution of **27a/b** (550 mg, 1.4 mmol) in THF (20 mL) was treated with pH-4 phosphate buffer (40 mL) followed by NaCNBH₃ (110 mg, 1.7 mmol). The reaction was stirred at room temperature and monitored by TLC. Upon completion it was diluted with brine (50 mL) and extracted with ethyl acetate (3 x 30 mL). The combined organic extracts were dried over Na₂SO₄ and concentrated *in vacuo*. The crude product was purified by column chromatography to afford **31a/b** (390 mg, 70%). A quantity was crystallized for the purpose of characterization affording an inseparable (by TLC) mixture of diastereomers.

Data for mixture of diastereomers. IR (thin film) 2974, 2933, 1693, 1617, 1550, 1496 cm⁻¹. ¹H NMR (300 MHz, CDCl₃) δ 6.91-6.77 (2H), 6.04-5.74 (1H), 5.75-5.54 (1H), 4.17-3.96 (1H), 3.91 (3H), 3.74-3.61 (1H), 3.54 (3H), 3.45 (5H), 2.24-1.93 (2H), 1.29-1.18 (3H). ¹³C NMR (75 MHz, CDCl₃) δ 190.3, 189.1, 150.3, 149.5, 148.9, 148.2, 141.1, 139.8, 126.9, 124.3, 123.5, 123.4, 122.1, 121.8, 120.7, 118.3, 112.6, 111.5, 111.4, 99.0, 96.6, 86.1, 83.9, 64.7, 56.5, 56.4, 55.4, 55.0, 46.0, 43.7, 43.2, 40.7, 39.9, 38.0, 36.5,

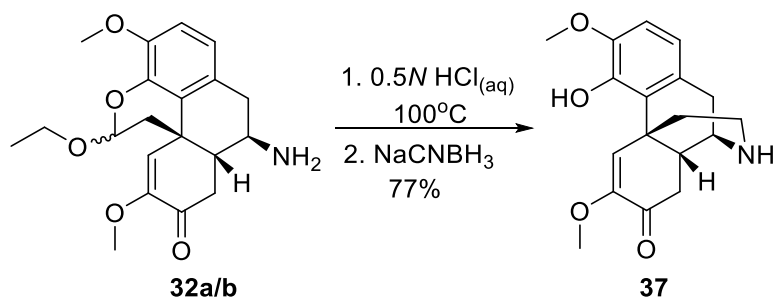
35.0, 33.6, 32.7, 15.4, 15.3.. HRMS calculated for $C_{20}H_{23}NO_7$ (M+Na)⁺ 412.1372, found (M+Na)⁺ 412.1370.



To a solution of **31a/b** (490 mg, 1.26 mmol) in THF (5 mL) and EtOH (5 mL) was added RaNi (2 mL of aqueous suspension). The reaction flask was then attached to an oil bubbler and 88% aqueous formic acid (15 mL) was added by a syringe. More formic acid was added until a very slow and steady bubbling of gas was observed. The reaction was monitored by TLC. Upon completion the reaction mixture was cooled in an ice bath and basified to pH 9 by a solution of 10% aqueous KOH. The product was extracted with 5% MeOH/CHCl₃ (3 x 25 mL). The combined organic extracts were washed with brine (50 mL), dried over Na₂SO₄ and concentrated *in vacuo* to afford **32a/b** (400 mg, 88%). No purification was necessary based on LCMS analysis. A quantity was recrystallized for the purpose of characterization affording a single diastereomer.

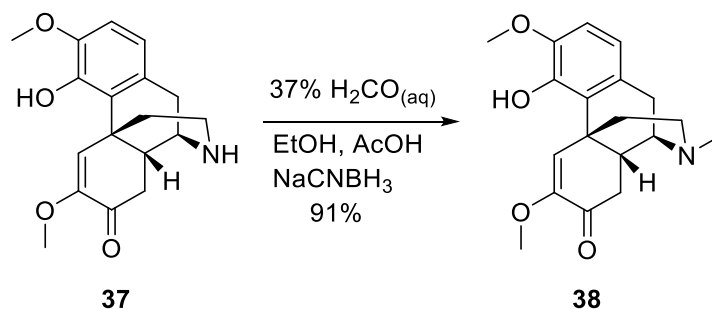
Data for diastereomer. IR (thin film) 3188, 2837, 1684 cm⁻¹. ¹H NMR (300 MHz, CD₃OD) δ 6.98 (1H, d, *J* = 8.1 Hz), 6.86 (1H, d, *J* = 8.1 Hz), 6.09 (1H, s), 5.55 (1H, s), 3.96 (1H, m), 3.71 (3H, s), 3.70-3.65 (1H, m), 3.62-3.58 (1H, m), 3.54 (3H, s), 3.26-3.15 (2H, m), 2.86 (2H, m), 2.70 (1H, d, *J* = 13.8 Hz), 2.25 (1H, dd, *J*'s = 13.7, 2.9 Hz), 2.05 (1H, m), 1.21 (3H, t, *J* = 7.2 Hz). ¹³C NMR (75 MHz, CD₃OD) δ 191.6, 149.3, 148.5,

140.1, 124.4, 124.1, 124.0, 120.9, 111.9, 96.6, 64.2, 55.7, 54.1, 51.7, 46.4, 40.2, 39.0, 34.7, 32.5, 14.4. HRMS calculated for $C_{20}H_{25}NO_5$ ($M+Na$)⁺ 382.1630, found ($M+Na$)⁺ 382.1620.



A solution of **32a/b** (400 mg, 1.13 mmol) in aqueous HCl (0.5N, 30 mL) was heated to 100 °C with stirring for 10 min. NaCNBH₃ (80 mg, 1.24 mmol) was added in two portions 5 min apart. The reaction was stirred for 20 min and cooled to room temperature. The solution was basified to pH 7 to 8 using a solution of 10% aqueous KOH and extracted with 5% MeOH/CHCl₃ (3 x 25 mL). The combined extracts were dried over Na₂SO₄ and concentrated *in vacuo* to afford **37** (270 mg, 77%). No purification was necessary based on LCMS analysis. A quantity was purified by prep-TLC for the purpose of characterization.

IR (thin film) 3397, 2961, 1684, 1622, 1488 cm⁻¹. ¹H NMR (500 MHz, CDCl₃) δ 6.78 (1H, d, *J* = 8.5 Hz), 6.70 (1H, d, *J* = 8.0 Hz), 6.64 (1H, s), 3.87 (3H, s), 3.78 (1H, d, *J* = 2 Hz), 3.68 (3H, s), 3.48 (1H, s), 3.25-3.20 (3H, m), 2.86-2.36 (2H, m), 2.49-2.35 (2H, m), 2.21 (1H, d, *J* = 11.5 Hz), 2.12 (1H, td, *J*'s = 26.8, 4.5 Hz), 1.26-1.18 (1H, m). ¹³C NMR (125 MHz, CDCl₃) δ 191.6, 149.0, 145.7, 143.9, 126.0, 124.0, 122.1, 119.3, 110.0, 56.2, 55.0, 50.8, 49.6, 40.2, 38.1, 36.9, 34.2, 28.2. HRMS calculated for C₁₈H₂₁NO₃ (M+Na)⁺ 338.1368, found (M+Na)⁺ 338.1360.

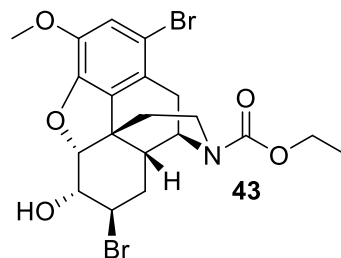


To a solution of **37** (270 mg, 0.87 mmol) in EtOH (5 mL) was added AcOH (0.5 mL) and a solution of 37% aqueous formaldehyde (1 mL). The reaction was stirred for 10 min and NaCNBH₃ (65 mg, 1.04 mmol) was added. The reaction was monitored by TLC. Upon completion the solution was diluted with brine (10 mL) and basified to pH 7 to 8 using a solution of 10% aqueous KOH. The product was extracted with 5% MeOH/CHCl₃ (3 x 20 mL), the combined extracts were dried over Na₂SO₄ and concentrated *in vacuo* to afford **38** (257 mg, 91%). No purification was necessary based on LCMS analysis. A quantity was purified by prep-TLC for the purpose of characterization.

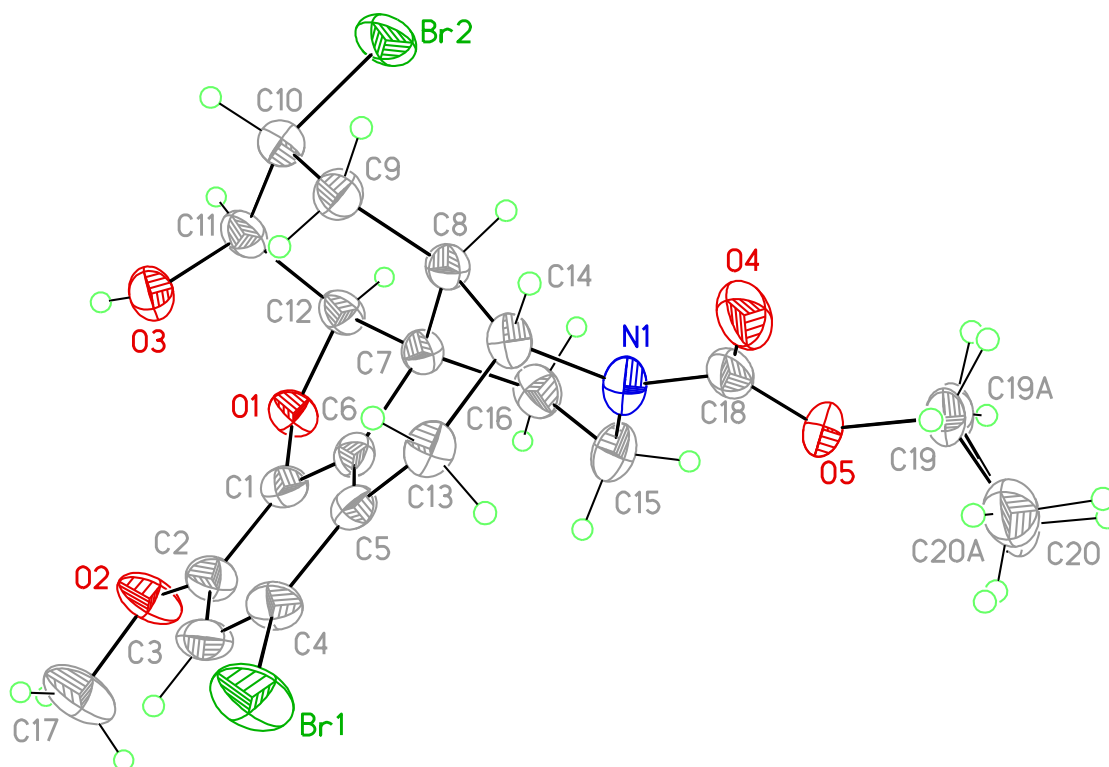
IR (thin film) 3420, 2938, 1684, 1617, 1487 cm⁻¹. ¹H NMR (300 MHz, CDCl₃) δ 6.76-6.71 (2H, m), 6.68 (1H, m), 3.87 (3H, s), 3.69 (3H, s), 3.05 (1H, d, *J* = 18.6 Hz), 3.01-2.96 (1H, m), 2.76 (1H, dd, *J*'s = 18.3, 5.4), 2.64-2.60 (2H, bd), 2.51 (2H, d, *J* = 16.5 Hz), 2.44 (3H, s), 2.23 (1H, td, *J*'s = 24.5, 3.5 Hz), 2.06 (1H, d, *J* = 12 Hz), 1.92 (1H, td, *J*'s = 24.9, 4.6 Hz), 1.25-1.15 (1H, m). ¹³C NMR (75 MHz, CD₃Cl) δ 194.0, 149.0, 145.4, 144.1, 129.2, 126.1, 124.0, 118.8, 109.5, 56.5, 56.4, 55.1, 47.7, 43.8, 42.7,

39.6, 37.6, 36.8, 23.6. HRMS calculated for $C_{19}H_{23}NO_4$ (M+H)⁺ 330.1661, found (M+H)⁺ 330.1694.

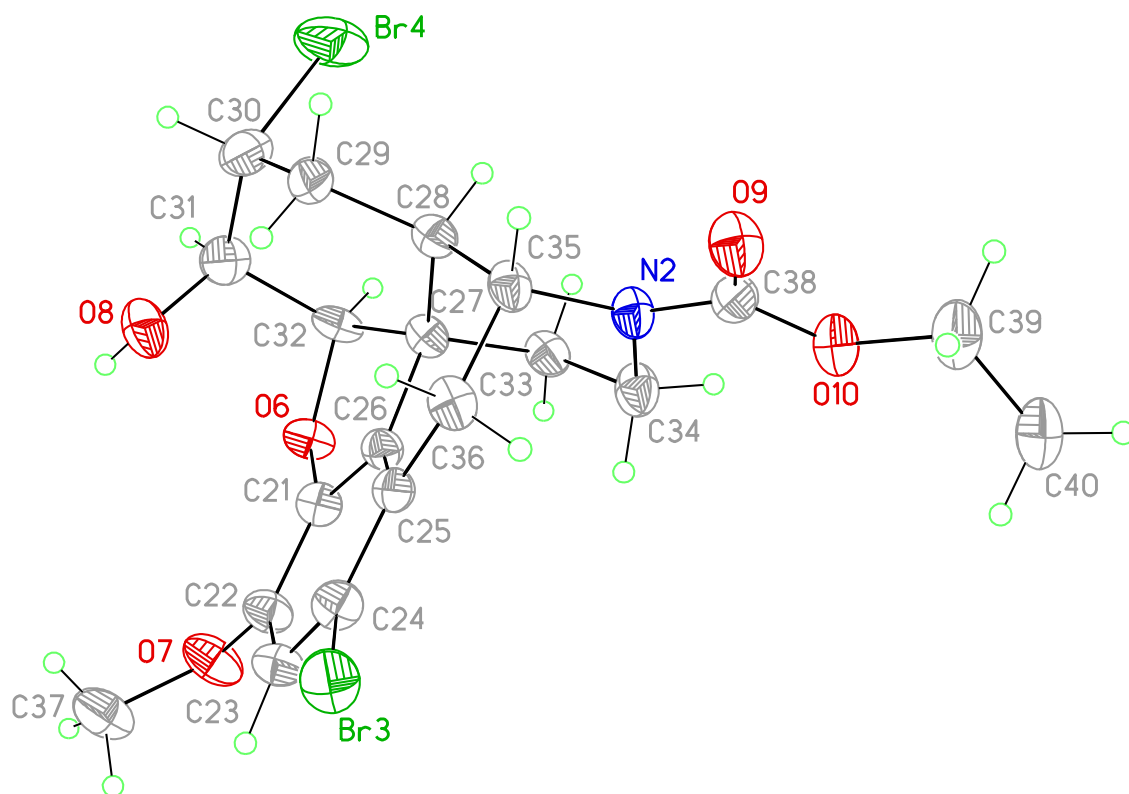
Appendix A. X-Ray Data.



View 1 of molecule **43** showing the atom labeling scheme. Displacement ellipsoids are scaled to the 50% probability level. The ethyl group disorder is shown.



View 2 of molecule **43** showing the atom labeling scheme. Displacement ellipsoids are scaled to the 50% probability level.



X-ray Experimental for $C_{20}H_{23}NO_5Br_2$: Crystals grew as clusters of colorless prisms by slow evaporation chloroform/hexanes. The data crystal was cut from a larger crystal and had approximate dimensions; 0.20 x 0.10 x 0.08 mm. The data were collected on a Rigaku SCX-Mini diffractometer with a Mercury 2 CCD using a graphite monochromator with $MoK\alpha$ radiation ($\lambda = 0.71075\text{\AA}$). A total of 1080 frames of data were collected using ω -scans with a scan range of 0.5° and a counting time of 30 seconds per frame. The data were collected at 223 K using a Rigaku Tech 50 low temperature device. Details of crystal data, data collection and structure refinement are listed in Table 1. Data reduction were performed using the Rigaku Americas Corporation's Crystal Clear version 1.40.¹ The structure was solved by direct methods using SIR97² and refined by full-matrix least-squares on F^2 with anisotropic displacement parameters for the non-H atoms using SHELXL-97.³ Structure analysis was aided by use of the programs PLATON98⁴ and WinGX.⁵ The hydrogen atoms on carbon were calculated in ideal positions with isotropic displacement parameters set to $1.2xU_{eq}$ of the attached atom ($1.5xU_{eq}$ for methyl hydrogen atoms). There are two crystallographically unique molecules in the asymmetric unit. The ethyl group on one molecule was disordered. The disorder was modeled by assigning the variable x to the site occupancy factor for one component of the disordered group and $(1-x)$ to the site occupancy factor for the alternate component. The variable x was refined while refining a common isotropic displacement parameter for the relevant atoms. In this way, the site occupancy factor for the major component consisting of atoms, C19 and C20 refined to 54(1)%. The geometry of the two

components was restrained to be equivalent throughout the refinement process. The function, $\sum w(|F_o|^2 - |F_c|^2)^2$, was minimized, where $w = 1/[(\sigma(F_o))^2 + (0.0343*P)^2 + (7.9623*P)]$ and $P = (|F_o|^2 + 2|F_c|^2)/3$. $R_w(F^2)$ refined to 0.118, with $R(F)$ equal to 0.0522 and a goodness of fit, S , = 1.00. Definitions used for calculating $R(F)$, $R_w(F^2)$ and the goodness of fit, S , are given below.⁶ The data were checked for secondary extinction but no correction was necessary. Neutral atom scattering factors and values used to calculate the linear absorption coefficient are from the International Tables for X-ray Crystallography (1992).⁷ All figures were generated using SHELXTL/PC.⁸ Tables of positional and thermal parameters, bond lengths and angles, torsion angles and figures are found elsewhere.

Table 1. Crystal data and structure refinement for **43**.

Empirical formula	C ₂₀ H ₂₃ Br ₂ N O ₅	
Formula weight	517.21	
Temperature	233(2) K	
Wavelength	0.71074 Å	
Crystal system	monoclinic	
Space group	P 21/c	
Unit cell dimensions	a = 16.2839(15) Å	α = 90°.
	b = 14.4371(13) Å	β = 110.846(2)°.
	c = 18.883(2) Å	γ = 90°.
Volume	4148.7(7) Å ³	
Z	8	
Density (calculated)	1.656 Mg/m ³	
Absorption coefficient	3.939 mm ⁻¹	
F(000)	2080	
Crystal size	0.200 x 0.100 x 0.080 mm	
Theta range for data collection	3.026 to 27.353°.	
Index ranges	-21 ≤ h ≤ 21, -18 ≤ k ≤ 18, -24 ≤ l ≤ 24	
Reflections collected	42393	
Independent reflections	9335 [R(int) = 0.0867]	
Completeness to theta = 25.242°	99.8 %	

Table 1, continued,

Absorption correction	Semi-empirical from equivalents
Max. and min. transmission	1.00 and 0.674
Refinement method	Full-matrix least-squares on F ²
Data / restraints / parameters	9335 / 25 / 532
Goodness-of-fit on F ²	1.004
Final R indices [I > 2σ(I)]	R1 = 0.0522, wR2 = 0.0983
R indices (all data)	R1 = 0.1007, wR2 = 0.1176
Extinction coefficient	n/a
Largest diff. peak and hole	0.654 and -0.533 e.Å ⁻³

Table 2. Atomic coordinates ($\times 10^4$) and equivalent isotropic displacement parameters ($\text{\AA}^2 \times 10^3$) for **43**. U(eq) is defined as one third of the trace of the orthogonalized U_{ij} tensor.

	x	y	z	U(eq)
Br1	1742(1)	6988(1)	6105(1)	60(1)
Br2	-1524(1)	8471(1)	8592(1)	58(1)
Br3	3470(1)	3996(1)	8764(1)	38(1)
Br4	6696(1)	5752(1)	6276(1)	59(1)
O1	337(2)	10045(2)	7532(2)	33(1)
O2	812(2)	10510(2)	6254(2)	48(1)
O3	-1043(2)	9022(2)	6635(2)	37(1)
O4	1736(2)	5557(3)	9368(2)	50(1)
O5	2809(2)	6566(3)	10010(2)	50(1)
O6	4767(2)	7174(2)	7372(2)	29(1)
O7	4158(2)	7571(2)	8610(2)	40(1)
O8	6216(2)	6193(2)	8252(2)	39(1)
O9	3393(2)	2613(2)	5690(2)	37(1)
O10	2337(2)	3627(2)	5000(2)	36(1)

Table 2, continued,

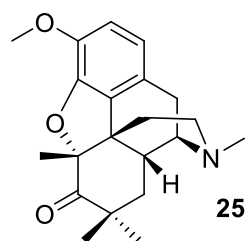
N1	1683(2)	7078(3)	8998(2)	36(1)
N2	3568(2)	4185(2)	5891(2)	28(1)
C1	760(3)	9452(3)	7191(2)	29(1)
C2	977(3)	9632(3)	6555(3)	35(1)
C3	1295(3)	8876(3)	6259(3)	37(1)
C4	1386(3)	8004(3)	6597(3)	33(1)
C5	1176(3)	7813(3)	7236(2)	28(1)
C6	887(3)	8577(3)	7522(2)	26(1)
C7	583(3)	8588(3)	8190(2)	27(1)
C8	195(3)	7644(3)	8278(2)	29(1)
C9	-707(3)	7464(3)	7682(3)	34(1)
C10	-1327(3)	8273(3)	7623(3)	39(1)
C11	-1004(3)	9177(3)	7396(2)	34(1)
C12	-60(3)	9431(3)	7945(2)	31(1)
C13	1156(3)	6869(3)	7589(2)	31(1)
C14	902(3)	6901(3)	8305(2)	32(1)
C15	2079(3)	8014(3)	9082(3)	40(1)
C16	1380(3)	8776(3)	8933(2)	37(1)
C17	1077(4)	10729(4)	5624(3)	65(2)
C18	2046(3)	6342(4)	9447(3)	38(1)

Table 2, continued,

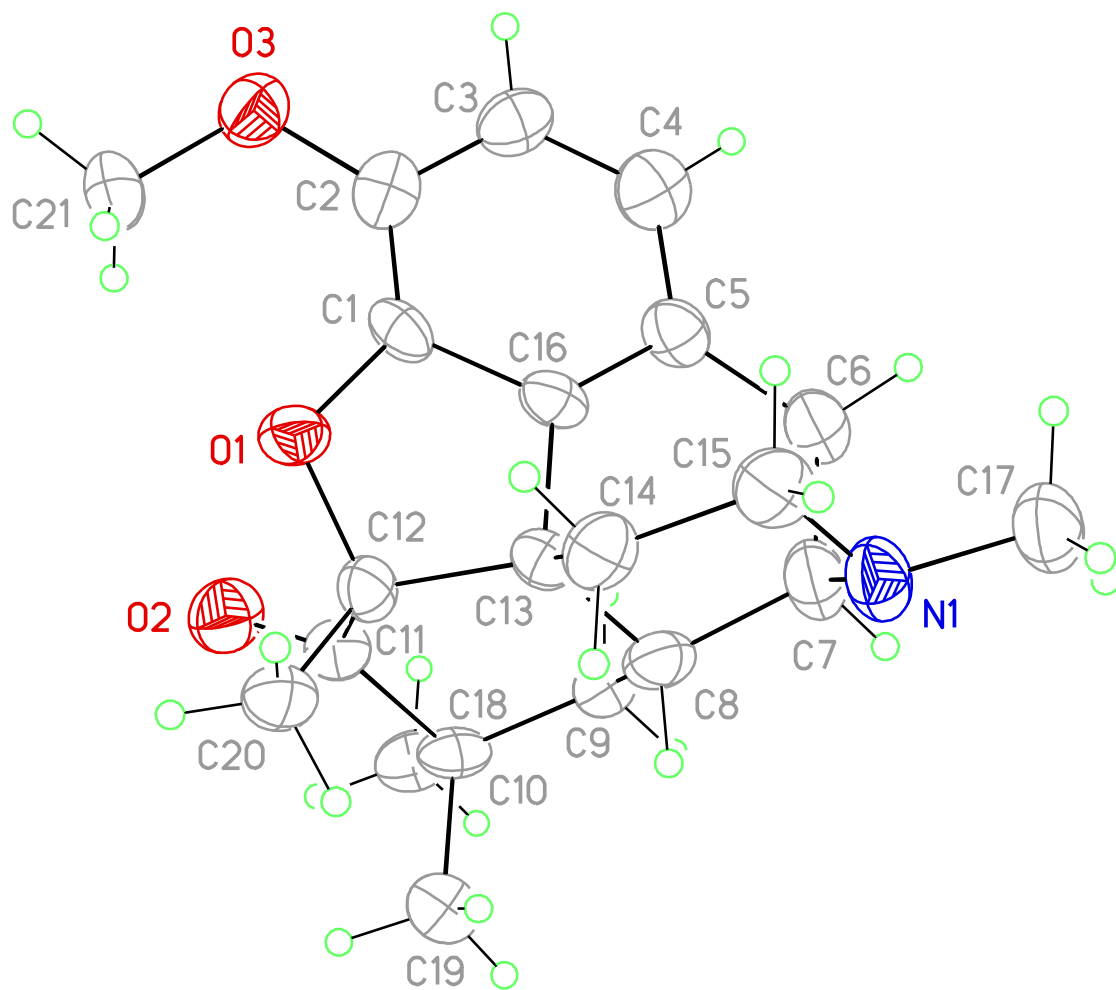
C19	3197(6)	5676(7)	10467(6)	32(2)
C20	4154(7)	5856(11)	10788(10)	50(4)
C19A	3265(8)	6075(9)	10699(7)	38(3)
C20A	3986(10)	5515(12)	10609(13)	51(5)
C21	4349(3)	6544(3)	7687(2)	26(1)
C22	4090(3)	6688(3)	8307(2)	29(1)
C23	3773(3)	5916(3)	8580(2)	31(1)
C24	3752(3)	5041(3)	8262(2)	28(1)
C25	3999(3)	4893(3)	7632(2)	23(1)
C26	4265(3)	5682(3)	7352(2)	23(1)
C27	4592(3)	5732(3)	6693(2)	24(1)
C28	5024(3)	4803(3)	6609(2)	26(1)
C29	5951(3)	4669(3)	7204(2)	32(1)
C30	6529(3)	5522(3)	7252(3)	37(1)
C31	6161(3)	6393(3)	7498(3)	34(1)
C32	5197(3)	6596(3)	6955(2)	29(1)
C33	3813(3)	5895(3)	5944(2)	29(1)
C34	3139(3)	5110(3)	5785(3)	33(1)
C35	4354(3)	4033(3)	6584(2)	27(1)
C36	4102(3)	3963(3)	7300(2)	28(1)

Table 2, continued,

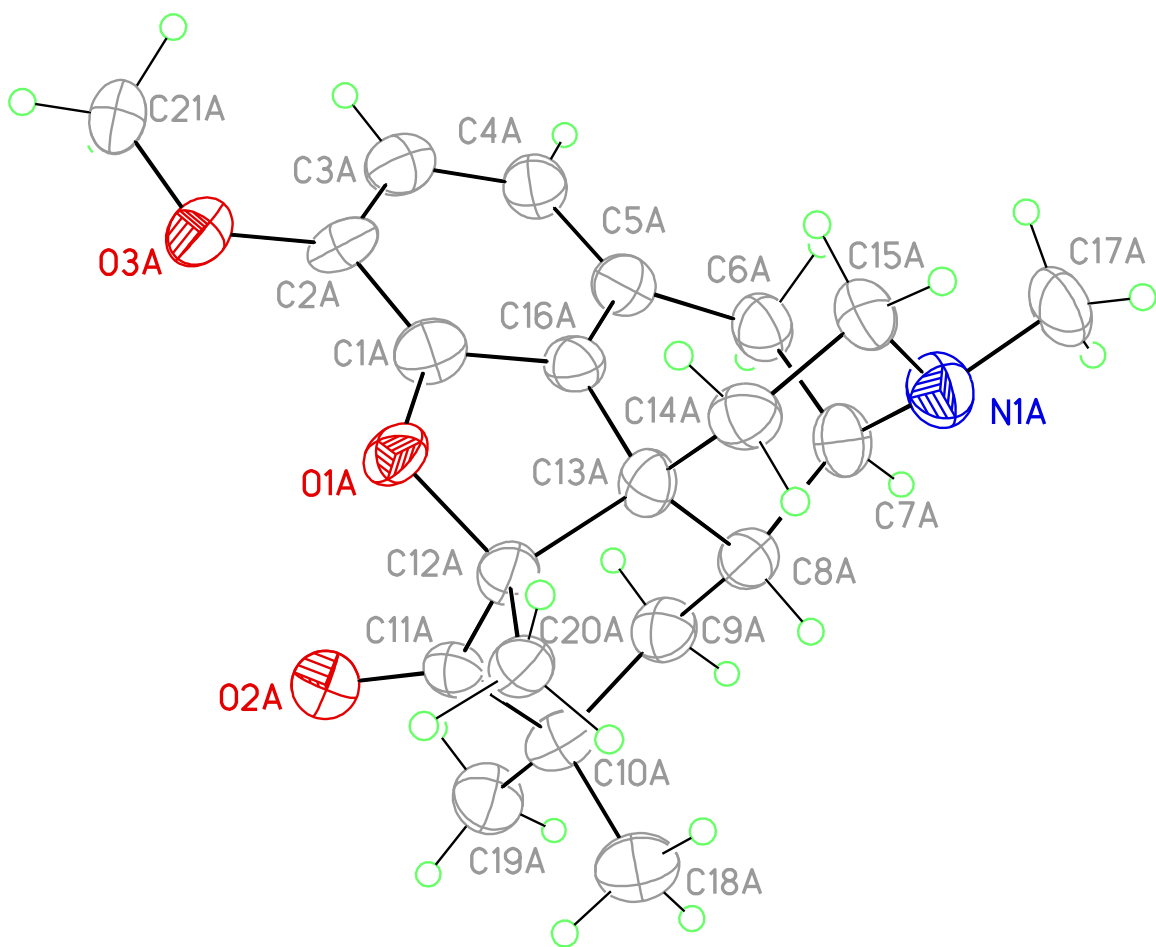
C37	4509(3)	7622(3)	9427(3)	45(1)
C38	3116(3)	3410(3)	5542(2)	29(1)
C39	1809(3)	2846(3)	4593(3)	44(1)
C40	872(3)	3146(4)	4293(3)	62(2)



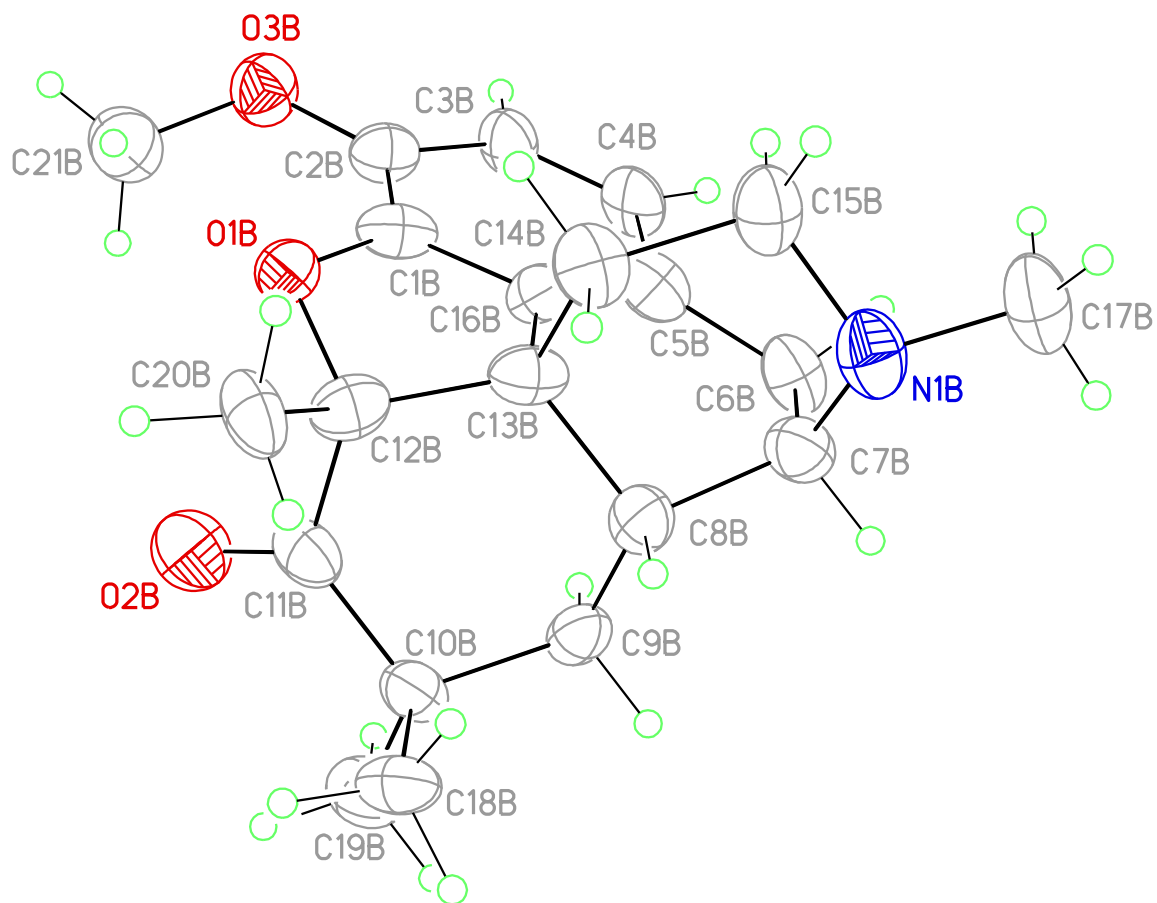
View 1 of molecule **25** showing the atom labeling scheme. Displacement ellipsoids are scaled to the 50% probability level.



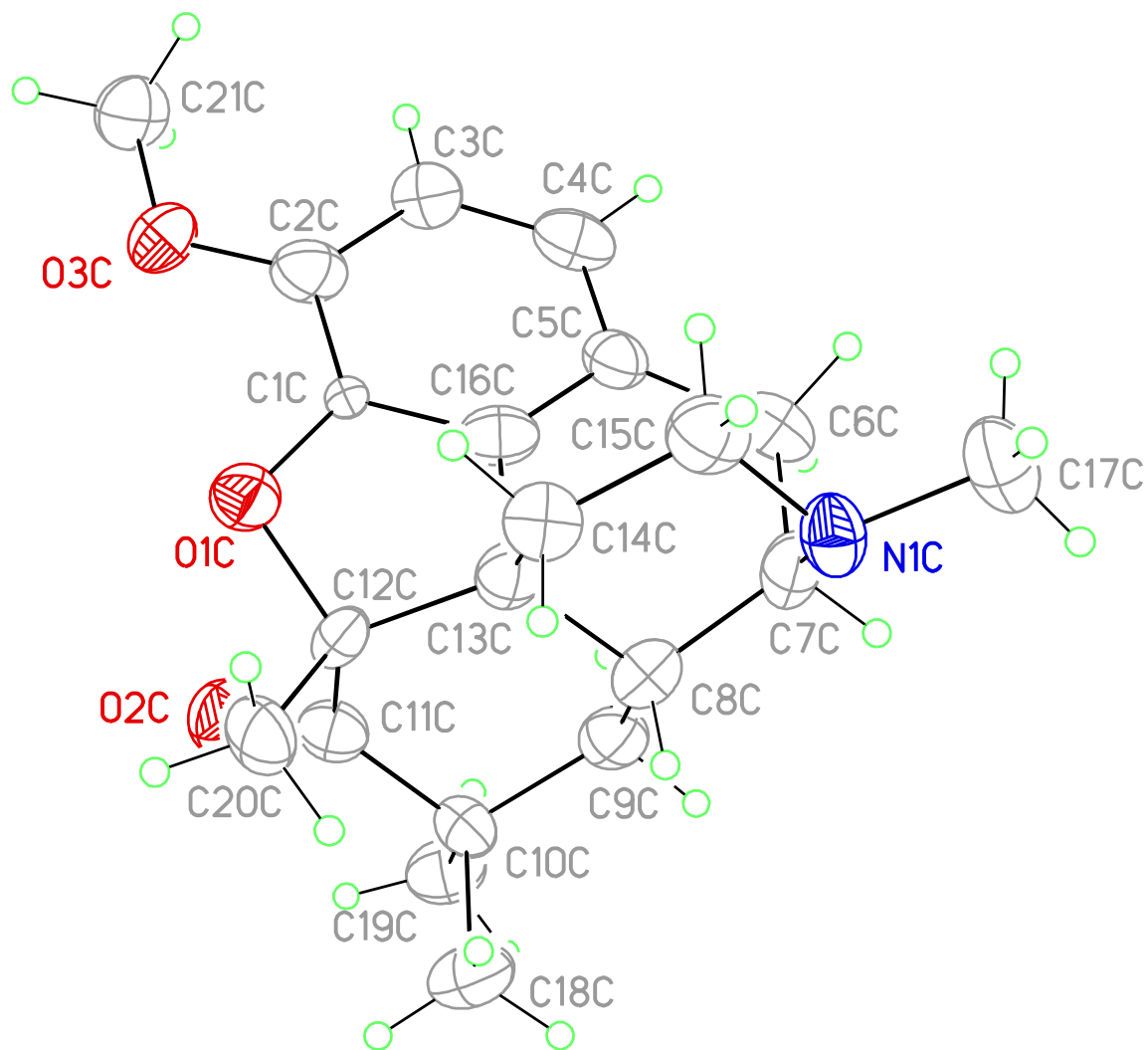
View 2 of molecule **25** showing the atom labeling scheme. Displacement ellipsoids are scaled to the 50% probability level.



View 3 of molecule **25** showing the atom labeling scheme. Displacement ellipsoids are scaled to the 50% probability level.



View 4 of molecule **25** showing the atom labeling scheme. Displacement ellipsoids are scaled to the 50% probability level.



X-ray Experimental for $C_{21}H_{27}NO_3$: Crystals grew as clusters of colorless prisms by slow evaporation chloroform/methanol/hexanes. The data crystal was cut from a large cluster and had approximate dimensions; 0.42 x 0.4 x 0.08 mm. The data were collected on a Rigaku AFC12 diffractometer with a Saturn 724+ CCD using a graphite monochromator with $MoK\alpha$ radiation ($\lambda = 0.71075\text{\AA}$). A total of 1872 frames of data were collected using ω -scans with a scan range of 0.5° and a counting time of 28 seconds per frame. The data were collected at 100 K using a Rigaku XStream low temperature device. Details of crystal data, data collection and structure refinement are listed in Table 1. Data reduction were performed using the Rigaku Americas Corporation's Crystal Clear version 1.40.¹ The structure was solved by direct methods using SIR97² and refined by full-matrix least-squares on F^2 with anisotropic displacement parameters for the non-H atoms using SHELXL-97.³ Structure analysis was aided by use of the programs PLATON98⁴ and WinGX.⁵ The hydrogen atoms were calculated in ideal positions with isotropic displacement parameters set to 1.2xUeq of the attached atom (1.5xUeq for methyl hydrogen atoms). The intensity statistics and the systematic absences indicated that the space group was the centrosymmetric space group, P21/c. However, the crystal was composed of an enantiopure molecule, of which there were four such molecules in the asymmetric unit. The absolute configuration was assigned on the basis of the known absolute configuration of the target molecule. The function, $\sum w(|F_O|^2 - |F_C|^2)^2$, was minimized, where $w = 1/[(\sigma(F_O))^2 + (0.10*P)^2]$ and $P = (|F_O|^2 + 2|F_C|^2)/3$. $R_w(F^2)$ refined to 0.286, with R(F) equal to 0.101 and a goodness of fit, S, = 1.46. Definitions

used for calculating $R(F)$, $R_w(F^2)$ and the goodness of fit, S , are given below.⁶ The data were checked for secondary extinction effects but no correction was necessary. Neutral atom scattering factors and values used to calculate the linear absorption coefficient are from the International Tables for X-ray Crystallography (1992).⁷ All figures were generated using SHELXTL/PC.⁸ Tables of positional and thermal parameters, bond lengths and angles, torsion angles and figures are found elsewhere.

Table 3. Crystal data and structure refinement for **25**.

Empirical formula	C ₂₁ H ₂₇ N O ₃	
Formula weight	341.44	
Temperature	100(2) K	
Wavelength	0.71075 Å	
Crystal system	Monoclinic	
Space group	P21	
Unit cell dimensions	a = 11.360(8) Å	α = 90°.
	b = 9.549(8) Å	β = 90.276(13)°.
	c = 33.13(2) Å	γ = 90°.
Volume	3594(4) Å ³	
Z	8	
Density (calculated)	1.262 Mg/m ³	
Absorption coefficient	0.084 mm ⁻¹	
F(000)	1472	
Crystal size	0.42 x 0.14 x 0.08 mm	
Theta range for data collection	1.23 to 25.00°.	
Index ranges	-13 ≤ h ≤ 13, -11 ≤ k ≤ 11, -39 ≤ l ≤ 39	
Reflections collected	49301	
Independent reflections	11803 [R(int) = 0.0761]	
Completeness to theta = 25.00°	100.0 %	

Table 3, continued,

Absorption correction	Semi-empirical from equivalents
Max. and min. transmission	1.00 and 0.521
Refinement method	Full-matrix-block least-squares on F^2
Data / restraints / parameters	11803 / 1 / 920
Goodness-of-fit on F^2	1.464
Final R indices [$I > 2\sigma(I)$]	R1 = 0.1009, wR2 = 0.2669
R indices (all data)	R1 = 0.1283, wR2 = 0.2857
Largest diff. peak and hole	0.680 and -0.328 e. \AA^{-3}

Table 4. Atomic coordinates ($\times 10^4$) and equivalent isotropic displacement parameters ($\text{\AA}^2 \times 10^3$) for **25**. U(eq) is defined as one third of the trace of the orthogonalized U_{ij} tensor.

	x	y	z	U(eq)
O1	1736(3)	5240(5)	1950(1)	36(1)
O2	735(4)	4606(6)	1235(1)	49(1)
O3	666(4)	8102(5)	2203(1)	46(1)
N1	6180(4)	5405(6)	1664(2)	44(1)
C1	2173(5)	6598(7)	1919(2)	31(1)
C2	1743(5)	7854(8)	2027(2)	39(2)
C3	2421(5)	9040(8)	1945(2)	41(2)
C4	3490(5)	8987(8)	1748(2)	47(2)
C5	3969(5)	7689(7)	1634(2)	37(1)
C6	5063(5)	7495(8)	1374(2)	42(2)
C7	5423(5)	5929(8)	1342(2)	44(2)
C8	4383(5)	4927(7)	1279(2)	37(1)
C9	3629(5)	5214(7)	907(2)	37(2)
C10	2567(5)	4280(7)	868(1)	33(1)
C11	1783(5)	4448(7)	1251(2)	38(1)

Table 4, continued,

C12	2410(5)	4346(7)	1679(2)	31(1)
C13	3652(5)	4990(7)	1670(2)	32(1)
C14	4462(5)	4483(8)	2021(2)	39(2)
C15	5573(5)	5322(8)	2055(2)	43(2)
C16	3334(5)	6534(6)	1733(2)	31(1)
C17	7307(5)	6136(9)	1700(2)	57(2)
C18	1802(5)	4709(8)	505(2)	43(2)
C19	2909(6)	2735(8)	830(2)	48(2)
C20	2300(5)	2846(7)	1833(2)	40(2)
C21	-138(5)	6945(8)	2214(2)	52(2)
O1A	6675(3)	1335(5)	590(1)	36(1)
O2A	5849(4)	1493(5)	1346(1)	47(1)
O3A	5090(4)	-594(5)	200(1)	46(1)
N1A	10987(4)	-91(7)	766(2)	47(2)
C1A	6890(5)	-59(7)	536(2)	39(2)
C2A	6168(5)	-1050(7)	352(2)	36(1)
C3A	6562(5)	-2424(8)	338(2)	43(2)
C4A	7656(5)	-2814(7)	508(2)	41(2)
C5A	8400(5)	-1827(7)	687(2)	37(2)
C6A	9553(5)	-2061(8)	907(2)	43(2)

Table 4, continued,

C7A	10190(5)	-759(7)	1063(2)	40(2)
C8A	9360(5)	422(7)	1213(2)	36(1)
C9A	8591(5)	-10(8)	1563(2)	41(2)
C10A	7705(6)	1139(8)	1684(2)	43(2)
C11A	6919(5)	1463(7)	1322(2)	32(1)
C12A	7490(5)	1783(7)	912(2)	36(1)
C13A	8599(5)	838(7)	836(2)	34(1)
C14A	9423(5)	1443(7)	503(2)	39(2)
C15A	10393(5)	402(8)	403(2)	42(2)
C16A	8016(5)	-442(7)	680(2)	33(1)
C17A	12024(5)	-968(8)	678(2)	53(2)
C18A	8335(6)	2513(8)	1824(2)	51(2)
C19A	6961(5)	620(9)	2035(2)	51(2)
C20A	7667(5)	3368(6)	860(2)	33(1)
C21A	4403(5)	-1608(8)	-10(2)	49(2)
O1B	8212(3)	1027(5)	3045(1)	35(1)
O2B	9273(4)	437(6)	3756(1)	54(1)
O3B	9257(3)	3835(5)	2756(1)	45(1)
N1B	3793(4)	1187(6)	3366(2)	43(1)
C1B	7759(5)	2367(7)	3071(2)	35(1)

Table 4, continued,

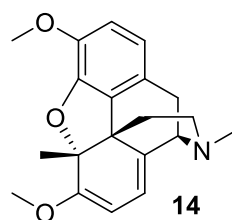
C2B	8214(5)	3626(7)	2950(2)	36(1)
C3B	7533(5)	4835(7)	3040(2)	38(2)
C4B	6509(5)	4800(7)	3239(2)	40(2)
C5B	6050(5)	3474(7)	3373(2)	40(2)
C6B	4967(5)	3346(7)	3635(2)	43(2)
C7B	4592(5)	1766(7)	3678(2)	38(1)
C8B	5626(5)	749(7)	3741(2)	35(1)
C9B	6398(5)	1072(7)	4105(2)	34(1)
C10B	7492(5)	108(7)	4133(2)	37(2)
C11B	8213(6)	267(7)	3751(2)	39(2)
C12B	7568(5)	154(7)	3338(2)	39(2)
C13B	6339(5)	813(7)	3340(2)	35(1)
C14B	5516(5)	245(7)	3007(2)	40(2)
C15B	4388(5)	1107(8)	2970(2)	44(2)
C16B	6654(5)	2322(8)	3267(2)	39(2)
C17B	2686(5)	1958(8)	3332(2)	51(2)
C18B	7143(6)	-1426(7)	4179(2)	41(2)
C19B	8249(6)	531(9)	4496(2)	51(2)
C20B	7702(5)	-1349(7)	3186(2)	41(2)
C21B	10151(6)	2781(9)	2804(2)	54(2)

Table 4, continued,

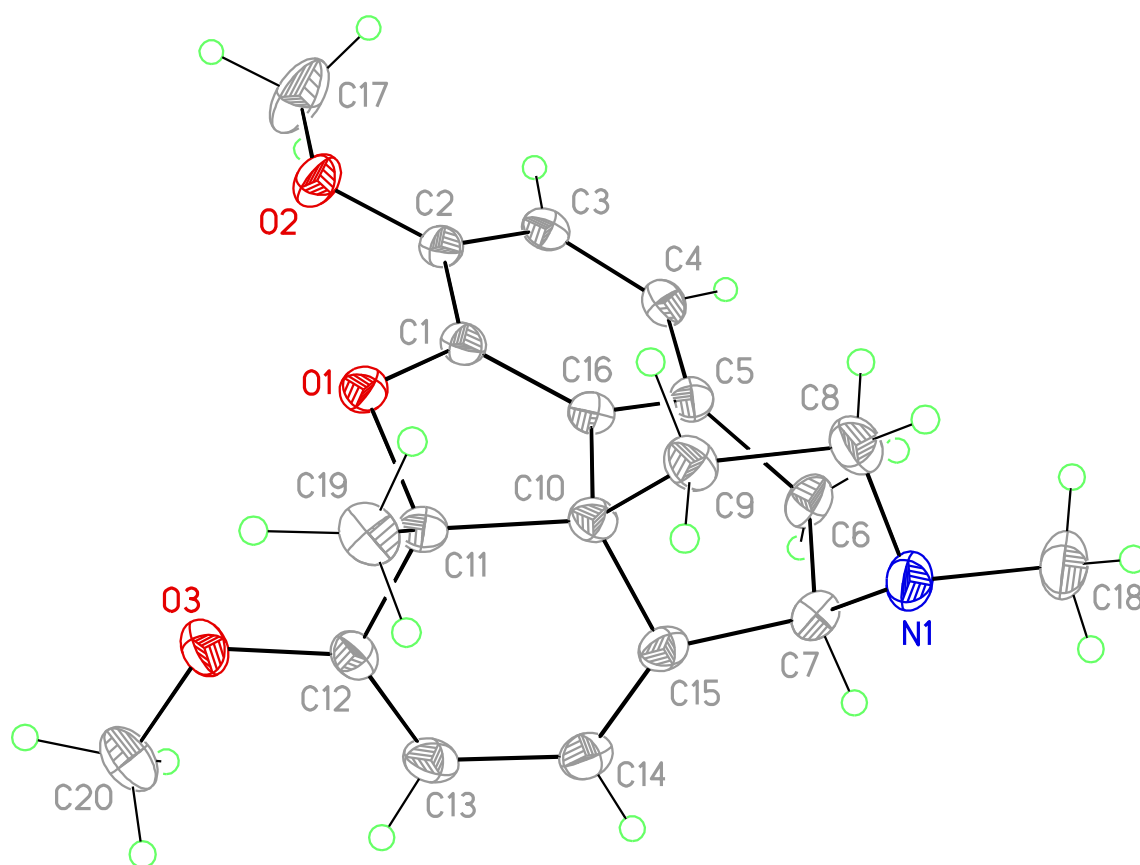
O1C	3360(3)	7157(5)	4400(1)	39(1)
O2C	4179(4)	7319(5)	3654(1)	47(1)
O3C	4899(3)	5238(5)	4803(1)	45(1)
N1C	-979(4)	5755(6)	4222(1)	38(1)
C1C	3140(4)	5744(6)	4454(1)	27(1)
C2C	3858(5)	4782(8)	4652(2)	42(2)
C3C	3457(5)	3374(7)	4662(2)	37(2)
C4C	2352(5)	3023(8)	4494(2)	43(2)
C5C	1625(5)	4012(7)	4315(2)	34(1)
C6C	449(5)	3737(7)	4096(2)	44(2)
C7C	-180(5)	5096(7)	3937(2)	39(2)
C8C	662(5)	6229(8)	3788(2)	38(2)
C9C	1409(5)	5796(7)	3429(2)	39(2)
C10C	2327(5)	6932(7)	3312(2)	35(1)
C11C	3103(5)	7290(7)	3673(2)	35(1)
C12C	2502(4)	7602(7)	4089(1)	29(1)
C13C	1408(5)	6676(7)	4156(2)	36(1)
C14C	576(5)	7264(7)	4486(2)	39(2)
C15C	-385(5)	6237(8)	4590(2)	45(2)
C16C	2026(5)	5385(7)	4314(2)	37(2)

Table 4, continued,

C17C	-2032(5)	4889(8)	4316(2)	51(2)
C18C	1692(6)	8295(8)	3166(2)	47(2)
C19C	3069(5)	6387(8)	2967(2)	46(2)
C20C	2322(5)	9166(7)	4128(2)	43(2)
C21C	5604(5)	4238(8)	5010(2)	46(2)



View of **14** showing the atom labeling scheme. Displacement ellipsoids are scaled to the 50% probability level.



X-ray Experimental for $C_{20}H_{23}NO_3$: Crystals grew as large, colorless prisms by slow evaporation ethyl acetate. The data crystal was cut from a larger crystal and had approximate dimensions; 0.37 x 0.30 x 0.15 mm. The data were collected on a Rigaku SCX-Mini diffractometer with a Mercury 2 CCD using a graphite monochromator with $MoK\alpha$ radiation ($\lambda = 0.71075\text{\AA}$). A total of 720 frames of data were collected using ω -scans with a scan range of 1° and a counting time of 45 seconds per frame. The data were collected at 153 K using a Rigaku XStream low temperature device. Details of crystal data, data collection and structure refinement are listed in Table 1. Data reduction were performed using the Rigaku Americas Corporation's Crystal Clear version 1.40.¹ The structure was solved by direct methods using SIR97² and refined by full-matrix least-squares on F^2 with anisotropic displacement parameters for the non-H atoms using SHELXL-97.³ Structure analysis was aided by use of the programs PLATON98⁴ and WinGX.⁵ The hydrogen atoms on carbon were calculated in ideal positions with isotropic displacement parameters set to 1.2xUeq of the attached atom (1.5xUeq for methyl hydrogen atoms). The absolute configuration was assigned on the basis of the known configuration of the molecule. The function, $\sum w(|F_o|^2 - |F_c|^2)^2$, was minimized, where $w = 1/[(\sigma(F_o))^2 + (0.0959*P)^2 + (0.0258*P)]$ and $P = (|F_o|^2 + 2|F_c|^2)/3$. $R_w(F^2)$ refined to 0.0912, with $R(F)$ equal to 0.0336 and a goodness of fit, S , = 1.06. Definitions used for calculating $R(F)$, $R_w(F^2)$ and the goodness of fit, S , are given below.⁶ The data were checked for secondary extinction but no correction was necessary. Neutral atom scattering factors and values used to calculate the linear absorption coefficient are from

the International Tables for X-ray Crystallography (1992).⁷ All figures were generated using SHELXTL/PC.⁸ Tables of positional and thermal parameters, bond lengths and angles, torsion angles and figures are found elsewhere.

Table 5. Crystal data and structure refinement for **14**.

Empirical formula	C ₂₀ H ₂₃ N O ₃	
Formula weight	325.39	
Temperature	153(2) K	
Wavelength	0.71075 Å	
Crystal system	Orthorhombic	
Space group	P212121	
Unit cell dimensions	a = 8.9446(4) Å	α = 90°.
	b = 10.6291(6) Å	β = 90°.
	c = 17.4821(9) Å	γ = 90°.
Volume	1662.08(15) Å ³	
Z	4	
Density (calculated)	1.300 Mg/m ³	
Absorption coefficient	0.087 mm ⁻¹	
F(000)	696	
Crystal size	0.37 x 0.30 x 0.15 mm	
Theta range for data collection	2.24 to 27.49°.	
Index ranges	-11 ≤ h ≤ 11, -13 ≤ k ≤ 13, -22 ≤ l ≤ 22	
Reflections collected	23721	
Independent reflections	3819 [R(int) = 0.0408]	
Completeness to theta = 27.49°	100.0 %	

Table 5, continued,

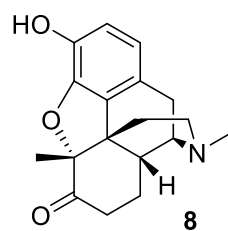
Absorption correction	Semi-empirical from equivalents
Max. and min. transmission	1.00 and 0.941
Refinement method	Full-matrix least-squares on F ²
Data / restraints / parameters	3819 / 0 / 221
Goodness-of-fit on F ²	1.058
Final R indices [I > 2σ(I)]	R1 = 0.0336, wR2 = 0.0900
R indices (all data)	R1 = 0.0348, wR2 = 0.0912
Absolute structure parameter	0.1(7)
Largest diff. peak and hole	0.162 and -0.211 e.Å ⁻³

Table 6. Atomic coordinates ($\times 10^4$) and equivalent isotropic displacement parameters ($\text{\AA}^2 \times 10^3$) for **14**. U(eq) is defined as one third of the trace of the orthogonalized U^{ij} tensor.

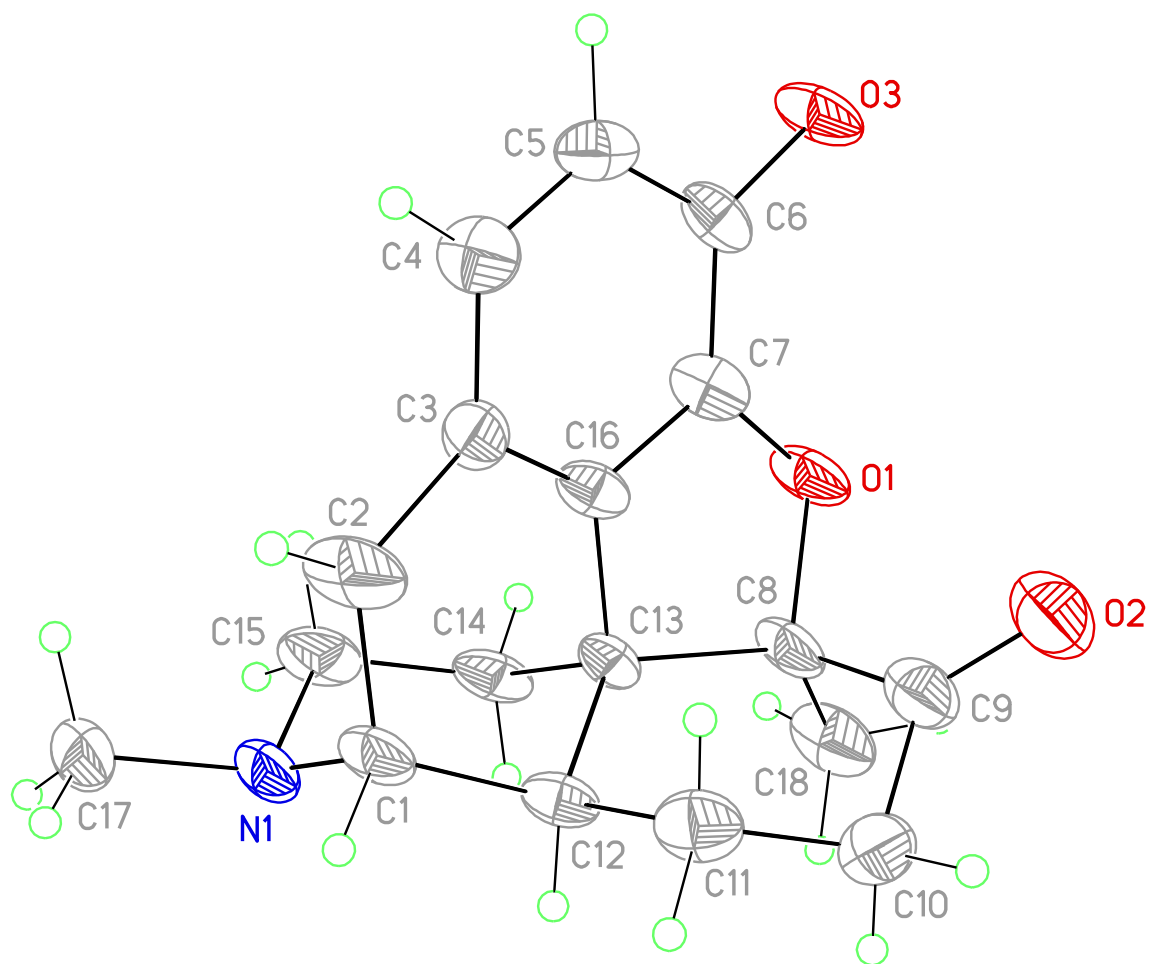
	x	y	z	U(eq)
C1	5470(1)	2739(1)	1857(1)	18(1)
C2	6824(1)	2575(1)	1472(1)	20(1)
C3	8066(1)	2255(1)	1920(1)	21(1)
C4	7950(1)	2071(1)	2714(1)	21(1)
C5	6587(1)	2238(1)	3094(1)	20(1)
C6	6289(1)	1872(1)	3922(1)	25(1)
C7	4627(1)	2088(1)	4184(1)	24(1)
C8	4603(1)	4352(1)	3989(1)	26(1)
C9	3670(1)	4209(1)	3266(1)	23(1)
C10	3825(1)	2883(1)	2906(1)	19(1)
C11	2956(1)	2747(1)	2133(1)	19(1)
C12	2315(1)	1435(1)	2033(1)	20(1)
C13	2189(1)	600(1)	2606(1)	24(1)
C14	2854(1)	826(1)	3356(1)	24(1)
C15	3593(1)	1888(1)	3508(1)	21(1)

Table 6, continued,

C16	5403(1)	2638(1)	2642(1)	18(1)
C17	8196(2)	2482(2)	306(1)	46(1)
C18	5132(2)	3527(2)	5240(1)	36(1)
C19	1736(1)	3719(1)	1977(1)	26(1)
C20	1058(2)	118(1)	1131(1)	31(1)
N1	4309(1)	3331(1)	4529(1)	27(1)
O1	4101(1)	2974(1)	1529(1)	21(1)
O2	6819(1)	2729(1)	693(1)	26(1)
O3	1769(1)	1283(1)	1306(1)	26(1)



View of **8** showing the atom labeling scheme. Displacement ellipsoids are scaled to the 50% probability level.



X-ray Experimental for $C_{18}H_{19}NO_3 - \frac{1}{2} C_6H_{14}$: Crystals grew as colorless needles by slow evaporation from hexanes, methanol and dichloromethane. The data crystal was cut from a larger crystal and had approximate dimensions; 0.20 x 0.08 x 0.05 mm. The data were collected on a Rigaku ACF-12 with a Saturn 724+ CCD using a graphite monochromator with $MoK\alpha$ radiation ($\lambda = 0.71075\text{\AA}$). A total of 1632 frames of data were collected using ω -scans with a scan range of 0.5° and a counting time of 29 seconds per frame. The data were collected at 100 K using a Rigaku XStream low temperature device. Details of crystal data, data collection and structure refinement are listed in Table 1. Data reduction were performed using the Rigaku Americas Corporation's Crystal Clear version 1.40.¹ The structure was solved by direct methods using SIR97² and refined by full-matrix least-squares on F^2 with anisotropic displacement parameters for the non-H atoms using SHELXL-97.³ A molecule of what appeared to be n-hexane was disordered in a cylindrical region along the c-axis. Attempts to model the disorder were unsatisfactory. The contributions to the scattering factors due to the solvent molecule was removed by use of the utility SQUEEZE⁴ in PLATON98.⁵ Structure analysis was aided by use of the programs PLATON98 as incorporated into WinGX.⁵ The hydrogen atoms on carbon were calculated in ideal positions with isotropic displacement parameters set to $1.2xU_{eq}$ of the attached atom ($1.5xU_{eq}$ for methyl hydrogen atoms). The function, $\sum w(|F_O|^2 - |F_C|^2)^2$, was minimized, where $w = 1/[(\sigma(F_O))^2 + (0.0973*P)^2 + (4.441*P)]$ and $P = (|F_O|^2 + 2|F_C|^2)/3$. $R_w(F^2)$ refined to 0.255, with $R(F)$ equal to 0.117 and a goodness of fit, S , = 1.12. Definitions used for calculating $R(F)$, $R_w(F^2)$ and the

goodness of fit, S , are given below.⁶ The data were checked for secondary extinction effects but no correction was necessary. Neutral atom scattering factors and values used to calculate the linear absorption coefficient are from the International Tables for X-ray Crystallography (1992).⁷ All figures were generated using SHELXTL/PC.⁸ Tables of positional and thermal parameters, bond lengths and angles, torsion angles and figures are found elsewhere.

Table 7. Crystal data and structure refinement for **8**.

Empirical formula	C ₂₁ H ₂₆ N O ₃	
Formula weight	340.43	
Temperature	100(2) K	
Wavelength	0.71073 Å	
Crystal system	trigonal	
Space group	P 31 2 1	
Unit cell dimensions	a = 11.7452(15) Å	α = 90°.
	b = 11.7452(15) Å	β = 90°.
	c = 21.772(2) Å	γ = 120°.
Volume	2601.1(7) Å ³	
Z	6	
Density (calculated)	1.304 Mg/m ³	
Absorption coefficient	0.086 mm ⁻¹	
F(000)	1098	
Crystal size	0.200 x 0.080 x 0.050 mm	
Theta range for data collection	3.449 to 27.484°.	
Index ranges	-15 ≤ h ≤ 15, -15 ≤ k ≤ 15, -28 ≤ l ≤ 28	
Reflections collected	46897	
Independent reflections	3982 [R(int) = ?]	
Completeness to theta = 25.242°	99.7 %	

Table 7, continued,

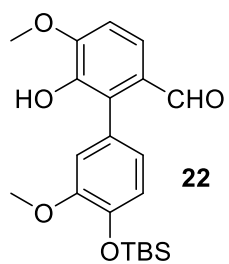
Absorption correction	Semi-empirical from equivalents
Max. and min. transmission	1.00 and 0.869
Refinement method	Full-matrix least-squares on F ²
Data / restraints / parameters	3982 / 0 / 201
Goodness-of-fit on F ²	1.123
Final R indices [I > 2σ(I)]	R1 = 0.1172, wR2 = 0.2433
R indices (all data)	R1 = 0.1372, wR2 = 0.2550
Absolute structure parameter	0.0(9)
Extinction coefficient	n/a
Largest diff. peak and hole	0.376 and -0.294 e.Å ⁻³

Table 8. Atomic coordinates ($\times 10^4$) and equivalent isotropic displacement parameters ($\text{\AA}^2 \times 10^3$) for **8**. U(eq) is defined as one third of the trace of the orthogonalized U_{ij} tensor.

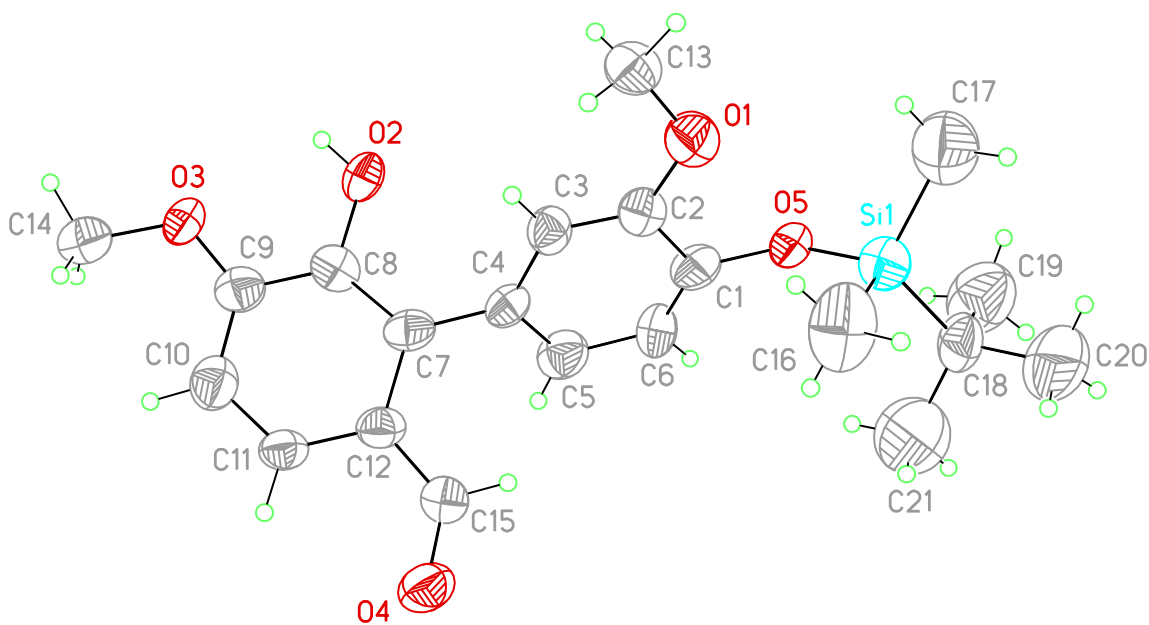
	x	y	z	U(eq)
C1	-2093(7)	-4753(7)	5224(3)	31(2)
C2	-1799(9)	-3428(7)	5518(3)	48(2)
C3	-2021(6)	-3519(6)	6209(3)	31(1)
C4	-1765(7)	-2473(7)	6594(3)	36(2)
C5	-2080(7)	-2661(7)	7210(3)	34(2)
C6	-2721(6)	-3912(7)	7484(3)	31(2)
C7	-2976(7)	-4942(7)	7092(3)	33(2)
C8	-4023(7)	-6962(7)	6631(3)	32(2)
C9	-5359(7)	-7106(7)	6449(3)	38(2)
C10	-5635(7)	-7203(7)	5765(3)	41(2)
C11	-4570(7)	-6049(7)	5422(3)	37(2)
C12	-3242(6)	-5992(6)	5507(2)	27(1)
C13	-2901(6)	-6027(6)	6189(2)	23(1)
C14	-1685(7)	-6206(7)	6206(3)	32(2)
C15	-542(7)	-5100(8)	5861(3)	39(2)

Table 8, continued,

C16	-2584(6)	-4740(6)	6487(3)	26(1)
C17	227(8)	-3913(9)	4896(3)	55(2)
C18	-4225(9)	-8348(7)	6730(3)	45(2)
N1	-922(6)	-4952(6)	5229(2)	37(1)
O1	-3641(5)	-6286(4)	7236(2)	37(1)
O2	-6112(6)	-7134(6)	6825(3)	53(2)
O3	-3017(5)	-4037(5)	8093(2)	40(1)



View of **22** showing the atom labeling scheme. Displacement ellipsoids are scaled to the 50% probability level.



X-ray Experimental for $C_{21}H_{28}O_5Si - \frac{1}{2} C_6H_{14}$: Crystals grew as colorless plates by slow evaporation from hexanes. The data were collected on a Nonius Kappa CCD diffractometer using a graphite monochromator with MoK α radiation ($\lambda = 0.71073\text{\AA}$). A total of 473 frames of data were collected using ω -scans with a scan range of 0.7° and a counting time of 108 seconds per frame. The data were collected at 153 K using an Oxford Cryostream low temperature device. Details of crystal data, data collection and structure refinement are listed in Table 1. Data reduction were performed using DENZO-SMN.¹ The structure was solved by direct methods using SIR97² and refined by full-matrix least-squares on F^2 with anisotropic displacement parameters for the non-H atoms using SHELXL-2013.³ The hydrogen atoms were calculated in ideal positions with isotropic displacement parameters set to 1.2xUeq of the attached atom (1.5xUeq for methyl hydrogen atoms).

A molecule of n-hexane was disordered along a cylindrical void near 0.085, $\frac{1}{4}$, z. Attempts to model the disorder were unsatisfactory. The contributions to the scattering factors due to this solvent molecule were removed by use of the utility SQUEEZE⁴ in PLATON98⁵. PLATON98 was used as incorporated in WinGX⁶. The function, $\sum w(|F_o|^2 - |F_c|^2)^2$, was minimized, where $w = 1/[(\sigma(F_o))^2 + (0.1656*P)^2]$ and $P = (|F_o|^2 + 2|F_c|^2)/3$. $R_w(F^2)$ refined to 0.566, with R(F) equal to 0.238 and a goodness of fit, S, = 2.26. Definitions used for calculating R(F), $R_w(F^2)$ and the goodness of fit, S, are given below.⁶ Neutral atom scattering factors and values used to calculate the linear absorption coefficient are from the International Tables for X-ray Crystallography (1992).⁷All

figures were generated using SHELXTL/PC.⁸ Tables of positional and thermal parameters, bond lengths and angles, torsion angles, figures and lists of observed and calculated structure factors are located in tables 1 through 7.

Table 9. Crystal data and structure refinement for **22**.

Empirical formula	C ₂₄ H ₃₅ O ₅ Si	
Formula weight	431.61	
Temperature	153(2) K	
Wavelength	0.71073 Å	
Crystal system	monoclinic	
Space group	P 21/c	
Unit cell dimensions	a = 20.3140(7) Å	α = 90°.
	b = 16.5310(17) Å	β = 94.265(6)°.
	c = 7.0680(17) Å	γ = 90°.
Volume	2366.9(6) Å ³	
Z	4	
Density (calculated)	1.211 Mg/m ³	
Absorption coefficient	0.130 mm ⁻¹	
F(000)	932	
Theta range for data collection	3.142 to 24.916°.	
Index ranges	-23 ≤ h ≤ 24, -19 ≤ k ≤ 19, -8 ≤ l ≤ 8	
Reflections collected	5964	
Independent reflections	3572 [R(int) = 0.1076]	
Completeness to theta = 25.242°	83.2 %	
Absorption correction	Semi-empirical from equivalents	
Max. and min. transmission	1.00 and 0.832	

Table 9, continued,

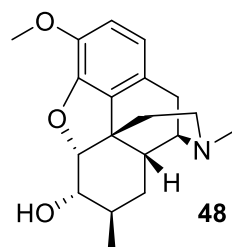
Refinement method	Full-matrix least-squares on F^2
Data / restraints / parameters	3572 / 162 / 252
Goodness-of-fit on F^2	2.257
Final R indices [$I > 2\sigma(I)$]	R1 = 0.2382, wR2 = 0.5343
R indices (all data)	R1 = 0.3309, wR2 = 0.5660
Extinction coefficient	n/a
Largest diff. peak and hole	0.779 and -0.621 e. \AA^{-3}

Table 10. Atomic coordinates ($\times 10^4$) and equivalent isotropic displacement parameters ($\text{\AA}^2 \times 10^3$) for **22**. U(eq) is defined as one third of the trace of the orthogonalized U_{ij} tensor.

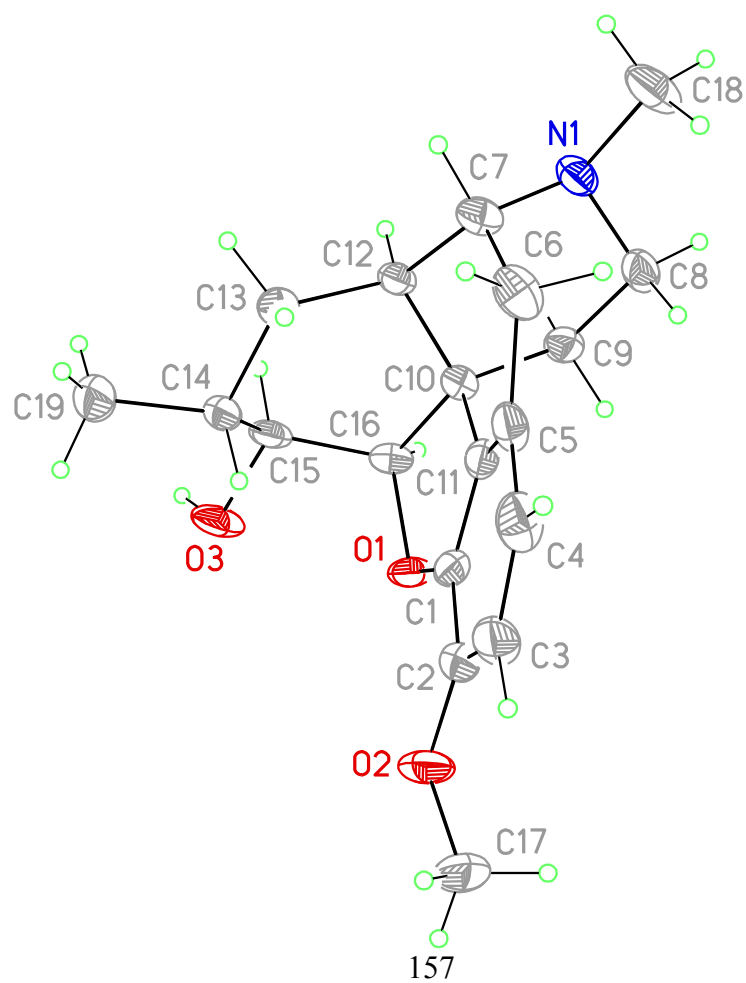
	x	y	z	U(eq)
Si1	1643(2)	5166(3)	9311(6)	61(2)
O1	2560(5)	3640(6)	10885(15)	63(3)
O2	4475(4)	2258(5)	8299(14)	50(3)
O3	5744(4)	1912(5)	8261(14)	52(3)
O4	5355(5)	5662(6)	7047(15)	65(3)
O5	1985(4)	4492(5)	7942(12)	49(3)
C1	2666(7)	4285(8)	7919(19)	48(4)
C2	2963(7)	3827(8)	9468(19)	44(4)
C3	3603(6)	3623(8)	9540(19)	44(4)
C4	3982(6)	3847(8)	7911(19)	43(4)
C5	3680(7)	4282(8)	6420(20)	57(4)
C6	2991(7)	4473(8)	6420(20)	51(4)
C7	4684(7)	3672(8)	8044(18)	46(4)
C8	4943(6)	2878(8)	8106(17)	40(3)
C9	5608(7)	2680(9)	8140(20)	49(4)

Table 10, continued,

C10	6052(7)	3309(9)	7910(20)	57(4)
C11	5830(6)	4106(8)	7808(18)	43(4)
C12	5162(6)	4308(8)	7793(18)	45(4)
C13	2828(7)	3074(9)	12301(19)	54(4)
C14	6420(7)	1666(9)	8190(20)	66(5)
C15	4992(6)	5104(8)	7585(17)	39(3)
C16	2325(8)	5653(12)	10910(30)	97(6)
C17	1026(9)	4650(12)	10630(30)	99(6)
C18	1253(7)	5931(10)	7710(20)	62(4)
C19	750(10)	5533(13)	6320(30)	113(7)
C20	887(10)	6559(13)	8770(30)	113(7)
C21	1762(11)	6376(15)	6550(40)	143(9)



View of **48** showing the atom labeling scheme. Displacement ellipsoids are scaled to the 50% probability level.



X-ray Experimental for C₁₉H₂₅NO₃ – H₂O: Crystals grew as colorless prisms by slow evaporation chloroform/methanol/hexanes. The data crystal was cut from a larger crystal and had approximate dimensions; 0.18 x 0.12 x 0.10 mm. The data were collected on a Rigaku AFC12 diffractometer with a Saturn 724+ CCD using a graphite monochromator with MoK α radiation ($\lambda = 0.71073\text{\AA}$). A total of 755 frames of data were collected using ω -scans with a scan range of 0.5° and a counting time of 23 seconds per frame. The data were collected at 100 K using a Rigaku XStream low temperature device. Details of crystal data, data collection and structure refinement are listed in Table 1. Data reduction were performed using the Rigaku Americas Corporation's Crystal Clear version 1.40.¹ The structure was solved by direct methods using SIR97² and refined by full-matrix least-squares on F² with anisotropic displacement parameters for the non-H atoms using SHELXL-97.³ Structure analysis was aided by use of the programs PLATON98⁴ and WinGX.⁵ The absolute configuration was assigned by internal comparison to the known absolute configuration of atoms ????. The hydrogen atoms on carbon were calculated in ideal positions with isotropic displacement parameters set to 1.2xUeq of the attached atom (1.5xUeq for methyl hydrogen atoms). The hydrogen atoms on the water molecule and the hydroxyl oxygen atom, O4 and O3, respectively, were observed in a ΔF map and refined with isotropic displacement parameters. The function, $\sum w(|F_o|^2 - |F_c|^2)^2$, was minimized, where $w = 1/[(\sigma(F_o))^2 + (0.0468*P)^2 + (0.3281*P)]$ and $P = (|F_o|^2 + 2|F_c|^2)/3$. R_w(F²) refined to 0.116, with R(F) equal to 0.0532 and a goodness of fit, S, = 1.21. Definitions used for calculating R(F), R_w(F²) and the goodness of fit, S, are given

below.⁶ The data were checked for secondary extinction effects but no correction was necessary. Neutral atom scattering factors and values used to calculate the linear absorption coefficient are from the International Tables for X-ray Crystallography (1992).⁷ All figures were generated using SHELXTL/PC.⁸ Tables of positional and thermal parameters, bond lengths and angles, torsion angles and figures are found elsewhere.

Table 11. Crystal data and structure refinement for **48**.

Empirical formula	C ₁₉ H ₂₇ N O ₄	
Formula weight	333.42	
Temperature	100(2) K	
Wavelength	0.71075 Å	
Crystal system	Orthorhombic	
Space group	P2 ₁ 2 ₁ 2 ₁	
Unit cell dimensions	a = 8.786(2) Å	α = 90°.
	b = 12.615(2) Å	β = 90°.
	c = 15.806(3) Å	γ = 90°.
Volume	1751.9(6) Å ³	
Z	4	
Density (calculated)	1.264 Mg/m ³	
Absorption coefficient	0.088 mm ⁻¹	
F(000)	720	
Crystal size	0.18 x 0.12 x 0.10 mm ³	
Theta range for data collection	3.04 to 27.41°.	
Index ranges	-11 ≤ h ≤ 11, -16 ≤ k ≤ 11, -19 ≤ l ≤ 20	
Reflections collected	15035	
Independent reflections	2278 [R(int) = 0.0642]	
Completeness to theta = 27.41°	99.6 %	

Table 11, continued,

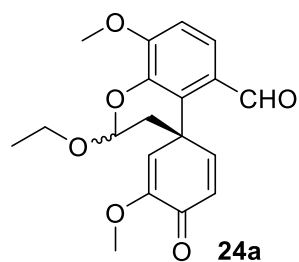
Absorption correction	None
Refinement method	Full-matrix least-squares on F^2
Data / restraints / parameters	2278 / 0 / 232
Goodness-of-fit on F^2	1.214
Final R indices [$I > 2\sigma(I)$]	R1 = 0.0532, wR2 = 0.1104
R indices (all data)	R1 = 0.0655, wR2 = 0.1165
Absolute structure parameter	n/a
Largest diff. peak and hole	0.201 and -0.215 e. \AA^{-3}

Table 12. Atomic coordinates ($\times 10^4$) and equivalent isotropic displacement parameters ($\text{\AA}^2 \times 10^3$) for **48**. U(eq) is defined as one third of the trace of the orthogonalized U_{ij} tensor.

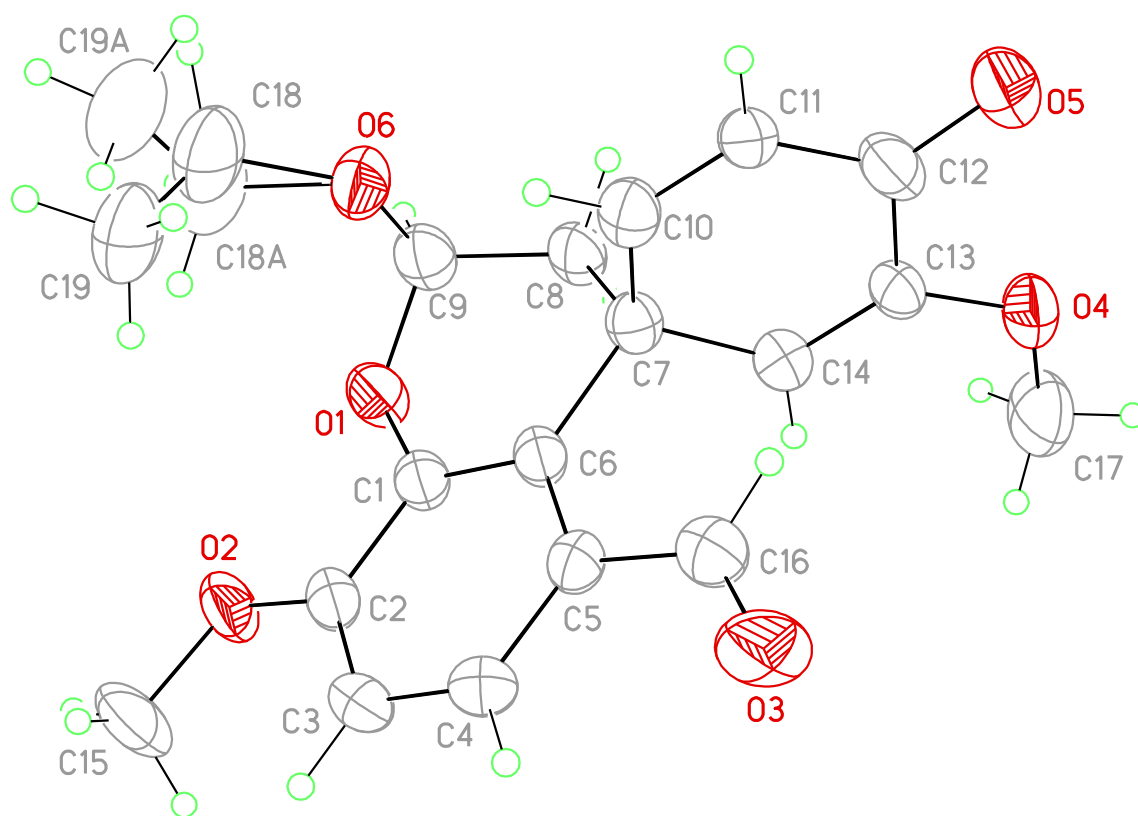
	x	y	z	U(eq)
C1	3077(3)	10401(2)	3995(2)	23(1)
C2	4263(4)	11050(2)	4262(2)	30(1)
C3	5723(4)	10615(3)	4245(2)	36(1)
C4	5982(4)	9590(3)	3937(2)	35(1)
C5	4778(3)	8939(2)	3675(2)	26(1)
C6	4925(3)	7864(3)	3230(2)	32(1)
C7	3406(3)	7422(2)	2847(2)	27(1)
C8	2199(3)	7098(2)	4221(2)	28(1)
C9	1188(3)	8067(2)	4094(2)	24(1)
C10	1864(3)	8872(2)	3465(2)	20(1)
C11	3330(3)	9360(2)	3757(2)	22(1)
C12	2226(3)	8297(2)	2626(2)	20(1)
C13	2774(3)	9060(2)	1921(2)	25(1)
C14	2158(3)	10208(2)	1979(2)	26(1)
C15	656(3)	10242(2)	2471(2)	25(1)

Table 12, continued,

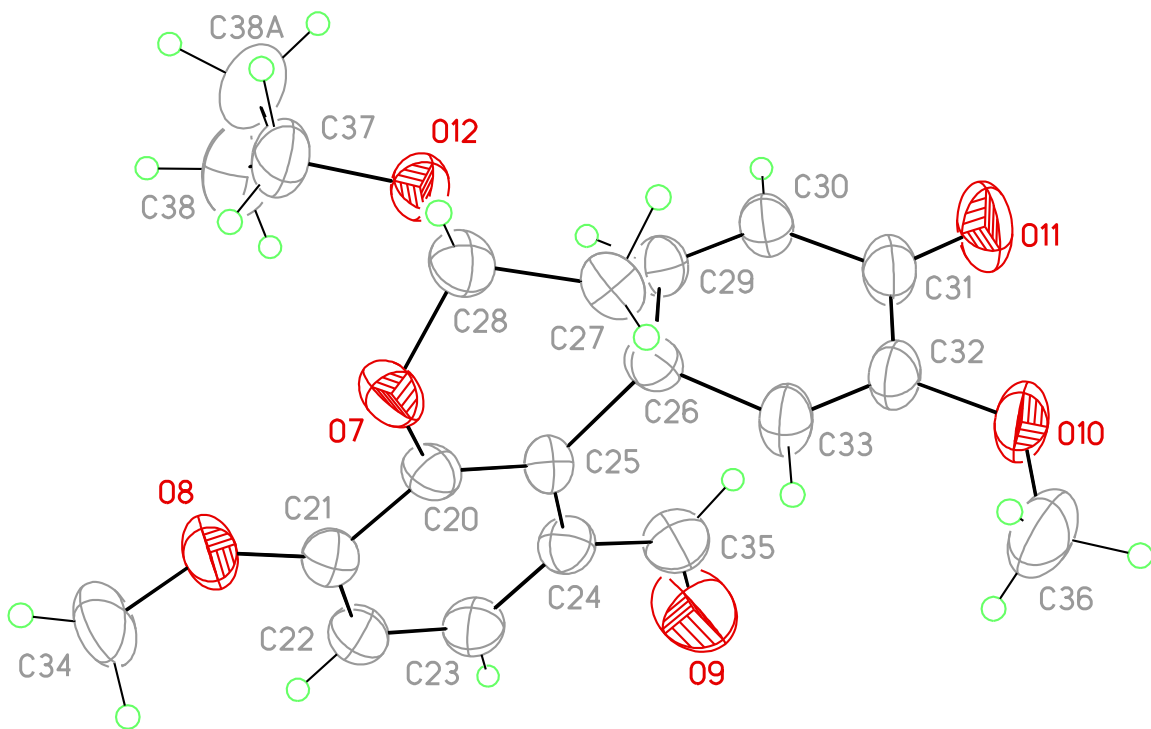
C16	846(3)	9871(2)	3383(2)	22(1)
C17	4976(4)	12669(3)	4963(2)	43(1)
C18	3449(4)	5635(3)	3494(2)	41(1)
C19	1968(4)	10678(3)	1091(2)	37(1)
N1	2606(3)	6634(2)	3397(2)	27(1)
O1	1587(2)	10715(2)	3888(1)	26(1)
O2	3885(3)	12085(2)	4482(1)	42(1)
O3	34(3)	11292(2)	2484(2)	35(1)
O4	1850(3)	13026(2)	3087(2)	37(1)



View 1 of molecule **24a** showing the atom labeling scheme. Displacement ellipsoids are scaled to the 30% probability level.



View 2 of molecule **24a** showing the atom labeling scheme. Displacement ellipsoids are scaled to the 30% probability level.



X-ray Experimental for C₁₉H₂₀O₆: Crystals grew as large, colorless prisms by slow evaporation of ethyl acetate. The data crystal was cut from a larger crystal and had approximate dimensions; 0.26 x 0.17 x 0.10 mm. The data were collected at room temperature on a Rigaku SCX-Mini diffractometer with a Mercury CCD using a graphite monochromator with MoK α radiation ($\lambda = 0.71073\text{\AA}$). A total of 540 frames of data were collected using ω -scans with a scan range of 1 $^\circ$ and a counting time of 120 seconds per frame. Details of crystal data, data collection and structure refinement are listed in Table 1. Data reduction were performed using the Rigaku Americas Corporation's Crystal Clear version 1.40.¹ The structure was solved by direct methods using SIR97² and refined by full-matrix least-squares on F² with anisotropic displacement parameters for the non-H atoms using SHELXL-97.³ Structure analysis was aided by use of the programs PLATON98⁴ and WinGX.⁵ The hydrogen atoms on carbon were calculated in ideal positions with isotropic displacement parameters set to 1.2xUeq of the attached atom (1.5xUeq for methyl hydrogen atoms).

There are two crystallographically unique molecules in the asymmetric unit. The ethyl group in both molecules is disordered. In one molecule, the disorder is seen in both methyl and methylene carbon atoms, C18 and C19. In the other molecule, the disorder impacts only the methyl carbon, C38. The disorder was modeled in the same fashion for both groups. For example, for the disorder of C18 and C19, the site occupancy factors for these atoms was assigned to the variable x, while (1-x) was assigned to the site occupancy factors for C18a and C19a. While refining x, a common isotropic

displacement parameter was refined for the four atoms and the geometry of the groups was restrained to be equivalent. In this way, the site occupancy factor for C18 and C19 refined to 64(2)%.

The function, $\Sigma w(|F_o|^2 - |F_c|^2)^2$, was minimized, where $w = 1/[(\sigma(F_o))^2 + (0.032*P)^2 + (0.3815*P)]$ and $P = (|F_o|^2 + 2|F_c|^2)/3$. $R_w(F^2)$ refined to 0.249, with $R(F)$ equal to 0.104 and a goodness of fit, S , = 1.36. Definitions used for calculating $R(F)$, $R_w(F^2)$ and the goodness of fit, S , are given below.⁶ The data were checked for secondary extinction effects but no correction was necessary. Neutral atom scattering factors and values used to calculate the linear absorption coefficient are from the International Tables for X-ray Crystallography (1992).⁷ All figures were generated using SHELXTL/PC.⁸ Tables of positional and thermal parameters, bond lengths and angles, torsion angles and figures are found elsewhere.

Table 13. Crystal data and structure refinement for **24a**.

Empirical formula	C ₁₉ H ₂₀ O ₆	
Formula weight	344.35	
Temperature	298(2) K	
Wavelength	0.71075 Å	
Crystal system	Monoclinic	
Space group	P2 ₁ /n	
Unit cell dimensions	a = 12.166(2) Å	α = 90°.
	b = 15.3530(3) Å	β = 97.195(4)°.
	c = 19.1590(3) Å	γ = 90°.
Volume	3550.4(6) Å ³	
Z	8	
Density (calculated)	1.288 Mg/m ³	
Absorption coefficient	0.096 mm ⁻¹	
F(000)	1456	
Crystal size	0.26 x 0.17 x 0.10 mm	
Theta range for data collection	3.15 to 25.00°.	
Index ranges	-14 ≤ h ≤ 14, -18 ≤ k ≤ 18, -22 ≤ l ≤ 22	
Reflections collected	29531	
Independent reflections	6251 [R(int) = 0.1460]	
Completeness to theta = 25.00°	99.8 %	

Table 13, continued,

Absorption correction	None
Refinement method	Full-matrix least-squares on F^2
Data / restraints / parameters	6251 / 73 / 488
Goodness-of-fit on F^2	1.355
Final R indices [$I > 2\sigma(I)$]	R1 = 0.1042, wR2 = 0.2149
R indices (all data)	R1 = 0.2105, wR2 = 0.2490
Largest diff. peak and hole	0.489 and -0.270 e. \AA^{-3}

Table 14. Atomic coordinates ($\times 10^4$) and equivalent isotropic displacement parameters ($\text{\AA}^2 \times 10^3$) for **24a**. $U(\text{eq})$ is defined as one third of the trace of the orthogonalized U_{ij} tensor.

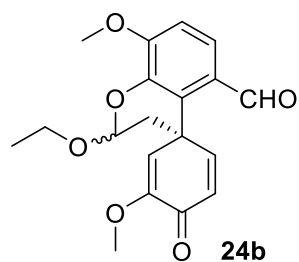
	x	y	z	U(eq)
O1	4023(3)	1876(2)	1420(2)	74(1)
O2	4431(3)	3237(2)	749(2)	82(1)
O3	2593(4)	4385(2)	3579(2)	102(2)
O4	553(3)	1437(2)	3658(2)	78(1)
O5	2147(3)	1057(3)	4674(2)	95(1)
O6	5164(4)	1221(2)	2328(2)	83(1)
C18	6227(9)	1201(10)	2054(8)	118(4)
C19	6747(8)	2066(7)	2139(6)	115(4)
C18A	6033(12)	1260(20)	1865(9)	117(5)
C19A	7085(9)	1392(15)	2324(11)	118(5)
C1	3790(4)	2639(3)	1748(3)	57(1)
C2	4056(4)	3386(3)	1372(3)	61(1)
C3	3901(4)	4192(3)	1645(3)	70(2)
C4	3492(4)	4264(3)	2277(3)	65(2)
C5	3217(4)	3533(3)	2646(3)	56(1)

Table 14, continued,

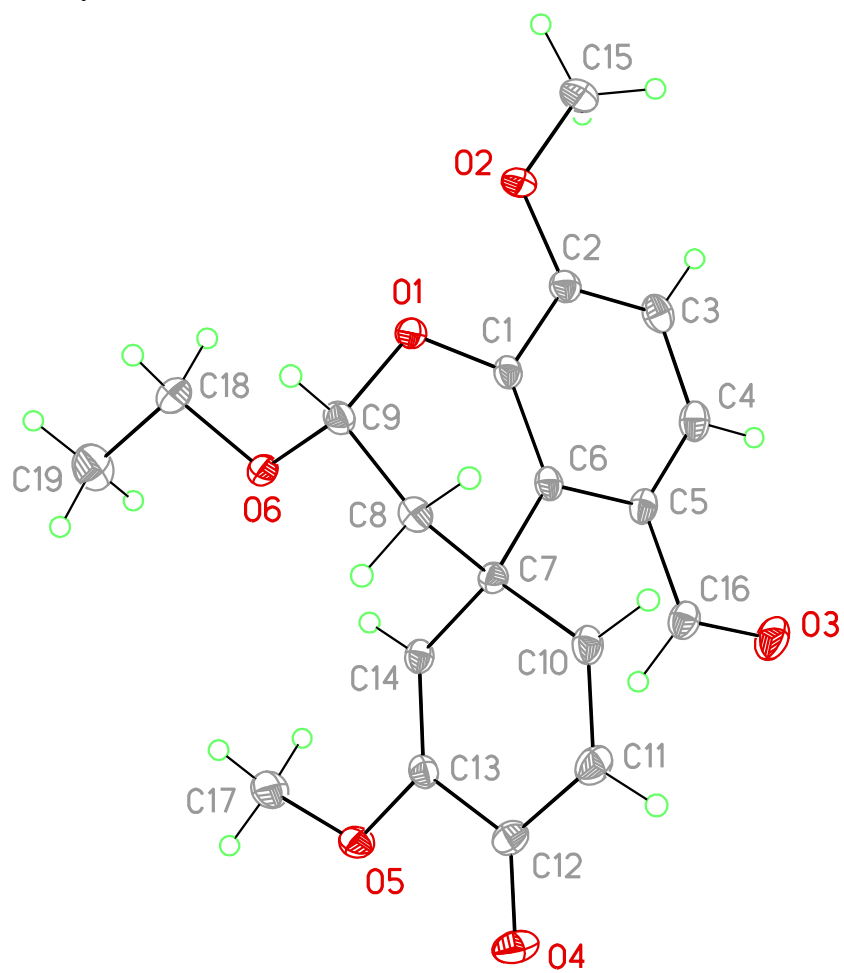
C6	3384(4)	2698(3)	2385(3)	53(1)
C7	3112(4)	1863(3)	2789(3)	54(1)
C8	3244(4)	1063(3)	2318(3)	66(2)
C9	4190(5)	1143(3)	1892(3)	73(2)
C10	3894(4)	1767(3)	3449(3)	62(2)
C11	3583(4)	1524(3)	4046(3)	56(1)
C12	2439(5)	1354(3)	4125(3)	71(2)
C13	1615(4)	1560(3)	3519(3)	53(1)
C14	1928(4)	1825(3)	2927(3)	61(1)
C15	4750(6)	3955(3)	357(3)	107(3)
C16	2801(5)	3696(4)	3327(3)	71(2)
C17	-311(5)	1575(4)	3093(4)	110(2)
O7	5728(3)	3149(2)	6221(2)	75(1)
O8	5197(3)	1741(2)	6775(2)	86(1)
O9	7258(5)	881(4)	3985(3)	160(2)
O10	9126(4)	3806(3)	3954(2)	100(1)
O11	7497(4)	4198(3)	2963(2)	131(2)
O12	4512(3)	3849(2)	5376(2)	75(1)
C20	5952(4)	2423(3)	5844(3)	61(1)
C21	5662(5)	1646(3)	6176(3)	66(2)

Table 14, continued,

C22	5868(5)	866(3)	5867(3)	77(2)
C23	6321(5)	856(3)	5242(3)	76(2)
C24	6569(4)	1623(3)	4907(3)	66(2)
C25	6378(4)	2424(3)	5215(3)	58(1)
C26	6610(4)	3291(3)	4854(3)	62(1)
C27	6433(5)	4064(3)	5367(3)	70(2)
C28	5521(5)	3926(3)	5803(3)	72(2)
C29	5809(4)	3421(3)	4202(3)	68(2)
C30	6097(5)	3703(3)	3597(3)	71(2)
C31	7235(6)	3886(4)	3509(3)	86(2)
C32	8066(5)	3679(4)	4110(3)	75(2)
C33	7773(5)	3397(3)	4710(3)	74(2)
C34	4785(7)	992(4)	7074(4)	123(3)
C35	6995(5)	1552(4)	4232(3)	87(2)
C36	9997(6)	3632(5)	4508(4)	133(3)
C37	3579(6)	3731(4)	5750(4)	102(2)
C38	2802(12)	3108(13)	5389(10)	124(10)
C38A	2562(8)	3650(11)	5272(7)	114(7)



View of **24b** showing the atom labeling scheme. Displacement ellipsoids are scaled to the 50% probability level.



X-ray Experimental for C₁₉H₂₀O₆: Crystals grew as colorless prisms by slow evaporation ethyl acetate. The data crystal was cut from a larger crystal and had approximate dimensions; 0.22 x 0.16 x 0.15 mm. The data were collected on a Rigaku AFC12 diffractometer with a Saturn 724+ CCD using a graphite monochromator with MoK α radiation ($\lambda = 0.71073\text{\AA}$). A total of 1960 frames of data were collected using ω -scans with a scan range of 0.5° and a counting time of 26 seconds per frame. The data were collected at 100 K using a Rigaku XStream low temperature device. Details of crystal data, data collection and structure refinement are listed in Table 1. Data reduction were performed using the Rigaku Americas Corporation's Crystal Clear version 1.40.¹ The structure was solved by direct methods using SIR97² and refined by full-matrix least-squares on F² with anisotropic displacement parameters for the non-H atoms using SHELXL-97.³ Structure analysis was aided by use of the programs PLATON98⁴ and WinGX.⁵ The data crystal was grown from a racemic mixture. The absolute configuration of the data crystal could not be determined from the anomalous scattering and, therefore, the Friedel pairs were averaged in the final refinement cycles. The hydrogen atoms were calculated in ideal positions with isotropic displacement parameters set to 1.2xUeq of the attached atom (1.5xUeq for methyl hydrogen atoms). The function, $\Sigma w(|F_o|^2 - |F_c|^2)^2$, was minimized, where $w = 1/[(\sigma(F_o))^2 + (0.0401*P)^2 + (0.3531*P)]$ and $P = (|F_o|^2 + 2|F_c|^2)/3$. R_w(F²) refined to 0.0753, with R(F) equal to 0.0289 and a goodness of fit, S, = 1.16. Definitions used for calculating R(F), R_w(F²) and the goodness of fit, S, are given below.⁶ The data were checked for secondary extinction

effects but no correction was necessary. Neutral atom scattering factors and values used to calculate the linear absorption coefficient are from the International Tables for X-ray Crystallography (1992).⁷ All figures were generated using SHELXTL/PC.⁸ Tables of positional and thermal parameters, bond lengths and angles, torsion angles and figures are found elsewhere.

Table 15. Crystal data and structure refinement for **24b**.

Empirical formula	C ₁₉ H ₂₀ O ₆	
Formula weight	344.35	
Temperature	100(2) K	
Wavelength	0.71075 Å	
Crystal system	Orthorhombic	
Space group	P212121	
Unit cell dimensions	a = 7.8437(15) Å	α = 90°.
	b = 13.259(2) Å	β = 90°.
	c = 16.120(2) Å	γ = 90°.
Volume	1676.5(5) Å ³	
Z	4	
Density (calculated)	1.364 Mg/m ³	
Absorption coefficient	0.102 mm ⁻¹	
F(000)	728	
Crystal size	0.22 x 0.16 x 0.15 mm	
Theta range for data collection	3.02 to 27.39°.	
Index ranges	-10 ≤ h ≤ 10, -16 ≤ k ≤ 17, -20 ≤ l ≤ 20	
Reflections collected	37065	
Independent reflections	2171 [R(int) = 0.0340]	
Completeness to theta = 27.39°	99.8 %	

Table 15, continued,

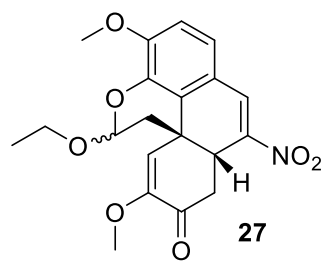
Absorption correction	Semi-empirical from equivalents
Max. and min. transmission	1.00 and 0.866
Refinement method	Full-matrix least-squares on F ²
Data / restraints / parameters	2171 / 0 / 229
Goodness-of-fit on F ²	1.159
Final R indices [I > 2σ(I)]	R1 = 0.0289, wR2 = 0.0745
R indices (all data)	R1 = 0.0302, wR2 = 0.0753
Absolute structure parameter	not determined
Largest diff. peak and hole	0.224 and -0.158 e.Å ⁻³

Table 16. Atomic coordinates ($\times 10^4$) and equivalent isotropic displacement parameters ($\text{\AA}^2 \times 10^3$) for **24b**. $U(\text{eq})$ is defined as one third of the trace of the orthogonalized U_{ij} tensor.

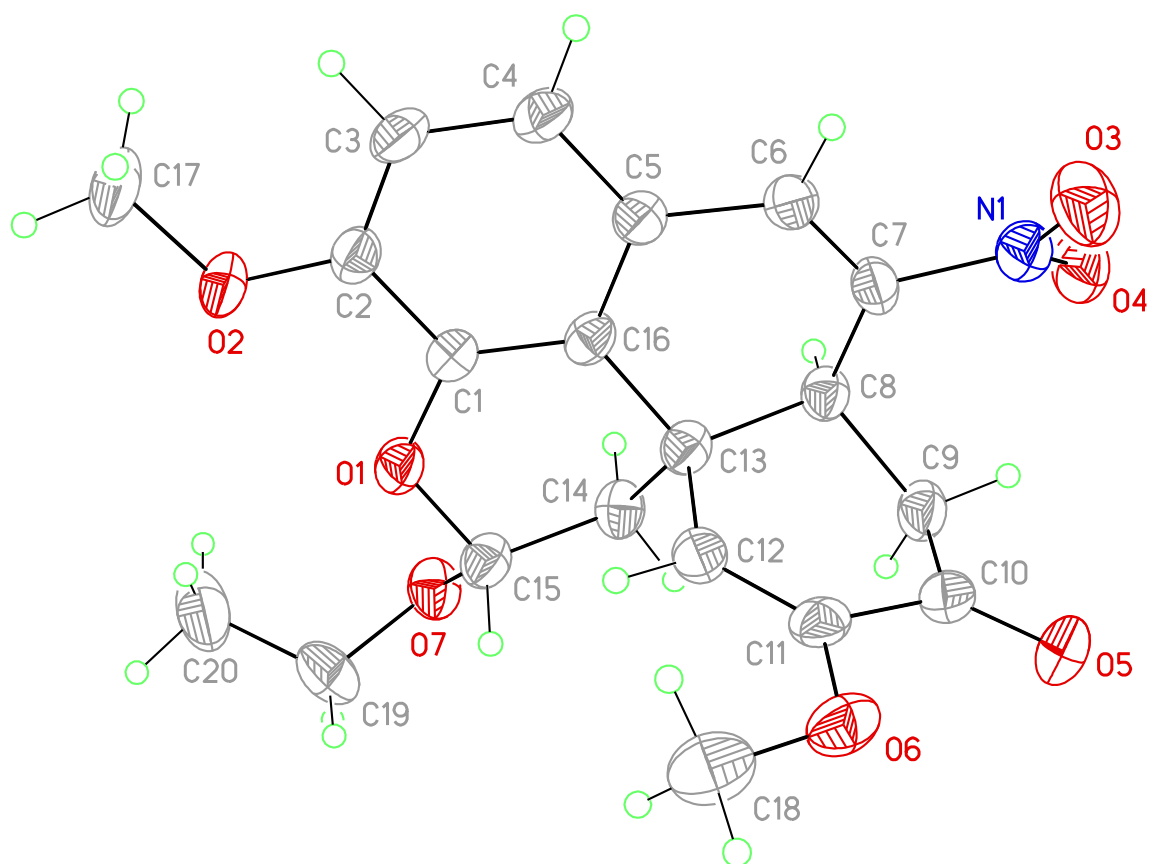
	x	y	z	$U(\text{eq})$
O1	2553(2)	-391(1)	4891(1)	16(1)
O2	5228(2)	-1488(1)	4959(1)	18(1)
O3	5543(2)	1137(1)	1637(1)	25(1)
O4	-265(2)	3219(1)	1941(1)	23(1)
O5	1100(2)	3776(1)	3380(1)	18(1)
O6	1374(2)	1163(1)	5290(1)	16(1)
C1	3649(2)	-264(1)	4232(1)	13(1)
C2	5133(2)	-883(1)	4279(1)	15(1)
C3	6347(2)	-837(1)	3654(1)	18(1)
C4	6130(2)	-165(1)	2997(1)	18(1)
C5	4683(2)	443(1)	2942(1)	15(1)
C6	3380(2)	377(1)	3558(1)	13(1)
C7	1652(2)	924(1)	3464(1)	13(1)
C8	346(2)	395(1)	4055(1)	14(1)
C9	1051(2)	225(1)	4918(1)	15(1)

Table 16, continued,

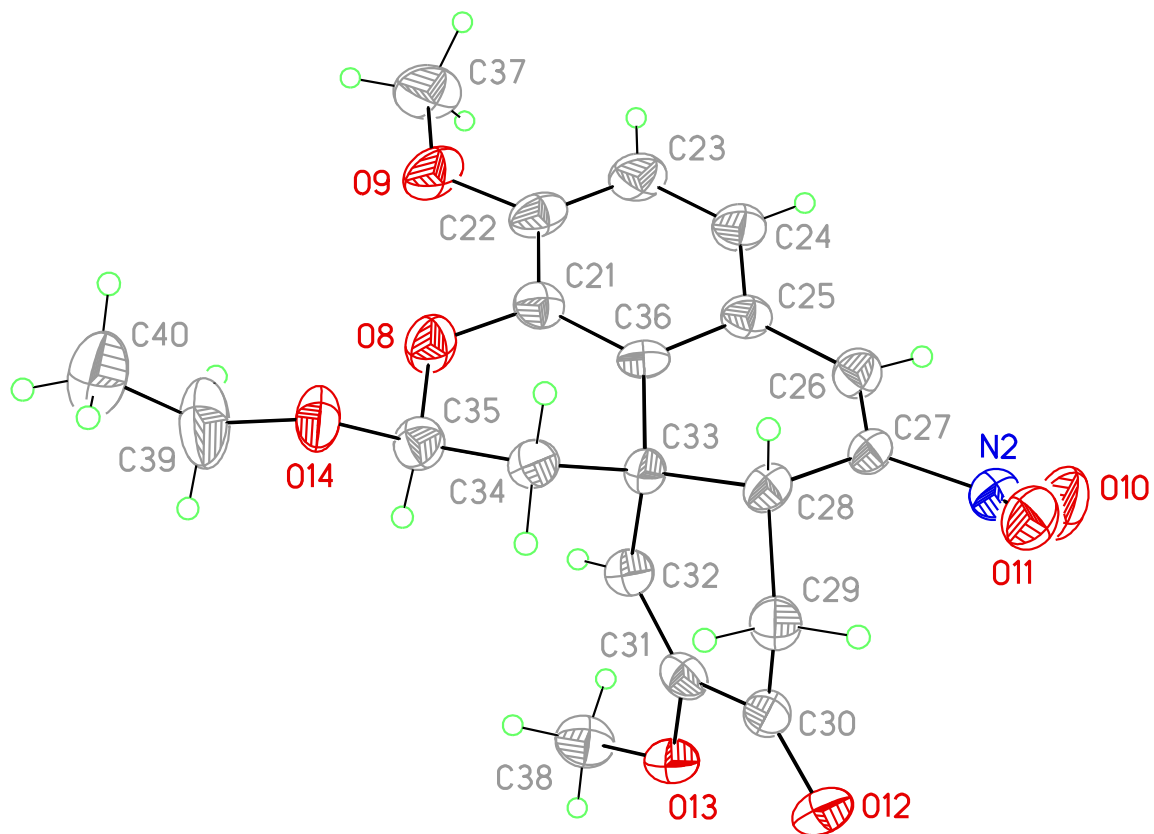
C10	914(2)	747(1)	2609(1)	16(1)
C11	277(2)	1477(1)	2131(1)	19(1)
C12	319(2)	2546(1)	2379(1)	16(1)
C13	1121(2)	2768(1)	3197(1)	14(1)
C14	1786(2)	2035(1)	3675(1)	14(1)
C15	6622(2)	-2197(1)	4990(1)	25(1)
C16	4627(2)	1185(1)	2250(1)	18(1)
C17	1673(3)	4055(1)	4192(1)	23(1)
C18	1671(2)	1108(1)	6172(1)	20(1)
C19	1640(3)	2172(2)	6504(1)	28(1)



View 1 of molecule **27** showing the atom labeling scheme. Displacement ellipsoids are scaled to the 50% probability level.



View 2 of molecule **27** showing the atom labeling scheme. Displacement ellipsoids are scaled to the 50% probability level.



X-ray Experimental for C₂₀H₂₁NO₇: Crystals grew as large, yellow prisms and needles by slow evaporation ethyl acetate/hexanes. The data crystal was cut from a long needle and had approximate dimensions; 0.42 x 0.09 x 0.08 mm. The data were collected on a Rigaku SCX-Mini diffractometer with a Mercury CCD using a graphite monochromator with MoK α radiation ($\lambda = 0.71075\text{\AA}$). A total of 720 frames of data were collected using ω -scans with a scan range of 1 $^\circ$ and a counting time of 40 seconds per frame. The data were collected at 153 K using a Rigaku XStream low temperature device. Details of crystal data, data collection and structure refinement are listed in Table 1. Data reduction were performed using the Rigaku Americas Corporation's Crystal Clear version 1.40.¹ The structure was solved by direct methods using SIR97² and refined by full-matrix least-squares on F² with anisotropic displacement parameters for the non-H atoms using SHELXL-97.³ Structure analysis was aided by use of the programs PLATON98⁴ and WinGX.⁵ The hydrogen atoms on carbon were calculated in ideal positions with isotropic displacement parameters set to 1.2xUeq of the attached atom (1.5xUeq for methyl hydrogen atoms). The function, $\Sigma w(|F_o|^2 - |F_c|^2)^2$, was minimized, where $w = 1/[(\sigma(F_o))^2 + (0.0492*P)^2 + (0.0787*P)]$ and $P = (|F_o|^2 + 2|F_c|^2)/3$. R_w(F²) refined to 0.190, with R(F) equal to 0.0839 and a goodness of fit, S, = 1.07. Definitions used for calculating R(F), R_w(F²) and the goodness of fit, S, are given below.⁶ The data were checked for secondary extinction effects but no correction was necessary. Neutral atom scattering factors and values used to calculate the linear absorption coefficient are from the International Tables for X-ray Crystallography (1992).⁷ All figures were generated

using SHELXTL/PC.⁸ Tables of positional and thermal parameters, bond lengths and angles, torsion angles and figures are found elsewhere.

Table 17. Crystal data and structure refinement for **27**.

Empirical formula	C ₂₀ H ₂₁ N O ₇	
Formula weight	387.38	
Temperature	153(2) K	
Wavelength	0.71075 Å	
Crystal system	Triclinic	
Space group	P-1	
Unit cell dimensions	a = 10.348(3) Å	α = 102.934(6)°.
	b = 10.853(3) Å	β = 93.21°.
	c = 17.384(5) Å	γ = 103.857(6)°.
Volume	1835.0(9) Å ³	
Z	4	
Density (calculated)	1.402 Mg/m ³	
Absorption coefficient	0.107 mm ⁻¹	
F(000)	816	
Crystal size	0.42 x 0.09 x 0.08 mm	
Theta range for data collection	3.16 to 27.48°.	
Index ranges	-13 ≤ h ≤ 12, -14 ≤ k ≤ 14, -22 ≤ l ≤ 22	
Reflections collected	18476	
Independent reflections	8273 [R(int) = 0.1030]	
Completeness to theta = 27.48°	98.4 %	

Table 17, continued,

Absorption correction	Semi-empirical from equivalents
Max. and min. transmission	1.00 and 0.576
Refinement method	Full-matrix least-squares on F ²
Data / restraints / parameters	8273 / 0 / 511
Goodness-of-fit on F ²	1.069
Final R indices [I > 2σ(I)]	R1 = 0.0839, wR2 = 0.1449
R indices (all data)	R1 = 0.2200, wR2 = 0.1902
Largest diff. peak and hole	0.300 and -0.313 e.Å ⁻³

Table 18. Atomic coordinates ($\times 10^4$) and equivalent isotropic displacement parameters ($\text{\AA}^2 \times 10^3$) for **27**. U(eq) is defined as one third of the trace of the orthogonalized U_{ij} tensor.

	x	y	z	U(eq)
O1	4144(3)	8195(2)	2700(2)	33(1)
O2	2709(3)	9551(2)	3500(2)	37(1)
O3	-786(3)	2917(3)	-99(2)	53(1)
O4	499(3)	1929(3)	415(2)	46(1)
O5	3107(3)	3694(3)	-847(2)	54(1)
O6	3550(3)	6285(3)	-609(2)	42(1)
O7	6051(3)	7555(3)	2927(2)	36(1)
N1	150(3)	2916(3)	364(2)	36(1)
C1	2782(4)	7697(4)	2529(2)	27(1)
C2	2002(4)	8452(4)	2957(2)	29(1)
C3	629(4)	8071(4)	2789(2)	34(1)
C4	10(4)	6948(4)	2211(2)	34(1)
C5	769(4)	6176(4)	1796(2)	30(1)
C6	173(4)	4986(4)	1194(2)	30(1)
C7	887(4)	4160(4)	904(2)	29(1)

Table 18, continued,

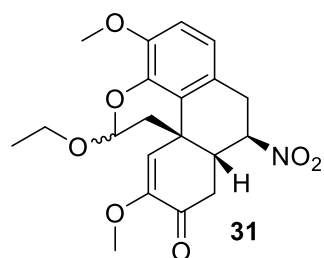
C8	2353(4)	4330(3)	1181(2)	28(1)
C9	3117(4)	3722(4)	529(2)	35(1)
C10	3170(4)	4328(4)	-165(2)	36(1)
C11	3357(4)	5767(4)	39(2)	31(1)
C12	3340(4)	6426(4)	781(2)	30(1)
C13	3035(4)	5810(4)	1481(2)	28(1)
C14	4340(4)	6019(3)	2027(2)	31(1)
C15	5027(4)	7445(4)	2343(2)	31(1)
C16	2182(4)	6566(4)	1963(2)	26(1)
C17	1960(4)	10385(4)	3922(3)	51(1)
C18	3837(4)	7686(4)	-448(2)	49(1)
C19	7067(4)	8775(4)	3120(3)	49(1)
C20	6810(5)	9798(4)	3765(3)	62(2)
O8	6299(3)	1670(2)	2297(2)	41(1)
O9	7925(3)	453(3)	1617(2)	48(1)
O10	10701(3)	7395(3)	5093(2)	57(1)
O11	9262(3)	8160(3)	4514(2)	45(1)
O12	6584(3)	6286(3)	5728(2)	48(1)
O13	6433(3)	3768(3)	5589(2)	36(1)
O14	4268(3)	2026(3)	2011(2)	40(1)

Table 18, continued,

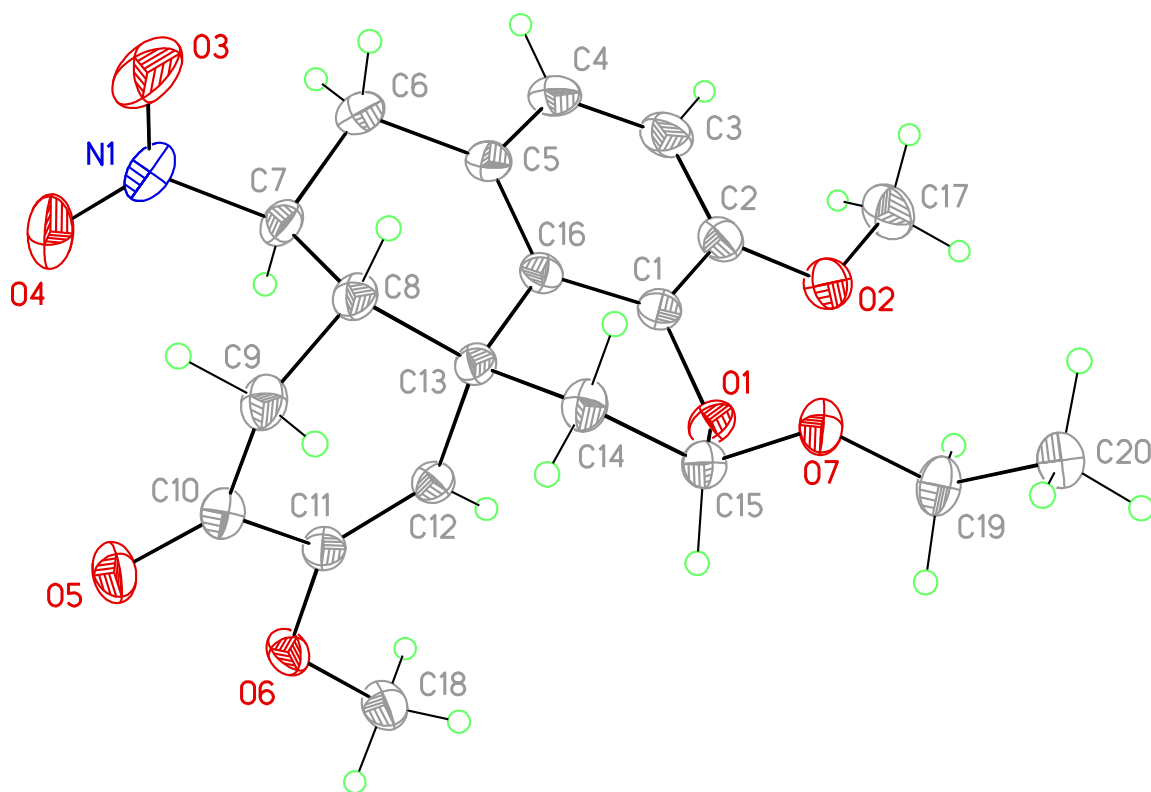
N2	9732(3)	7252(3)	4608(2)	38(1)
C21	7631(4)	2278(4)	2513(2)	31(1)
C22	8525(5)	1597(4)	2165(2)	38(1)
C23	9885(5)	2113(4)	2372(3)	43(1)
C24	10360(4)	3272(4)	2942(2)	38(1)
C25	9485(4)	3962(4)	3290(2)	30(1)
C26	9949(4)	5204(4)	3877(2)	33(1)
C27	9128(4)	5956(4)	4101(2)	28(1)
C28	7668(4)	5627(3)	3770(2)	29(1)
C29	6769(4)	6179(4)	4343(2)	32(1)
C30	6690(4)	5643(4)	5074(2)	33(1)
C31	6671(4)	4245(4)	4927(2)	30(1)
C32	6826(4)	3561(4)	4219(2)	30(1)
C33	7113(4)	4123(3)	3499(2)	26(1)
C34	5834(4)	3758(4)	2915(2)	30(1)
C35	5300(4)	2297(4)	2620(2)	35(1)
C36	8093(4)	3453(4)	3078(2)	27(1)
C37	8765(5)	-354(4)	1273(3)	61(2)
C38	6153(4)	2371(4)	5467(2)	43(1)
C39	3524(5)	666(5)	1805(3)	71(2)

Table 18, continued,

C40	2631(5)	358(5)	1087(3)	69(2)
-----	---------	--------	---------	-------



View of **31** showing the atom labeling scheme. Displacement ellipsoids are scaled to the 50% probability level.



X-ray Experimental for C₂₀H₂₇NO₇: Crystals grew as large, colorless prisms by slow evaporation of ethanol. The data crystal was cut from a larger crystal and had approximate dimensions; 0.60 x 0.50 x 0.40 mm. The data were collected on a Rigaku SCX-Mini diffractometer with a Mercury 2 CCD using a graphite monochromator with MoK α radiation ($\lambda = 0.71073\text{\AA}$). A total of 1080 frames of data were collected using ω -scans with a scan range of 0.5° and a counting time of 24 seconds per frame. The data were collected at 153 K using a Rigaku XStream low temperature device. Details of crystal data, data collection and structure refinement are listed in Table 1. Data reduction were performed using the Rigaku Americas Corporation's Crystal Clear version 1.40.¹ The structure was solved by direct methods using SIR97² and refined by full-matrix least-squares on F² with anisotropic displacement parameters for the non-H atoms using SHELXL-97.³ Structure analysis was aided by use of the programs PLATON98⁴ and WinGX.⁵ The hydrogen atoms on carbon were calculated in ideal positions with isotropic displacement parameters set to 1.2xUeq of the attached atom (1.5xUeq for methyl hydrogen atoms). The function, $\sum w(|F_o|^2 - |F_c|^2)^2$, was minimized, where $w = 1/[(\sigma(F_o))^2 + (0.0515*P)^2 + (0.3302*P)]$ and $P = (|F_o|^2 + 2|F_c|^2)/3$. R_w(F²) refined to 0.109, with R(F) equal to 0.0406 and a goodness of fit, S, = 1.04. Definitions used for calculating R(F), R_w(F²) and the goodness of fit, S, are given below.⁶ The data were checked for secondary extinction but no correction was necessary. Neutral atom scattering factors and values used to calculate the linear absorption coefficient are from the International Tables for X-ray Crystallography (1992).⁷ All figures were generated

using SHELXTL/PC.⁸ Tables of positional and thermal parameters, bond lengths and angles, torsion angles and figures are found elsewhere.

Table 19. Crystal data and structure refinement for **31**.

Empirical formula	C ₂₀ H ₂₃ N O ₇	
Formula weight	389.39	
Temperature	153(2) K	
Wavelength	0.71073 Å	
Crystal system	triclinic	
Space group	P -1	
Unit cell dimensions	a = 9.0867(15) Å	α = 70.291(3)°.
	b = 10.101(2) Å	β = 82.861(3)°.
	c = 11.628(2) Å	γ = 67.216(3)°.
Volume	926.3(3) Å ³	
Z	2	
Density (calculated)	1.396 Mg/m ³	
Absorption coefficient	0.106 mm ⁻¹	
F(000)	412	
Crystal size	0.600 x 0.500 x 0.400 mm	
Theta range for data collection	3.051 to 27.476°.	
Index ranges	-11 ≤ h ≤ 11, -13 ≤ k ≤ 13, -15 ≤ l ≤ 15	
Reflections collected	9212	
Independent reflections	4198 [R(int) = 0.0208]	
Completeness to theta = 25.242°	99.7 %	

Table 19, continued,

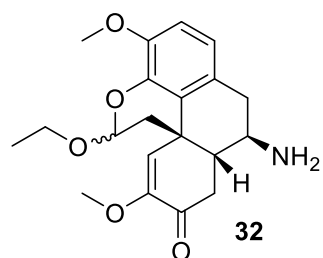
Absorption correction	Semi-empirical from equivalents
Max. and min. transmission	1.00 and 0.884
Refinement method	Full-matrix least-squares on F ²
Data / restraints / parameters	4198 / 0 / 256
Goodness-of-fit on F ²	1.038
Final R indices [I > 2σ(I)]	R1 = 0.0406, wR2 = 0.1060
R indices (all data)	R1 = 0.0446, wR2 = 0.1089
Extinction coefficient	n/a
Largest diff. peak and hole	0.315 and -0.211 e.Å ⁻³

Table 20. Atomic coordinates ($\times 10^4$) and equivalent isotropic displacement parameters ($\text{\AA}^2 \times 10^3$) for **31**. U(eq) is defined as one third of the trace of the orthogonalized U^{ij} tensor.

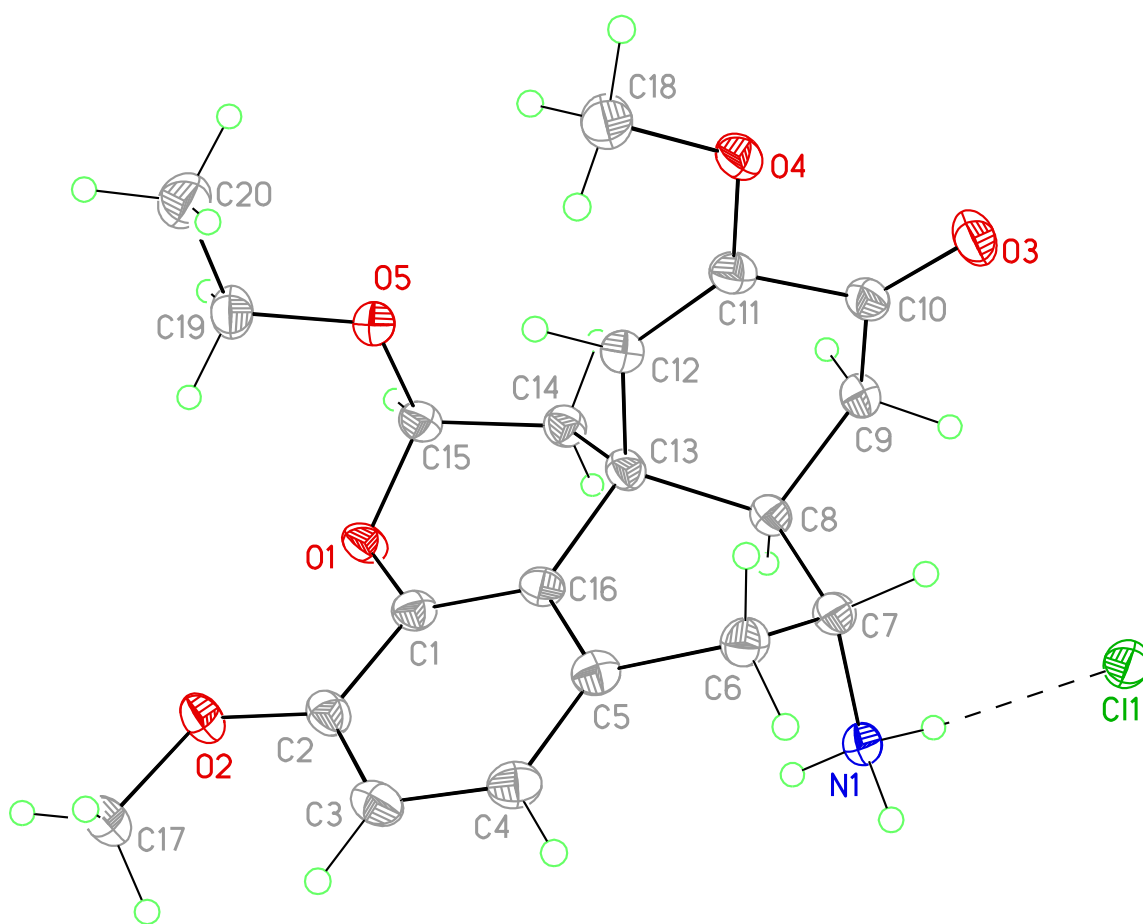
	x	y	z	U(eq)
O1	1516(1)	8379(1)	5364(1)	24(1)
O2	3166(1)	9807(1)	3722(1)	33(1)
O3	6734(2)	1441(1)	9060(1)	62(1)
O4	5933(1)	2411(1)	10526(1)	44(1)
O5	1734(1)	4019(1)	10965(1)	32(1)
O6	715(1)	6997(1)	9984(1)	26(1)
O7	403(1)	7206(1)	4502(1)	26(1)
N1	6060(1)	2517(1)	9442(1)	35(1)
C1	3153(1)	7749(1)	5449(1)	22(1)
C2	4028(2)	8516(1)	4605(1)	26(1)
C3	5681(2)	7931(2)	4735(1)	33(1)
C4	6438(2)	6608(2)	5671(1)	32(1)
C5	5572(1)	5842(1)	6510(1)	25(1)
C6	6421(2)	4376(2)	7495(1)	30(1)
C7	5273(1)	4060(1)	8524(1)	25(1)

Table 20, continued,

C8	3745(1)	4092(1)	8048(1)	23(1)
C9	2699(2)	3511(1)	9081(1)	25(1)
C10	1998(2)	4510(1)	9882(1)	24(1)
C11	1549(1)	6161(1)	9241(1)	21(1)
C12	1920(1)	6709(1)	8070(1)	20(1)
C13	2804(1)	5735(1)	7265(1)	20(1)
C14	1579(2)	5764(1)	6432(1)	24(1)
C15	678(1)	7365(1)	5596(1)	22(1)
C16	3903(1)	6440(1)	6403(1)	21(1)
C17	4059(2)	10538(2)	2803(1)	38(1)
C18	-106(2)	8573(1)	9372(1)	30(1)
C19	-579(2)	8606(1)	3653(1)	28(1)
C20	-1044(2)	8210(2)	2648(1)	29(1)



View of **32** showing the atom labeling scheme. Displacement ellipsoids are scaled to the 50% probability level.



X-ray Experimental for $C_{20}H_{27}NO_7$: Crystals grew as large, colorless prisms by slow evaporation chloroform/methanol/hexanes. The data crystal was cut from a larger crystal and had approximate dimensions; 0.60 x 0.50 x 0.40 mm. The data were collected on a Rigaku SCX-Mini diffractometer with a Mercury 2 CCD using a graphite monochromator with $MoK\alpha$ radiation ($\lambda = 0.71073\text{\AA}$). A total of 1080 frames of data were collected using ω -scans with a scan range of 0.5° and a counting time of 24 seconds per frame. The data were collected at 153 K using a Rigaku XStream low temperature device. Details of crystal data, data collection and structure refinement are listed in Table 1. Data reduction were performed using the Rigaku Americas Corporation's Crystal Clear version 1.40.¹ The structure was solved by direct methods using SIR97² and refined by full-matrix least-squares on F^2 with anisotropic displacement parameters for the non-H atoms using SHELXL-97.³ Structure analysis was aided by use of the programs PLATON98⁴ and WinGX.⁵ The hydrogen atoms on carbon were calculated in ideal positions with isotropic displacement parameters set to 1.2xUeq of the attached atom (1.5xUeq for methyl hydrogen atoms). The function, $\sum w(|F_o|^2 - |F_c|^2)^2$, was minimized, where $w = 1/[(\sigma(F_o))^2 + (0.0515*P)^2 + (0.3302*P)]$ and $P = (|F_o|^2 + 2|F_c|^2)/3$. $R_w(F^2)$ refined to 0.109, with R(F) equal to 0.0406 and a goodness of fit, S, = 1.04. Definitions used for calculating R(F), $R_w(F^2)$ and the goodness of fit, S, are given below.⁶ The data were checked for secondary extinction but no correction was necessary. Neutral atom scattering factors and values used to calculate the linear absorption coefficient are from the International Tables for X-ray Crystallography (1992).⁷ All figures were generated

using SHELXTL/PC.⁸ Tables of positional and thermal parameters, bond lengths and angles, torsion angles and figures are found elsewhere.

Table 21. Crystal data and structure refinement for **32**.

Empirical formula	C ₂₀ H ₂₃ N O ₇	
Formula weight	389.39	
Temperature	153(2) K	
Wavelength	0.71073 Å	
Crystal system	triclinic	
Space group	P -1	
Unit cell dimensions	a = 9.0867(15) Å	α = 70.291(3)°.
	b = 10.101(2) Å	β = 82.861(3)°.
	c = 11.628(2) Å	γ = 67.216(3)°.
Volume	926.3(3) Å ³	
Z	2	
Density (calculated)	1.396 Mg/m ³	
Absorption coefficient	0.106 mm ⁻¹	
F(000)	412	
Crystal size	0.600 x 0.500 x 0.400 mm	
Theta range for data collection	3.051 to 27.476°.	
Index ranges	-11 ≤ h ≤ 11, -13 ≤ k ≤ 13, -15 ≤ l ≤ 15	
Reflections collected	9212	
Independent reflections	4198 [R(int) = 0.0208]	
Completeness to theta = 25.242°	99.7 %	

Table 21, continued,

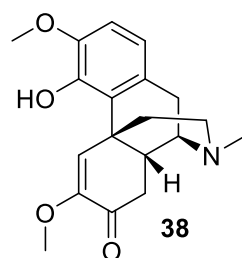
Absorption correction	Semi-empirical from equivalents
Max. and min. transmission	1.00 and 0.884
Refinement method	Full-matrix least-squares on F ²
Data / restraints / parameters	4198 / 0 / 256
Goodness-of-fit on F ²	1.038
Final R indices [I > 2σ(I)]	R1 = 0.0406, wR2 = 0.1060
R indices (all data)	R1 = 0.0446, wR2 = 0.1089
Extinction coefficient	n/a
Largest diff. peak and hole	0.315 and -0.211 e.Å ⁻³

Table 22. Atomic coordinates ($\times 10^4$) and equivalent isotropic displacement parameters ($\text{\AA}^2 \times 10^3$) for **32**. U(eq) is defined as one third of the trace of the orthogonalized U_{ij} tensor.

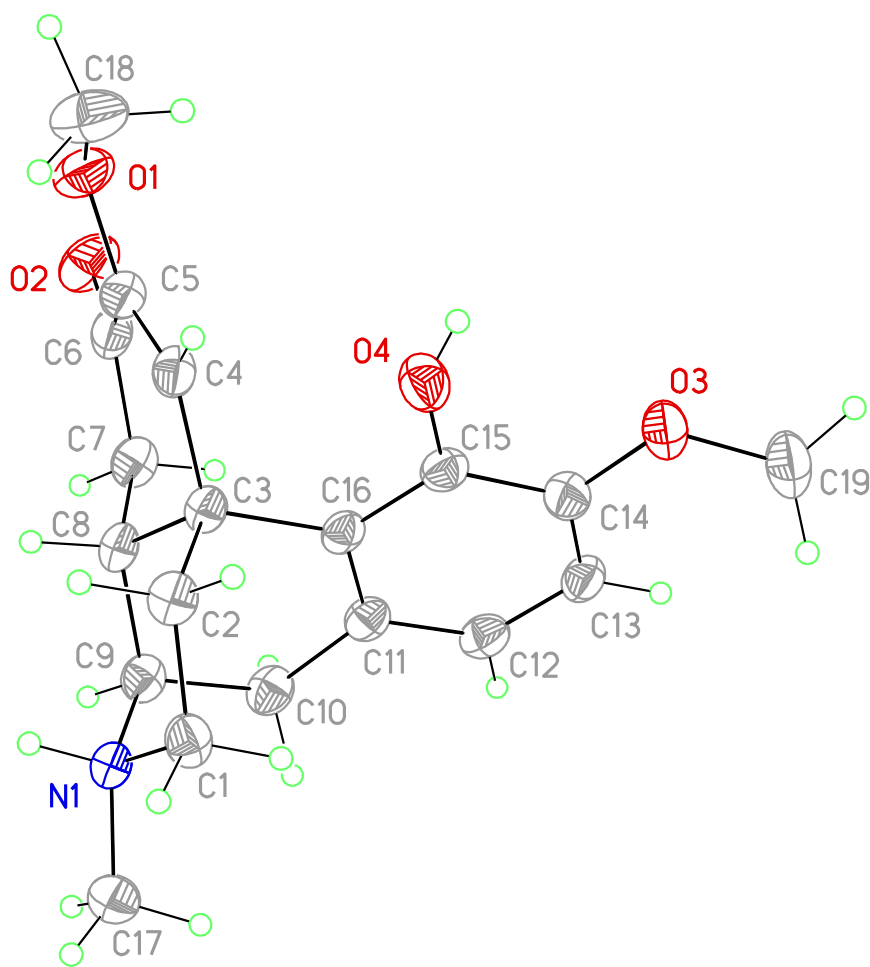
	x	y	z	U(eq)
O1	1516(1)	8379(1)	5364(1)	24(1)
O2	3166(1)	9807(1)	3722(1)	33(1)
O3	6734(2)	1441(1)	9060(1)	62(1)
O4	5933(1)	2411(1)	10526(1)	44(1)
O5	1734(1)	4019(1)	10965(1)	32(1)
O6	715(1)	6997(1)	9984(1)	26(1)
O7	403(1)	7206(1)	4502(1)	26(1)
N1	6060(1)	2517(1)	9442(1)	35(1)
C1	3153(1)	7749(1)	5449(1)	22(1)
C2	4028(2)	8516(1)	4605(1)	26(1)
C3	5681(2)	7931(2)	4735(1)	33(1)
C4	6438(2)	6608(2)	5671(1)	32(1)
C5	5572(1)	5842(1)	6510(1)	25(1)
C6	6421(2)	4376(2)	7495(1)	30(1)
C7	5273(1)	4060(1)	8524(1)	25(1)

Table 22, continued,

C8	3745(1)	4092(1)	8048(1)	23(1)
C9	2699(2)	3511(1)	9081(1)	25(1)
C10	1998(2)	4510(1)	9882(1)	24(1)
C11	1549(1)	6161(1)	9241(1)	21(1)
C12	1920(1)	6709(1)	8070(1)	20(1)
C13	2804(1)	5735(1)	7265(1)	20(1)
C14	1579(2)	5764(1)	6432(1)	24(1)
C15	678(1)	7365(1)	5596(1)	22(1)
C16	3903(1)	6440(1)	6403(1)	21(1)
C17	4059(2)	10538(2)	2803(1)	38(1)
C18	-106(2)	8573(1)	9372(1)	30(1)
C19	-579(2)	8606(1)	3653(1)	28(1)
C20	-1044(2)	8210(2)	2648(1)	29(1)



View of the cation in **38** showing the atom labeling scheme. Displacement ellipsoids are scaled to the 50% probability level.



X-ray Experimental for $C_{19}H_{24}NO_4^{1+} Cl^{1-} - H_2O$: Crystals grew as clusters of colorless prisms by slow evaporation chloroform/methanol/hexanes. The data crystal was cut from a larger crystal and had approximate dimensions; 0.25 x 0.10 x 0.10 mm. The data were collected on a Rigaku SCX-Mini diffractometer with a Mercury 2 CCD using a graphite monochromator with $MoK\alpha$ radiation ($\lambda = 0.71075\text{\AA}$). A total of 900 frames of data were collected using ω -scans with a scan range of 1° and a counting time of 30 seconds per frame. The data were collected at 163 K using a Rigaku XStream low temperature device. Details of crystal data, data collection and structure refinement are listed in Table 1. Data reduction were performed using the Rigaku Americas Corporation's Crystal Clear version 1.40.¹ The structure was solved by direct methods using SIR97² and refined by full-matrix least-squares on F^2 with anisotropic displacement parameters for the non-H atoms using SHELXL-97.³ Structure analysis was aided by use of the programs PLATON98⁴ and WinGX.⁵ The hydrogen atoms on carbon were calculated in ideal positions with isotropic displacement parameters set to 1.2xUeq of the attached atom (1.5xUeq for methyl hydrogen atoms). The hydrogen atoms on the N atom and the oxygen atoms were observed in a ΔF map and refined with isotropic displacement parameters. The function, $\sum w(|F_o|^2 - |F_c|^2)^2$, was minimized, where $w = 1/[(\sigma(F_o))^2 + (0.0573*P)^2 + (0.3775*P)]$ and $P = (|F_o|^2 + 2|F_c|^2)/3$. $R_w(F^2)$ refined to 0.117, with $R(F)$ equal to 0.0478 and a goodness of fit, S , = 1.17. Definitions used for calculating $R(F)$, $R_w(F^2)$ and the goodness of fit, S , are given below.⁶ The data were checked for secondary extinction but no correction was necessary. Neutral atom scattering factors and

values used to calculate the linear absorption coefficient are from the International Tables for X-ray Crystallography (1992).⁷ All figures were generated using SHELXTL/PC.⁸ Tables of positional and thermal parameters, bond lengths and angles, torsion angles and figures are found elsewhere.

Table 23. Crystal data and structure refinement for **38**.

Empirical formula	C ₁₉ H ₂₆ Cl N O ₅	
Formula weight	383.86	
Temperature	173(2) K	
Wavelength	0.71073 Å	
Crystal system	Orthorhombic	
Space group	Pna21	
Unit cell dimensions	a = 15.833(4) Å	α = 90°.
	b = 10.199(2) Å	β = 90°.
	c = 11.895(3) Å	γ = 90°.
Volume	1920.8(8) Å ³	
Z	4	
Density (calculated)	1.327 Mg/m ³	
Absorption coefficient	0.228 mm ⁻¹	
F(000)	816	
Crystal size	0.25 x 0.10 x 0.10 mm	
Theta range for data collection	3.09 to 27.45°.	
Index ranges	-20 ≤ h ≤ 20, -13 ≤ k ≤ 13, -15 ≤ l ≤ 15	
Reflections collected	31933	
Independent reflections	4370 [R(int) = 0.0551]	
Completeness to theta = 27.45°	99.5 %	

Table 23, continued,

Absorption correction	Semi-empirical from equivalents
Max. and min. transmission	1.00 and 0.850
Refinement method	Full-matrix least-squares on F^2
Data / restraints / parameters	4370 / 1 / 255
Goodness-of-fit on F^2	1.169
Final R indices [$I > 2\sigma(I)$]	R1 = 0.0478, wR2 = 0.1118
R indices (all data)	R1 = 0.0581, wR2 = 0.1169
Absolute structure parameter	0.10(8)
Largest diff. peak and hole	0.578 and -0.232 e. \AA^{-3}

Table 24. Atomic coordinates ($\times 10^4$) and equivalent isotropic displacement parameters ($\text{\AA}^2 \times 10^3$) for **38**. U(eq) is defined as one third of the trace of the orthogonalized U_{ij} tensor.

	x	y	z	U(eq)
C1	9088(2)	3413(2)	4719(2)	28(1)
C2	8606(2)	4672(2)	4944(2)	27(1)
C3	7759(1)	4415(2)	5567(2)	23(1)
C4	7367(2)	5730(2)	5875(2)	27(1)
C5	6970(2)	5953(2)	6854(2)	30(1)
C6	6773(2)	4882(3)	7653(2)	32(1)
C7	7189(2)	3561(2)	7424(2)	29(1)
C8	7975(2)	3703(2)	6685(2)	25(1)
C9	8396(2)	2379(2)	6436(2)	26(1)
C10	7791(2)	1478(2)	5806(2)	30(1)
C11	7226(2)	2147(2)	4947(2)	25(1)
C12	6723(2)	1374(2)	4248(2)	29(1)
C13	6227(2)	1898(2)	3402(2)	30(1)
C14	6229(2)	3253(3)	3241(2)	30(1)
C15	6708(2)	4074(2)	3957(2)	26(1)

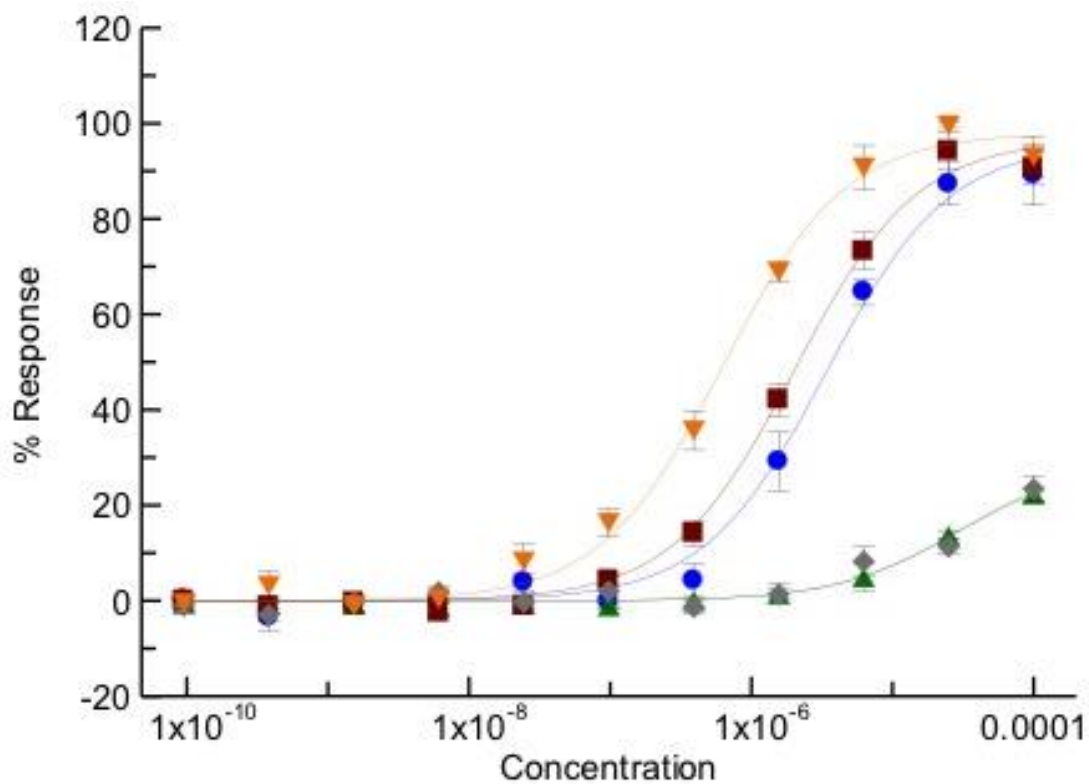
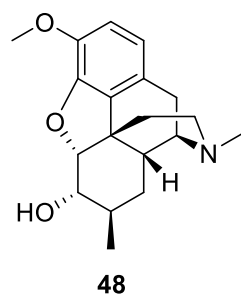
Table 24, continued,

C16	7202(1)	3531(2)	4816(2)	23(1)
C17	9759(2)	1493(3)	5639(3)	38(1)
C18	6810(2)	8239(3)	6503(3)	50(1)
C19	5361(2)	3066(3)	1618(3)	48(1)
Cl1	9706(1)	5802(1)	2472(1)	44(1)
N1	9216(1)	2667(2)	5807(2)	28(1)
O1	6656(1)	7134(2)	7211(2)	40(1)
O2	6288(1)	5035(2)	8443(2)	45(1)
O3	5786(1)	3895(2)	2404(2)	40(1)
O4	6721(1)	5401(2)	3776(2)	34(1)
O5	5184(2)	6589(3)	3787(2)	47(1)

References: X-rays

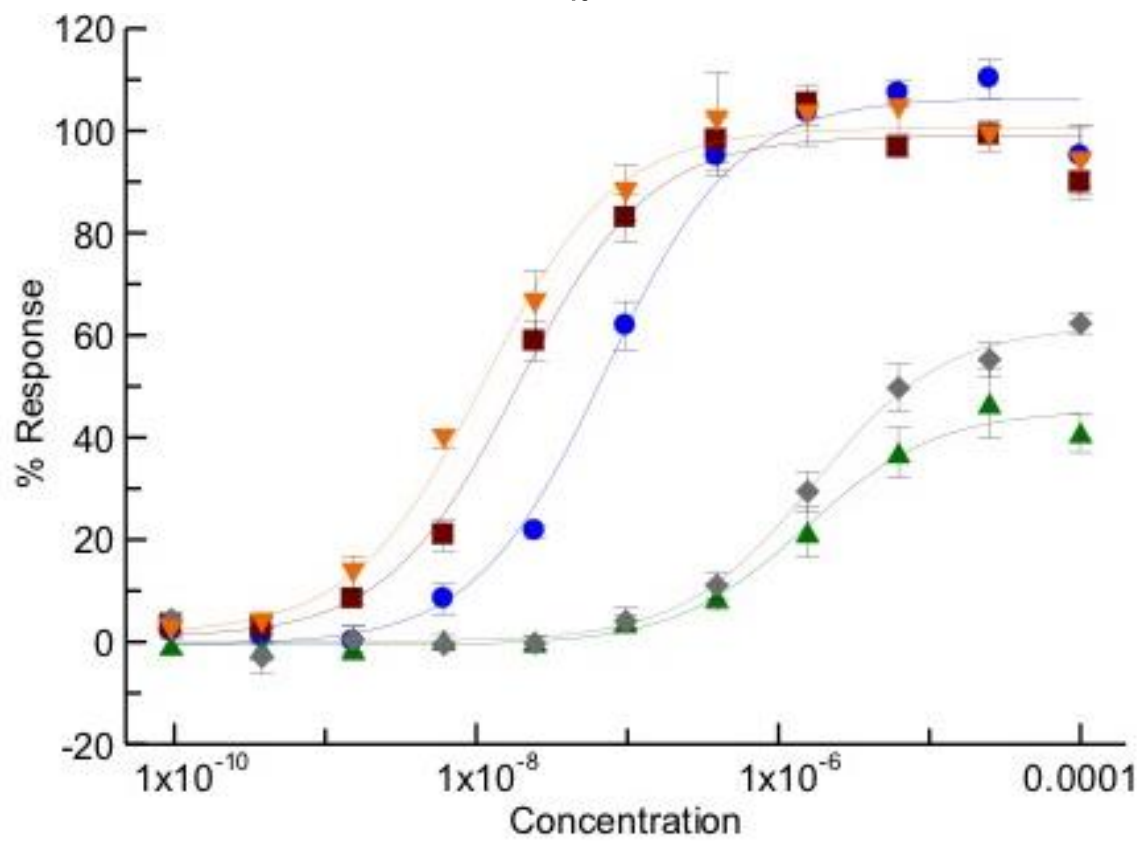
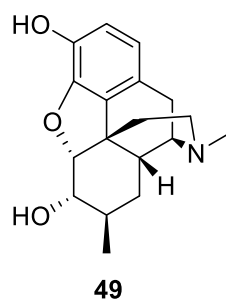
- 1) CrystalClear 1.40 (2008). Rigaku Americas Corporation, The Woodlands, TX.
- 2) SIR97. (1999). A program for crystal structure solution. Altomare, A., Burla, M. C., Camalli, M., Cascarano, G. L., Giacovazzo, C., Guagliardi, A., Moliterni, A. G. G., Polidori, G. and Spagna, R. J. Appl. Cryst. 32, 115-119.
- 3) Sheldrick, G. M. (2008). SHELXL97. Program for the Refinement of Crystal Structures. Acta Cryst., A64, 112-122.
- 4) Spek, A. L. (1998). PLATON, A Multipurpose Crystallographic Tool. Utrecht University, The Netherlands.
- 5) WinGX 1.64. (1999). An Integrated System of Windows Programs for the Solution, Refinement and Analysis of Single Crystal X-ray Diffraction Data. Farrugia, L. J. J. Appl. Cryst. 32. 837-838.
- 6) $R_w(F^2) = \{\sum w(|F_o|^2 - |F_c|^2)^2 / \sum w(|F_o|^4)\}^{1/2}$ where w is the weight given each reflection.
 $R(F) = \sum(|F_o| - |F_c|) / \sum |F_o|$ for reflections with $F_o > 4(\sigma(F_o))$.
 $S = [\sum w(|F_o|^2 - |F_c|^2)^2 / (n - p)]^{1/2}$, where n is the number of reflections and p is the number of refined parameters.
- 7) International Tables for X-ray Crystallography (1992). Vol. C, Tables 4.2.6.8 and 6.1.1.4, A. J. C. Wilson, editor, Boston: Kluwer Academic Press.
- 8) Sheldrick, G. M. (1994). SHELXTL/PC (Version 5.03). Siemens Analytical X-ray Instruments, Inc., Madison, Wisconsin, USA.

Appendix B. Biological Data.

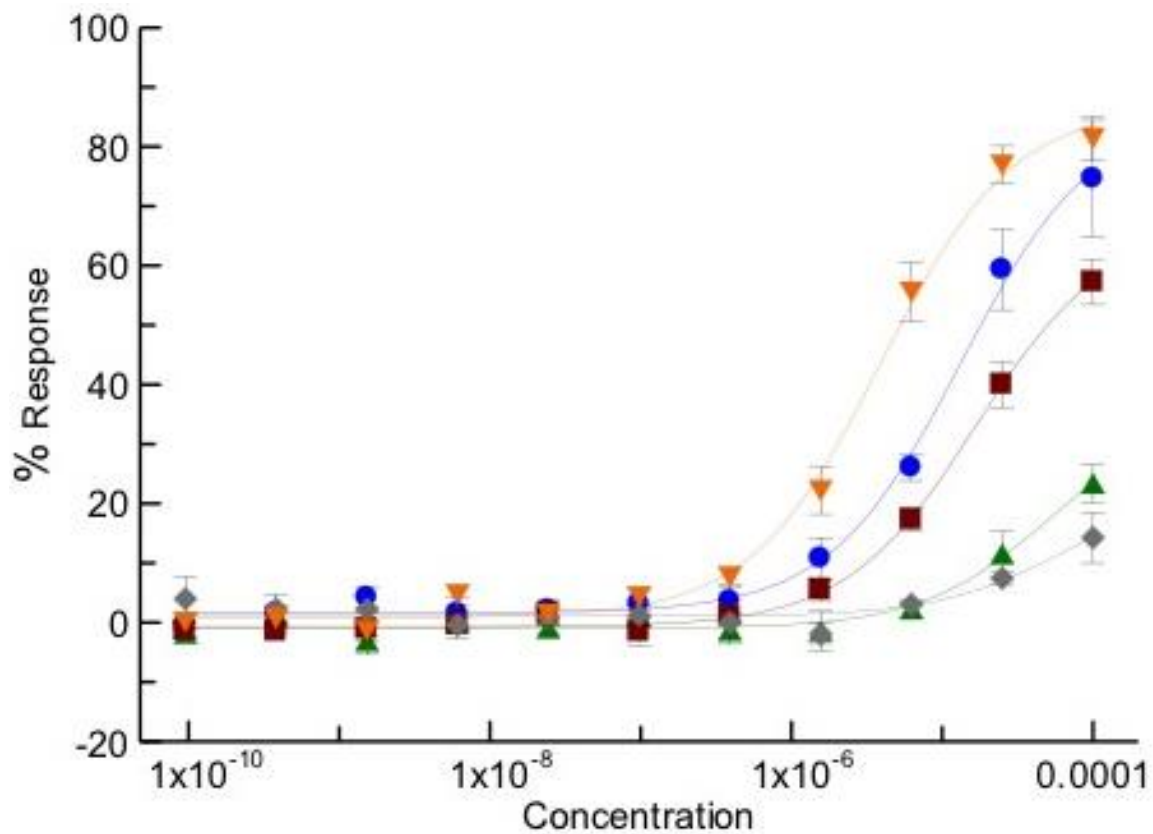
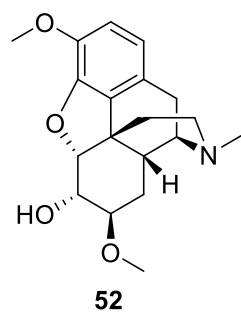


Compound 48 ● Human μOR ● Mouse μOR ● Human κOR ◆ Mouse κOR

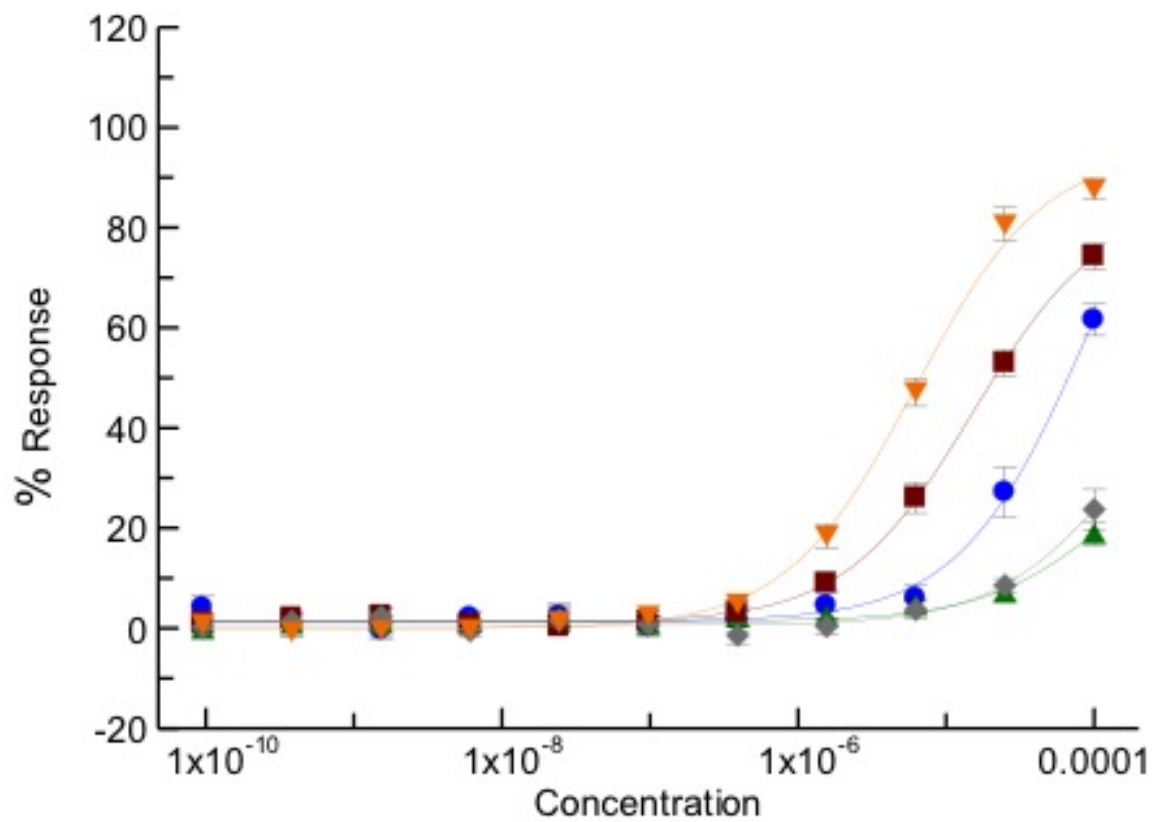
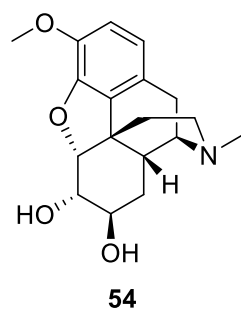
● Human δOR



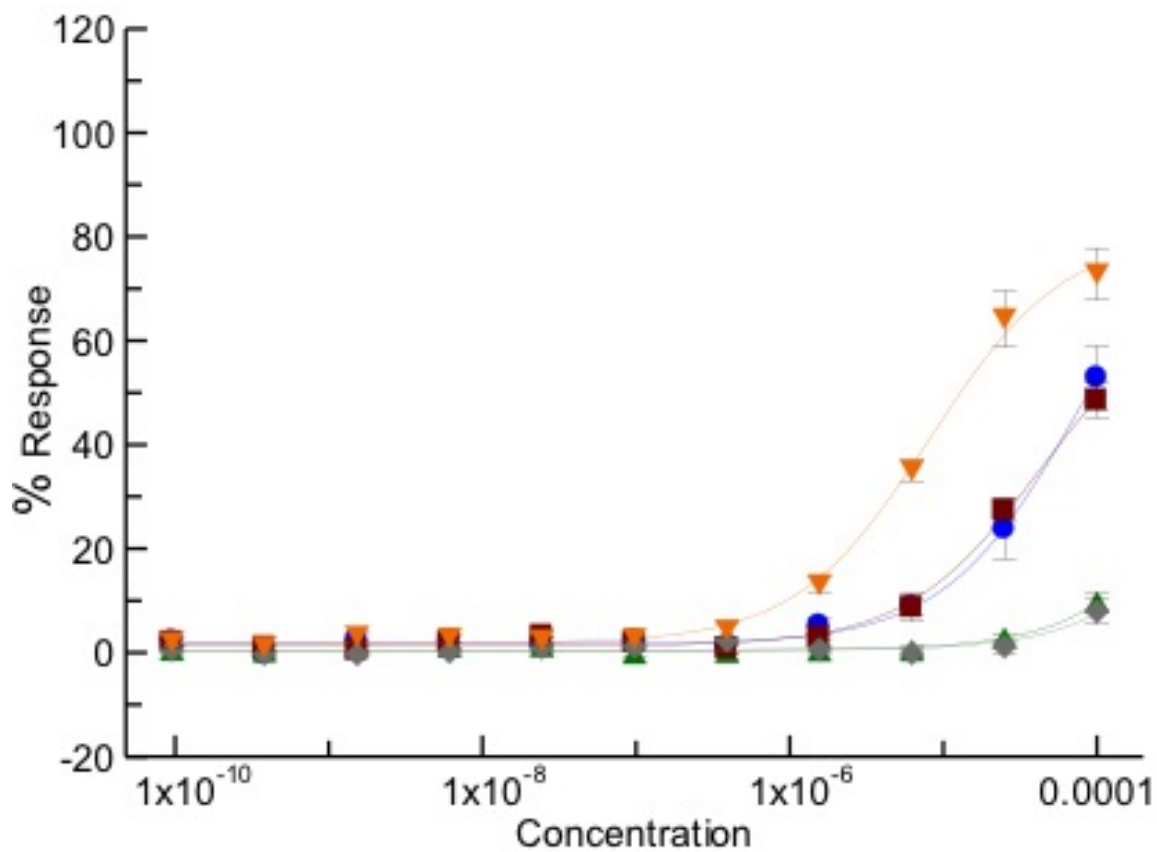
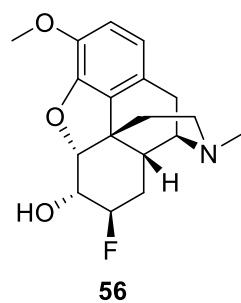
Compound **49** ● Human μ OR ● Mouse μ OR ● Human κ OR ◆ Mouse κ OR
 ● Human δ OR



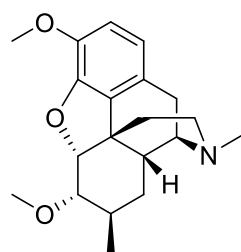
Compound **52** ● Human μ OR ▼ Mouse μ OR ▲ Human κ OR ◆ Mouse κ OR
● Human δ OR



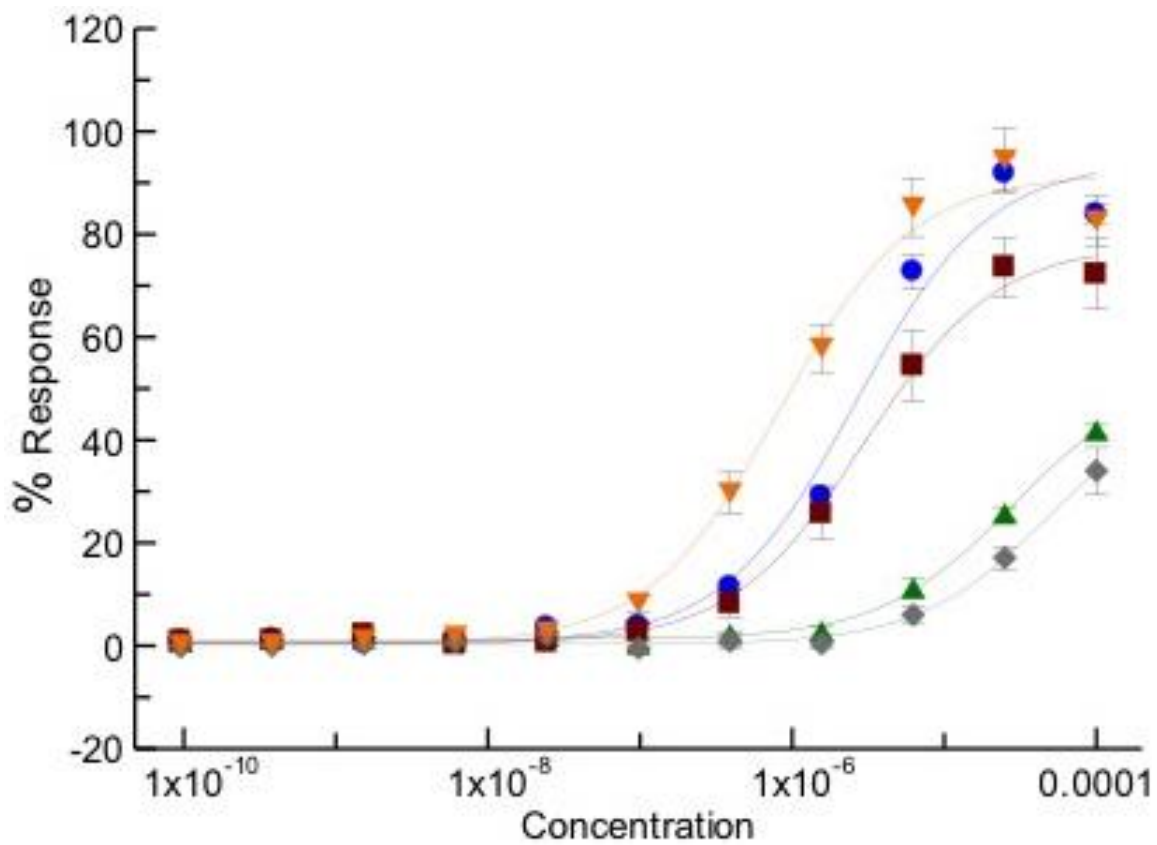
Compound **54** ◻ Human μ OR ◻ Mouse μ OR ◻ Human κ OR ◻ Mouse κ OR
◻ Human δ OR



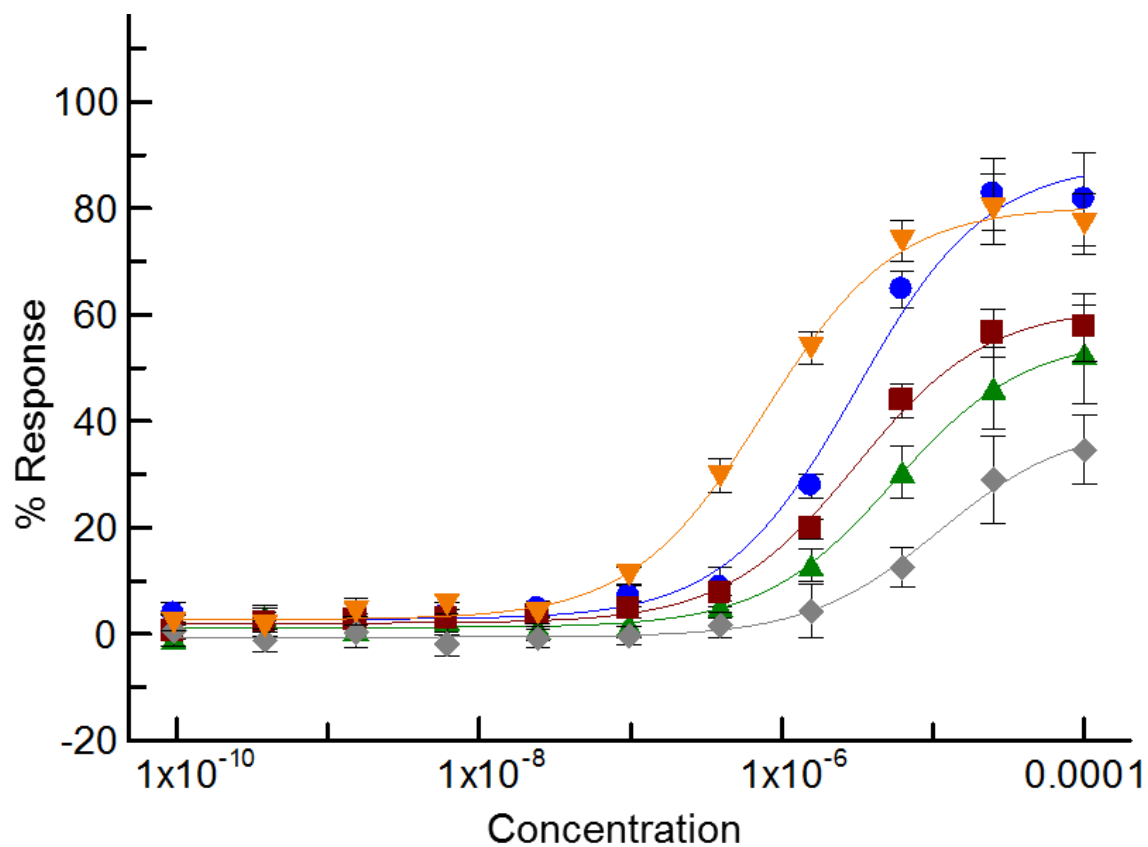
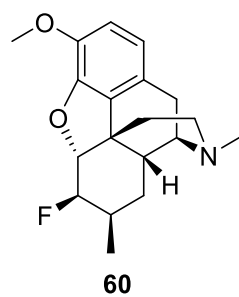
Compound **56** ● Human μ OR ● Mouse μ OR ● Human κ OR ◆ Mouse κ OR
● Human δ OR



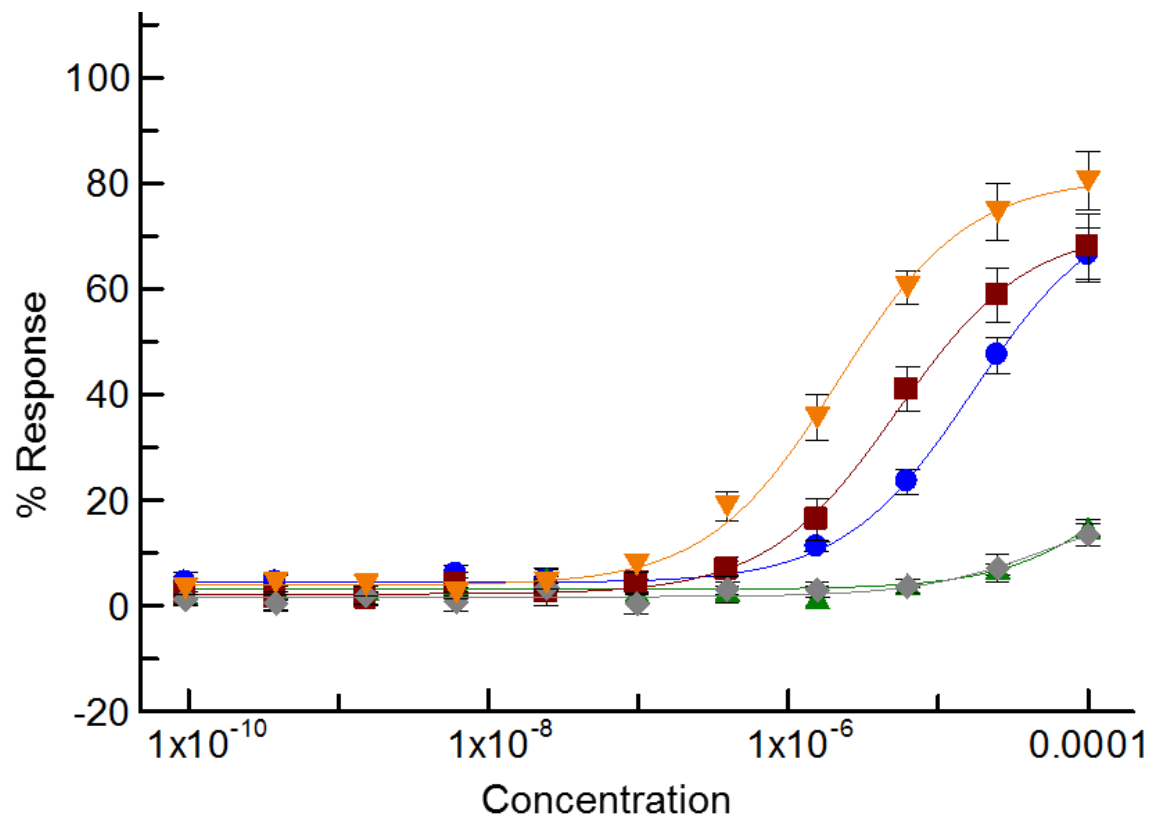
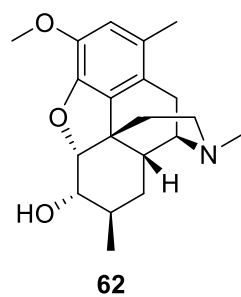
58



Compound **58** ● Human μ OR ▼ Mouse μ OR ▲ Human κ OR ◆ Mouse κ OR
● Human δ OR



Compound **60** ● Human μ OR ▼ Mouse μ OR ▲ Human κ OR ◆ Mouse κ OR
● Human δ OR

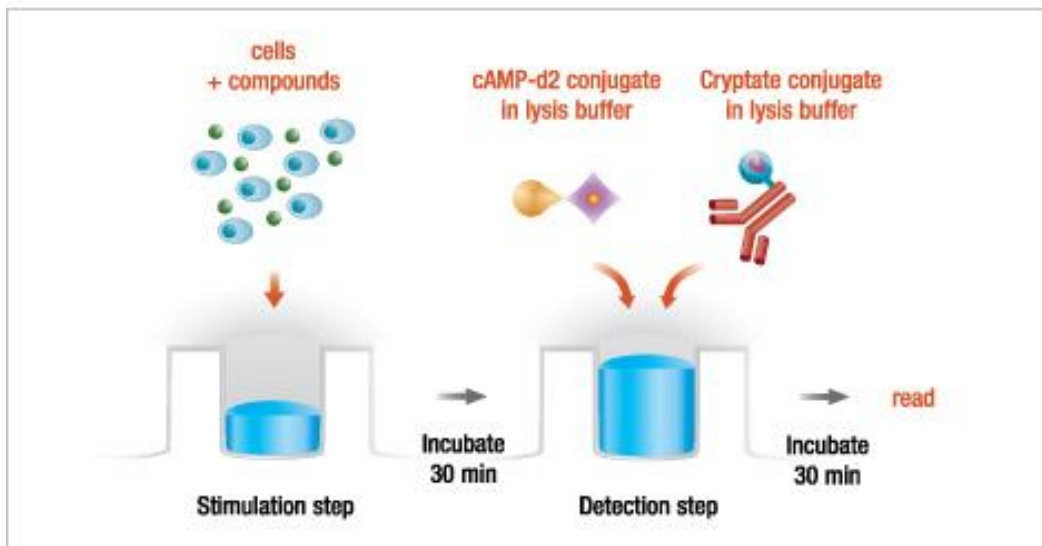


Compound **62**
 ● Human μ OR
 ▼ Mouse μ OR
 ● Human κ OR
 ◆ Mouse κ OR
● Human δ OR

Measurement of Forskolin-stimulated Adenylyl Cyclase Activity

Opioid receptors elicit analgesia by coupling to Gai, which among other signals leads to inhibition of adenylyl cyclase. This activity can be measured as inhibition of forskolin-stimulated adenylyl cyclase activity. Activity of cAMP was measured with a cell-based assay (from Cisbio®) in a 384-well plate. Titrations of test compounds are diluted in buffer containing forskolin and incubated for 30 minutes. Cells are then lysed and cAMP concentration is read by time-resolved FRET Receptor activation is reported as “% response”, the % of cAMP inhibition relative to a reference compound: DAMGO for MOR, U69, 593 for DOR, and DPDPE for KOR.

Two step protocol after cell stimulation



REFERENCES

- ¹ (a) Small, L.; Fitch, H. M.; Smith, W. E. *J. Am. Chem. Soc.* **1936**, *58*, 1457; (b) Small, L.; Turnbull, G.; Fitch, H. M. *J. Org. Chem.* **1938**, *3*, 204.
- ² Stork, G.; Bauer, L. *J. Am. Chem. Soc.* **1953**, *75*, 4373.
- ³ Boden, R. M.; Gates, M.; Ho, S. P.; Sundararaman, P. *J. Org. Chem.* **1982**, *47*, 1347.
- ⁴ Gates, M.; Boden, R. M.; Sundararaman, P. *J. Org. Chem.* **1989**, *54*, 972.
- ⁵ (a) Eddy, N. B. *Can. M. A. J.* **1948**, *58*, 79; (b) Eddy, N. B. *Public Health Reports* **1949**, *64*, 93; (c) Schmidhammer, H.; Latasch, L. *Anesth. Analg.* **2000**, *90*, 1359; (d) Schmidhammer, H.; Spetea, M. *Int. J. Med. Chem.* **2012**, *1*. Article ID 208039.
- ⁶ See any morphine-centric or equianalgesic chart.
- ⁷ Coop, A.; MacKerell, A. D., Jr. *Am. J. Pharm. Ed.* **2002**, *66*, 153.
- ⁸ Corbett, A.D.; Henderson, G.; McKnight, A. T.; Paterson, S. J. *Br. J. Pharmacol.* **2006**, *147*, S153.
- ⁹ Nordal, A. *UN Office Drugs Bull. Narc.* 1956.
- ¹⁰ Magnus, P.; Sane, N.; Fauber, B. P.; Lynch, V. *J. Am. Chem. Soc.* **2009**, *131*, 16045.
- ¹¹ (a) Kotick, M. P.; Leland, D. L.; Polazzi, J. O.; Howes, J. F.; Bousquet, A. R. *J. Med. Chem.* **1981**, *24*, 1445; (b) Leland, D. L.; Kotick, M. P. *J. Med. Chem.* **1981**, *24*, 717; (c) Kotick, M. P. *J. Med. Chem.* **1981**, *24*, 722.
- ¹² See, for example, Likhovtsov, I.; Lisowski, J. J. US 6,946,556 B1
- ¹³ (a) Carroll, R. J.; Leisch, H.; Rochon, L.; Hudlicky, T.; Cox, D. P. *J. Org. Chem.* **2009**, *74*, 747; (b) Leisch, H.; Carroll, R. J.; Hudlicky, T.; Cox, D. P. *Tet. Lett.* **2007**, *48*, 3979.
- ¹⁴ (a) Bentley, K. W.; Boura, A. L.; Fitzgerald, A. E.; Hardy, D. G.; McCoubrey, A.; Aikman, M. L.; Lister, R. E. *Nature* **1965**, *206*, 102; (b) Bentley, K. W.; Hardy, D. G. *J. Am. Chem. Soc.* **1967**, *89*, 3267; (c) Bentley, K. W.; Hardy, D. G.; Meek, B. *J. Am. Chem. Soc.* **1967**, *89*, 3273; (d) Bentley, K. W.; Hardy, D. G. *J. Am. Chem. Soc.* **1967**, *89*, 3281; (e) Bentley, K. W.; Hardy, D. G.; Meek, B. *J. Am. Chem. Soc.* **1967**, *89*, 3293.
- ¹⁵ Dianion Chemistry in Organic Synthesis by Charles M. Thompson. ISBN 0-8493-7868-0; Aug 19, 1994.
- ¹⁶ (a) Myers, A. G.; Zheng, B. *Tetrahedron Lett.* **1996**, *37*, 4841; (b) Myers, A. G.; Zheng, B.; Movassaghi, M. *J. Org. Chem.* **1997**, *62*, 7507; (c) Myers, A. G.; Movassaghi, M.; Zheng, B. *J. Am. Chem. Soc.* **1997**, *119*, 8572.
- ¹⁷ Magnus, P.; Ghavimi, B.; Coe, J. W. *Bioorg. Med. Chem. Lett.* **2013**, *23*, 4870.
- ¹⁸ Bedos, P. *Compl. rend.* **1929**, *189*, 255.
- ¹⁹ (a) Bartlett, P. D.; Berry, C. M. *J. Am. Chem. Soc.* **1934**, *56*, 2683; (b) Naqvi, S. M.; Horwitz, J. P.; Filler, R. *J. Am. Chem. Soc.* **1957**, *79*, 6283.

-
- ²⁰ Anslyn, Eric V.; Dougherty, Dennis A. (2006). *Modern Physical Organic Chemistry*. Sausalito, CA: University Science Books. pp. 104–105.
- ²¹ (a) Schlenk, W.; Schlenk, W., Jr. *Chem. Ber.* **1929**, 62, 920; (b) Whiteside, G. M.; Root, K. S.; Hill, C. L.; Lawrence, L. M. *J. Am. Chem. Soc.* **1989**, 111, 5405.
- ²² Anslyn, Eric V.; Dougherty, Dennis A. (2006). *Modern Physical Organic Chemistry*. Sausalito, CA: University Science Books. pp. 104–105.
- ²³ Metcalf, M. D.; Aceto, M. D.; Harris, L. S.; Woods, J. H.; Traynor, J. R.; Coop, A.; May, E. L. *Bioorg. Med. Chem.*, **2008**, 16, 869.
- ²⁴ DeWire, S. M.; Yamashita, D. S.; Rominger, D. H.; Liu, G.; Cowan, C. L.; Graczyk, T. M.; Chen, X. -T.; Pitis, P. M.; Gotchev, D.; Yuan, C.; Koblish, M.; Lark, M. W.; Violin, J. D. *J. Pharmacol. Exp. Ther.*, **2013**, 344, 708.
- ²⁵ (a) Snyder, S. H., Pasternak, G. W. *Trends Pharmacol. Sci.* **2003**, 24, 198; (b) Coop, A.; MacKerell, A. D., Jr. *Am. J. Pharm. Ed.* **2002**, 66, 153.
- ²⁶ (a) Clark, J. A.; Liu, L.; Price, M.; Hersh, B.; Edelson, M.; Pasternak, G. W. *J. Pharmacol. Exp. Ther.* **1989**, 251, 461; (b) Pasternak, G. W. *Neuropharmacology* **2004**, 47, 312.
- ²⁷ Corbett, A.D.; Henderson, G.; McKnight, A. T.; Paterson, S. J. *Br. J. Pharmacol.* **2006**, 147, S153.
- ²⁸ (a) Ananthan, S. *AAPS J.* **2006**, 8, E118; (b) Berger, A. C.; Whistler, J. L. *Ann. Neurol.* **2010**, 67, 559; (c) Negus, S. S.; Morrissey, E. M.; Folk, J. E.; Rice, K. C. *Pain Res. Treat.* **2012**, 1. Article ID 867067.
- ²⁹ McLaughlin, J. P.; Nowak, D.; Sebastian, A.; Schultz, A. G.; Archer, S.; Bidlack, J. M. *Eur. J. Pharm.* **1995**, 294, 201.
- ³⁰ Pasternak, G. W. *Neuropharmacology* **2004**, 47, 312.
- ³¹ McLaughlin, J. P.; Nowak, D.; Sebastian, A.; Schultz, A. G.; Archer, S.; Bidlack, J. M. *Eur. J. Pharm.* **1995**, 294, 201.
- ³² Vecchiotti, V.; Casagrande, C.; Ferrari, G.; Danieli, B.; Palmisano, G. *J. Chem. Soc., Perkin Trans. 1.* **1981**, 578.
- ³³ (a) Kutchan, T. M. *The Alkaloids: Chemistry and Biology*, Ed.: Cordell, G. A., Academic Press, London, **1998**, 50, 257; (b) Barton, D. H. R.; Cohen, T. *Festschrift Arthur Stoll*, Birkhauser, Basel, **1957**, 117. (c) Barton, D. H. R.; Kirby, G. W.; Steglich, W.; Thomas, G. M. *Proc. Chem. Soc.* **1963**, 203.
- ³⁴ Cavalcante, H. M. M.; Riberio, T. P.; Silva, D. F.; Nunes, X. P.; Barbosa-Filho, J. M.; Diniz, M. F. F. M.; Correia, N. A.; Braga, V. A.; Medeiros, I. A. *Basic & Clinical Pharmacology & Toxicology* **2010**, 108, 122.

-
- ³⁵ Melo, P. S.; Cavalcante, H. M. M.; Barbosa-Filho, J. M.; Diniz, M. F. F. M.; de Medeiros, I. A.; Haun, M. *Toxicology Letters* **2003**, *142*, 143.
- ³⁶ Wei, Y.; Jin, Q. *Zhongguo Yaolixue Tongbao* **1997**, *13*, 180.
- ³⁷ Haynes, L. J.; Stuart, K. L. *J. Chem. Soc.*, **1963**, 1784.
- ³⁸ (a) Haynes, L. J.; Husbands, G. E. M.; Stuart, K. L. *Chem. Comm.* **1967**, 15; (b) Haynes, L. J.; Husbands, G. E. M.; Stuart, K. L. *J. Chem. Soc. (C)* **1968**, 951.
- ³⁹ Stuart, K. L.; Woo-Ming, R. B. *Phytochemistry* **1969**, *8*, 777.
- ⁴⁰ Mukhtar, M. R.; Hadi, A. H. A.; Litaudon, M.; Awang, K. *Fitoterapia* **2004**, *75*, 792.
- ⁴¹ Haynes, L. J.; Stuart, K. L. *J. Chem. Soc.*, **1963**, 1784.
- ⁴² Haynes, L. J.; Husbands, G. E. M.; Stuart, K. L. *J. Chem. Soc. (C)* **1968**, 951.
- ⁴³ Haynes, L. J.; Husbands, G. E. M.; Stuart, K. L. *Chem. Comm.* **1967**, 15.
- ⁴⁴ Stuart, K. L.; Woo-Ming, R. B. *Phytochemistry* **1969**, *8*, 777.
- ⁴⁵ Sasaki, Y.; Ueda, S. *Yakugaku, Zasshi* **1958**, *78*, 44.
- ⁴⁶ Sasaki, Y.; Ueda, S. *Yakugaku, Zasshi* **1963**, *83*, 418.
- ⁴⁷ Barton, D. H. R.; Kirby, A. J.; Kirby, G. W. *J. Chem. Soc. (C)* **1968**, 929.
- ⁴⁸ Okabe, K.; Kuno, H.; Sawa, Y. K. *Chem. Pharm. Bull.* **1968**, *16*, 1611.
- ⁴⁹ Freitas, M. R.; Alencar, J. L.; Da-Cunha, E. V. L.; Barbosa-Filho, J. M.; Gray, A. I. *Phytochemistry* **1995**, *40*, 1553.
- ⁵⁰ Vecchiotti, V.; Casagrande, C.; Ferrari, G. *Tet. Lett.* **1976**, *19*, 1631.
- ⁵¹ Vecchiotti, V.; Casagrande, C.; Ferrari, G. *Tet. Lett.* **1976**, *19*, 1631.
- ⁵² Magnus, P.; Sane, N.; Fauber, B. P.; Lynch, V. *J. Am. Chem. Soc.* **2009**, *131*, 16045.
- ⁵³ Bahman Ghavimi and Philip Magnus *Org. Lett.* **2014**, *16*, 1708.
- ⁵⁴ (a) Henry, L. C. R. *Acad. Sci. Ser. C.* **1895**, 1265; (b) Henry, L. *Bull. Soc. Chim. Fr.* **1895**, *13*, 999; (c) Luzzio, F. A. *Tetrahedron* **2001**, *57*, 915.
- ⁵⁵ Magnus, P.; Sane, N.; Fauber, B. P.; Lynch, V. *J. Am. Chem. Soc.* **2009**, *131*, 16045.
- ⁵⁶ (a) Noboru Ono, *The Nitro Group In Organic Synthesis*, 2001, ISBN 0-471-31611-3; (b) Kabalka, G.W.; Varma, R. S. *Org. Prep. Proced. Int.* **1987**, *19*, 283.
- ⁵⁷ Posner, G. H. *Angew. Chemie. Int. Ed. Engl.* **1978**, *17*, 487.
- ⁵⁸ *Superbases for Organic Synthesis: Guanidines, Amidines, Phosphazenes and Related Organocatalysts* Edited by Tsutomu Ishikawa John Wiley & Sons, Ltd. **2009**, ISBN 978-0-470-51800-7.
- ⁵⁹ Caubere, P. *Chem. Rev.* **1993**, *93*, 2317.
- ⁶⁰ *Superbases for Organic Synthesis: Guanidines, Amidines, Phosphazenes and Related Organocatalysts* Edited by Tsutomu Ishikawa John Wiley & Sons, Ltd. **2009**, ISBN 978-0-470-51800-7.

-
- ⁶¹ (a) Gund, P.J. *J. Chem. Ed.* **1972**, *49*, 100; (b) Gobi, A.; Frenking, G. *J. Am. Chem. Soc.* **1993**, *115*, 2363; (c) Raczynska, E. D.; Cyranski, M. K.; Gutowski, M. *J. Phys. Org. Chem.* **2003**, *16*, 91.
- ⁶² Magnus, P.; Sane, N.; Fauber, B. P.; Lynch, V. *J. Am. Chem. Soc.* **2009**, *131*, 16045.
- ⁶³ Lane, C. F. *Synthesis* **1975**, *3*, 135.
- ⁶⁴ Gamble, A. B.; Garner, J.; Gordon, C. P.; O'Conner, S. M. J.; Keller, P. A. *Synth. Commun.* **2007**, *37*, 2777.
- ⁶⁵ Leminger, O. *Chemicky Prumysl* **1972**, *22*, 553.
- ⁶⁶ (a) Pitts, M. R.; Harrison, J. R.; Moody, C. J. *J. Chem. Soc., Perkin Trans. 1* **2001**, *9*, 955. (b) Banik, B. K.; Suhendra, M.; Banik, I.; Becker, F. F. *Synth. Commun.* **2000**, *30*, 3745.
- ⁶⁷ Gabriele, B.; Salerno, G.; Veltri, L.; Costa, M.; Massera, C. *Eur. J. Org. Chem.* **2001**, 4607.
- ⁶⁸ (a) (a) Ram, S.; Ehrenkanfer, R. E. *Tet. Lett.* **1984**, *25*, 3415. (b) Kabalka, G. W.; Pace, R. D.; Wadgaonkar, P. P. *Synth. Commun.* **1990**, *20*, 2453. (c) Gowda, D.; Mahesh, B.; Shankare, G. *Ind. J. Chem. Sect. B* **2001**, *40*, 75.
- ⁶⁹ (a) Gowda, S.; Gowda, B. K. K.; Gowda, D. C. *Syn. Comm.* **2003**, *33*, 281. (b) Abiraj, K.; Gowda, S.; Gowda, D. C. *Synth. React. Inorg. Met.-Org. Chem.* **2002**, *32*, 1409.
- ⁷⁰ Osby, J.O.; Ganem, B. *Tet. Lett.* **1985**, *52*, 6413.
- ⁷¹ (a) Gowda, D. C.; Gowda, A. S. P.; Baba, A. R.; Gowda, S. *Synth. Commun.* **2000**, *30*, 2889. (b) Yuste, F.; Saldana, M.; Walls, F. *Tet. Lett.* **1982**, *23*, 147.
- ⁷² (a) Murphy, W.; Wattanasin, S. *Chem. Soc. Rev.* **1983**, *12*, 213; (b) Magnus, P.; Sane, N.; Fauber, B. P.; Lynch, V. *J. Am. Chem. Soc.* **2009**, *131*, 16045.
- ⁷³ (a) Eschweiler, W. *Ber.* **1905**, *38*, 880; (b) Clark, H. T.; Gillespie, H. B.; Weisshaus, S. *Z. J. Am. Chem. Soc.* **1933**, *55*, 4571; (c) Moore, M. L. *Org. React.* **1949**, *5*, 301; (d) Frakas, E.; Sunman, C. J. *J. Org. Chem.* **1985**, *50*, 1110.